# INTERNATIONAL JOURNAL
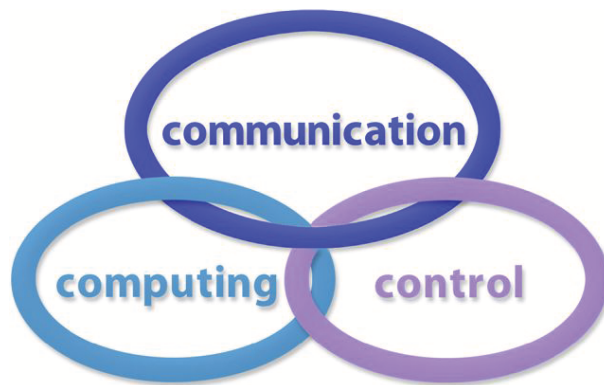
## of

## COMPUTERS COMMUNICATIONS & CONTROL

A Bimonthly Journal
With Emphasis on the Integration of Three Technologies

This journal is a member of, and subscribes to the principles of, the Committee on Publication Ethics (COPE).

## BRIEF DESCRIPTION OF JOURNAL

**Publication Name:** International Journal of Computers Communications & Control.
**Acronym:** IJCCC; **Starting year of IJCCC:** 2006.
**Abbreviated Journal Title in JCR:** INT J COMPUT COMMUN.
**International Standard Serial Number:** ISSN 1841-9836.
**Publisher:** CCC Publications - Agora University of Oradea.
**Publication frequency:** Bimonthly: Issue 1 (February); Issue 2 (April); Issue 3 (June);
Issue 4 (August); Issue 5 (October); Issue 6 (December).
**Founders of IJCCC:** Ioan DZITAC, Florin Gheorghe FILIP and Mişu-Jan MANOLESCU.
**Logo:**
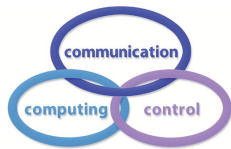


**Indexing/Coverage:**

- Since 2006, Vol. 1 (S), IJCCC is covered by Thomson Reuters and is indexed in ISI Web of Science/Knowledge: Science Citation Index Expanded.

- Journal Citation Reports (JCR2014 - Science Edition): IF/3 years = 0.746,
  IF/5 years = 0.739.
  Subject Category:

  - Automation & Control Systems: Q4 (47 of 58);
  - Computer Science, Information Systems: Q3 (96 of 139).

- Since 2008 IJCCC is covered by Scopus (2014: SNIP = 1.029, IPP = 0.619, SJR = 0.450).
  Subject Category:

  - Computational Theory and Mathematics: Q3;
  - Computer Networks and Communications: Q2;
  - Computer Science Applications: Q2.

- Since 2007, 2(1), IJCCC is covered in EBSCO.

**Focus & Scope:** International Journal of Computers Communications & Control is directed to the international communities of scientific researchers in computer and control from the universities, research units and industry.

To differentiate from other similar journals, the editorial policy of IJCCC encourages the submission of original scientific papers that focus on the integration of the 3 "C" (Computing, Communication, Control).

In particular the following topics are expected to be addressed by authors:

- Integrated solutions in computer-based control and communications;

- Computational intelligence methods (with particular emphasis on fuzzy logic-based methods, ANN, evolutionary computing, collective/swarm intelligence);

- Advanced decision support systems (with particular emphasis on the usage of combined solvers and/or web technologies).

**Gheorghe Păun**
Institute of Math. of Romanian Academy
Bucharest, PO Box 1-764, Romania
gpaun@us.es

**Mario de J. Pérez Jiménez**
Dept. of CS and Artificial Intelligence
University of Seville, Sevilla,
Avda. Reina Mercedes s/n, 41012, Spain
marper@us.es

**Dana Petcu**
Computer Science Department
Western University of Timisoara
V.Parvan 4, 300223 Timisoara, Romania
petcu@info.uvt.ro

**Radu Popescu-Zeletin**
Fraunhofer Institute for Open
Communication Systems
Technical University Berlin, Germany
rpz@cs.tu-berlin.de

**Imre J. Rudas**
Óbuda University
Budapest, Hungary
rudas@bmf.hu

**Yong Shi**
School of Management
Chinese Academy of Sciences
Beijing 100190, China &
University of Nebraska at Omaha
Omaha, NE 68182, U.S.A.
yshi@gucas.ac.cn, yshi@unomaha.edu

**Athanasios D. Styliadis**
University of Kavala
Institute of Technology
65404 Kavala, Greece
styliadis@teikav.edu.gr

**Gheorghe Tecuci**
Learning Agents Center
George Mason University
U.S.A.
University Drive 4440, Fairfax VA
tecuci@gmu.edu

**Horia-Nicolai Teodorescu**
Faculty of Electronics and
Telecommunications
Technical University "Gh. Asachi" Iasi
Iasi, Bd. Carol I 11, 700506, Romania
hteodor@etc.tuiasi.ro

**Dan Tufiş**
Research Institute for Artificial Intelligence
of the Romanian Academy
Bucharest, "13 Septembrie" 13, 050711,
Romania
tufis@racai.ro

**Lotfi A. Zadeh**
Director,
Berkeley Initiative in Soft Computing (BISC)
Computer Science Division
University of California Berkeley,
Berkeley, CA 94720-1776
U.S.A.
zadeh@eecs.berkeley.edu

"Research Excellence Award will recognize outstanding scientific journals as seen by modern bibliometric methods. To identify such journals, SNIP - Source Normalized Impact per Paper indicator is used, based on the data from Scopus database.

SNIP (Source Normalized Impact per Paper) measures a source's contextual citation impact by weighting citations based on the total number of citations in a subject field. It helps you make a direct comparison of sources in different subject fields.

SNIP takes into account characteristics of the source's subject field, which is the set of documents citing that source. SNIP especially considers: the frequency at which authors cite other papers in their reference lists; the speed at which citation impact matures; the extent to which the database used in the assessment covers the field's literature.

SNIP is the ratio of a source's average citation count per paper and the citation potential of its subject field.

The citation potential of a source's subject field is the average number of references per document citing that source. It represents the likelihood of being cited for documents in a particular field. A source in a field with a high citation potential tends to have a high impact per paper.

Citation potential is important because it accounts for the fact that typical citation counts vary widely between research disciplines. For example, they tend to be higher in life sciences than in mathematics or social sciences. If papers in one subject field contain an average of 40 cited references while those in another contain an average of 10, then the former field has a citation potential that is 4 times higher than that of the latter.

Citation potential also varies between subject fields within a discipline. For instance, basic journals tend to show higher citation potentials than applied or clinical journals, and journals covering emerging topics tend to have higher citation potentials than periodicals in well established areas."

# Interview with Editor-in-Chief Ioan Dzitac

**Elsevier**: How do you feel about being nominated for Scopus Awards 2015?

**Editor-in-Chief Ioan Dzitac**: The whole team is honored by the nomination which we believe is an acknowledgement of all the hard work that stands behind the publishing of International Journal of Computers Communication & Control (IJCCC). We would like to thank our authors, reviewers and the entire team for all their dedication, originality and hard work.

**Elsevier**: What gap do you think your journal fills in your respective field of research?

**Editor-in-Chief Ioan Dzitac**: IJCCC has been focused from the very beginning on promoting research that integrates the "3Cs" - Computing, Communication and Control as to N. Wiener's theory in order to try and differentiate ourselves from the other journals indexed in the same category by Scopus.

**Elsevier**: If you could pick 5 articles of great importance for your field of research that have been published in your journal which would those be and why?

**Editor-in-Chief Ioan Dzitac**: I have decided to choose 5 of the most cited articles according to international databases such as Scopus and SCI Expanded:

(1) Spiking neural P systems with anti-spikes, by L. Pan, G. Paun, 2009.

(2) Tissue P systems with cell division, by G. Paun, M.J. Pérez-Jiménez, A. Riscos-Núnez, 2008.

(3) Computing Nash equilibria by means of evolutionary computation, by R.I. Lung, D. Dumitrescu, 2008.

(4) Lorenz system stabilization using fuzzy controllers, by R.E. Precup, M.L. Tomescu, S. Preitl, 2007.

(5) Neuro-fuzzy based approach for inverse kinematics solution of industrial robot manipulators, by S. Alavandar, M.J. Nigam, 2008.

**Elsevier**: For you, as Editor-in-chief, what is the most important development objective for 2016?

**Editor-in-Chief Ioan Dzitac**: Reinforcing the intellectual current we have created through publishing high quality articles that bring new ideas and multidisciplinary approaches.

**Elsevier**: Why did you choose to publish your journal Open Access?

**Editor-in-Chief Ioan Dzitac**: We have never followed financial gain as our main goal has been to publish high quality articles with a real effect on the evolution of society.

**Elsevier**: What do you think makes your journal stand out?

**Editor-in-Chief Ioan Dzitac**: First of all it stands out through the approach of the subject by integrating the 3Cs. On top of this I would add the geographical distribution of the authors that come from over 45 countries and are affiliated to more than 150 universities. The prestige of the editorial board that included researchers from 14 countries.

The editorial team is another strong point as it includes researchers affiliated to high ranked universities from top 100 QS (1. Massachusetts Institute of Technology (MIT), 17. Cornell University, 24. McGill University, 25. Tsinghua University, 26. University of California Berkeley, Berkeley (UCB), 56. Tokyo Institute of Technology, 70. Shanghai Jiao Tong University, 80. University of Sheffield, 89. Purdue University, 96. University of Alberta).

Finally I would like to point out our association with the International Conference on Computers Communications and Control.

**IEEE - ICCCC2016**:

The International Conference on Computers Communications and Control (ICCCC) has been founded in 2006 by I. Dzitac, F.G. Filip and M.-J. Manolescu and organized every even year by Agora University of Oradea, under the aegis of the Information Science and Technology Section of Romanian Academy and IEEE - Romania Section.

2016 edition is Co-Sponsored by IEEE Region 8 - Europe, Middle East, Africa.

The goal of this conference is to bring together international researchers, scientists in academia and industry to present and discuss in a friendly environment their latest research findings on a broad array of topics in computer networking and control.

The Program Committee is soliciting paper describing original, previously unpublished, completed research, not currently under review by another conference or journal, addressing state-of-the-art research and development in all areas related to computer networking and control.

In particular the following topics are expected to be addressed by authors:

1) Integrated solutions in computer-based control and communications;

2) Network Optimization and Security;

3) Computational intelligence methods (with particular emphasis on fuzzy logic-based methods, ANN, evolutionary computing, collective/swarm intelligence);

4) Data Mining and Intelligent Knowledge Management;

5) Advanced decision support systems with particular emphasis on on sustainable energy;

6) Membrane Computing - Theory and Aplications;

7) Stereovision Based Perception for Autonomous Mobile Systems and Advanced Driving Assistance.

# Contents

# Biometrics Systems and Technologies: A survey

I. Buciu, A. Gacsadi

**Ioan Buciu\*, Alexandru Gacsadi**

Department of Electronics and Telecommunications
Faculty of Electrical Engineering and Information Technology
University of Oradea, 410087, Romania
\*Corresponding author: ibuciu@uoradea.ro

**Abstract:** In a nutshell, a biometric security system requires a user to provide some biometric features which are then verified against some stored biometric templates. Nowadays, the traditional password based authentication method tends to be replaced by advanced biometrics technologies. Biometric based authentication is becoming increasingly appealing and common for most of the human-computer interaction devices. To give only one recent example, *Microsoft* augmented its brand new Windows 10 OS version with the capability of supporting face recognition when the user login in. This chapter does not intend to cover a comprehensive and detailed list of biometric techniques. The chapter rather aims at briefly discussing biometric related items, including principles, definitions, biometric modalities and technologies along with their advantages, disadvantages or limitations, and biometric standards, targeting unfamiliar readers. It also mentions the attributes of a biometric system as well as attacks on biometrics. Important reference sources are pointed out so that the interested reader may gain deeper in-depth knowledge by consulting them.
**Keywords:** biometric modalities, biometric attacks, biometric standards.

## 1 Biometrics - Introduction

Let us begin with a simple scenario. Let us assume a user wants to remotely access a tele-presence group with secured and restricted credentials. The access is done by launching a verification application requiring a password and user ID. Unfortunately, for some reasons, the user does not remember the password. In this case, the application or system provides a link for *Forgot Password*. The user needs then to type his e-mail address to which a new temporary password is sent by the verification system. The user enters his e-mail account, copies the temporary password and the system asks the user to change again the temporary password with a new more meaningful password. Moreover, the brand new password must be re-typed to avoid any typo mistake. The whole process may take several minutes and requires the use of the keyboard for several times, not mentioning memorizing or writing down the brand new password. The action may become very frustrating and inconvenient for the user who might become angry soon. Let us now consider there is another application which can get the user access easily and very fast without requiring any typing and with a minimum user interaction or effort. Such applications already exist and they are based on user's biometric features.

A biometric feature can be defined as a physiological (face, fingerprints, iris, etc.) or behavioural (gait, voice, signature, etc.) attribute of a human being that can discriminate one individual from another. Nowadays, the great interest for biometric recognition systems can be justified due to increased demand for security. The goal of a biometric based recognition system is either automatic identification or verification of identities, given input data comprising images, speech or videos. Unlike the traditional ways, such as password, biometric traits have some advantages: they cannot be stolen (although spoof attacks may exist to tamper the biometric system), lost or forget. However, to be reliable, biometric traits should be unique and persistent

over time. Some other criteria should be met such as user convenience and acceptability (mainly due to privacy reasons). Biometric recognition is usually performed by extracting a biometric template in query from the input device and compare it against some enrolled biometric templates. The comparison is processed using of the two modes: a) verification (or authentication) and b) identification (or recognition). *Verification* is an one-to-one process where the query face is compared against the user claiming his genuine identity to verify his claimed ID. The output is binary, either accept or reject, based on a matching procedure. We should note here that a biometric authentication technology may be used in conjunction with traditional authentication methods such as password, passports, PIN, smart cards, access tokens, etc, employed as second factor authentication. *Identification* is one-to-many process where the query is compared against each enrolled biometric template (multiple templates) from the database to search for the identity of the query. Identification is a bit more complex than verification as the system serves as both identifier and authenticator. A biometric based recognition system needs an *enrollment* procedure which allows the registration of persons in a biometric database that may be later used for identification or verification. The acquired initial data may undergo some pre-processing steps depending on the biometric modality. For instance, in the case of images, histogram equalization may help when the image suffers from illumination imbalance. For audio data, voice separation from the background may be also a pre-processing step. Biometric features are constructed by feature extraction step resulting a biometric template, further stored in the database. After a person is enrolled, the person's biometrics are scanned and matched against the enrolled biometric templates. *Matching* is a complex pattern recognition problem between the enrolled samples and the test one. A *matching score* is computed to reflect the similarity between two biometric templates. Overall, the person's recognition process is challenging because the representation of the same biometric is basically taken either by different sensors or, more often, at two or multiple different points in time, so that the acquisition conditions between the enroll and test samples may greatly vary due to various factors: noise, change in illumination, partial occlusion, different resolution, etc. This issue translates in a matching score lower than its optimum value. A *threshold level* is next setup for a final decision. A matching score higher than the threshold would give a match and consequently an accept, while a lower score would lead to rejection.

The associated risks for any biometric system are *false accept* (when an unauthorized person is wrongly accepted), represented by *False Acceptance Rate* (FAR) and *false reject* (when an authorized person is incorrectly denied for access), represented by *False Rejection Rate* (FRR). An ideal biometric system should have both FAR = FRR = 0. In real life, no such biometric system or technology exists. While connected to the threshold level, FAR and FRR are inversely proportional. More precisely, a low threshold level would decrease FRR and increase FAR. This situation is preferred for applications where the level of security is not critical. However, for applications demanding high security level, the threshold is set to a very high value to favour low FAR in detriment of high (possible disturbing) FRR. One such applications is the authorized and secure remote access for telepresence requiring very strict authorization. When FRR equals FAR we have Equal Error Rate (EER), a measure that is often reported when the performance of a biometric system or technology is addressed.

Biometric systems or technologies can be categorized based on several classifications: a) physiological versus behavioural; b) cooperative versus non-cooperative; c) mono-modal versus multimodal biometric systems; d) contact versus touchless versus "at distance" (or remote) technology, e) server based versus mobile based biometric technology; f) human versus no human monitoring for data acquisition. The appropriateness of each classification is highly depending on the application type. For instance, a biometric based surveillance technology may operate with full a) category (face as physiological and gait as behavioural) using non-cooperative user interaction, remote sensors and server based processing (involving large video data), while the

contact based biometric type is fully absent. Similarly, a biometric authorization based access for telepresence application might also require either contact or contactless sensing technology, but no human monitoring is typically involved at the sensory remote spot.

# 2 Physiological versus Behavioural Biometrics

Physiological biometrics addresses direct measurement from parts of the human body, while behavioural biometrics relates to measurements derived from human actions. In terms of acquisition, behavioural biometrics need measurements acquired over a certain period of time which is an important factor.

## 2.1 Physiological Biometrics

The majority of commercial biometrics technologies involve physiological measurements which are considered to remain steady over relatively large time interval. Such measurements may include the following modalities:

- face recognition

- facial thermography

- fingerprint recognition

- hand geometry based recognition

- ear geometry based recognition

- iris recognition

- retina recognition

- vascular pattern recognition

The above biometric modalities have, more or less, reached maturity. However, the performance of such technologies are greatly dependent of application class. If, for a controlled acquisition environment (high image resolution, good quality light, occlusion free and steady images - a process preferable under external human monitoring) a face recognition technology may easily acquire a very high matching score for an genuine individual, the matching score may significantly degrade for different environmental conditions in the absence of a watching guard compensating the ideal conditions. This case is specific for surveillance applications or, more generally, when the remote biometric sensor is separated by the processing module location. Moreover, in the absence of any preventive or detective control, an attacker can get access by attacking the system with stolen biometric data (a printed photo of the genuine's face, fingerprint, video record, etc.). The scenario is closely related to *network authentication* such as telepresence, automated teller machine access, internet banking, mobile based biometrics, cloud technology. For a centralized biometric network, authentication the user who needs to be authenticated is physically present at the same site with the sensor while the recognition process takes place on a general - purpose computer or server, located some distance away from the sensor. The remote access is granted or rejected based on server decision which communicates with the sensor.

## Face Recognition

Face identification and verification dates back to 60's when the computer vision community has started to address the problem. While the face recognition technology is somehow inferior as performance compared to other biometric modalities (such as iris recognition for example), it is more accepted due to its major advantage: it is the only physiological biometric that can be reliable measured at distance and, moreover, the authentication of the users can happen without their explicit interaction with the sensor or their knowledge. The performance of face recognition systems can vary considerable depending upon the context and various factors. The modifications of facial features are caused by both long-term and short-term changes. Long-terms changes refer to aging where prominent and wrinkles may appear upon the face and permanently change the facial texture. In this case, periodic enrollment is necessary to update the biometric template. Short - term changes may refer to weight loss or gain. Other factors affecting the system's accuracy are partial occlusions (growing beard or moustache, glasses, hat, scarf) or various environment conditions (distance from camera, varying lighting conditions, noise, motion blur, etc). Another factor is given by face position. While the enrollment is usually taken in frontal pose, the matching process may suffer from non-frontal pose acquisition, where pose estimation might be needed.

The face recognition systems and technologies are based either on 2D or 3D representation of the face appearance. The 2D based face biometrics systems are pose variant and rely on the information conveyed in the gray level structure of the facial image (2D face texture), while the 3D approaches are pose invariant and involve the volumetric structure of the face along with its depth map. The 3D image acquisition technologies come with different cost and approaches. The most cost-effective solution called stereo acquisition is to use several calibrated 2D cameras to acquire images simultaneously followed by 3D reconstruction. While the acquisition is fast, this approach is highly light sensitive. Changes in illumination can lead to image artifacts compromising the performance of the 3D face recognition system. An alternative is to project a structured light pattern on the facial surface during acquisition. A third solution relies on active sensing where a laser beam is scanning the face surface generating a reflected facial pattern. Once the facial data are acquired, either as 2D or 3D, an automatic landmarking process is necessary to detect facial interest points such as eyes, eyebrows, mouth contour, nose, chin, etc. These landmarks are further used for face registration so that facial features (landmarks) are localized at the same position (geometrical coordinates) across multiple face images. The process continues with feature extraction and matching. For feature extraction, various techniques were proposed, including subspace methods (principal component analysis, linear discriminant analysis, independent component analysis), filtering approaches (different implementation of Gabor wavelets) or statistical approaches (including vacuous versions of local binary patterns). For the last step, matching, methods starting from distance based classifiers (Euclidean distance, cosine similarity measure) up to complex classifiers (neural networks or support vector machines) were implemented. The literature presents an abundant source of methods and it is impossible to provide references for all representative proposed techniques. The reader my consult the most recent edited or authored face recognition books such as [1], [2], [3], [4], [5], [6], where all related aspects and techniques are presented in great details.

## Facial Thermography

A very challenging issue for conventional face recognition systems is when they are operating under low illumination environment. Off-the-shell methods to cope with this issue exist, but their outcome is typically very noisy and the overall performance of this biometric system is slightly improved. One solution is to shift from visible spectrum to infrared (IR) or near infrared

(NIR) range that requires dedicated sensors. For long-wave IR (8 - 14 $\mu m$) the human body is a light source emitting heat due to the blood flow under the skin and the resulting thermal patterns can be collected in total darkness [7], [8], [9]. While an external light is not necessary, these sensors are completely useless when the system operates in daylight, as usually happens. This is because the body thermal patterns strongly interferes with the surrounding temperature coming from artificial light or sunlight. Alternatively, less heat sensitive near infrared spectrum - NIR (0.8 - 2.5 $\mu m$) can also be used. For a reliable functioning, the NIR sensor need an ambient light. Studies have reported, however, modest performances of somewhere between 84% and 93% [10], [11]. This is due to the fact that many facial texture patterns that are clearly distinctive in the visible spectrum are absent in the IR or even NIR facial imagery, thus lowering the discriminant capability of facial thermography based biometrics systems. Facial thermography is affected by medical conditions such as, for example, fever.

**Fingerprint Recognition**

The fingerprint recognition is perhaps the most used biometric having applications in both law enforcement and computer systems, having a mature and widely accepted technology. The technology is implemented on various platforms and devices, including laptops, mobile phones or personal digital assistants. Conventional fingerprint systems belong to touch-based sensing technology and require touching or rolling a finger onto a rigid surface with a live-scan device. One disadvantage is the usability aspect as the system depends on the finger placement, finger scarfs or skin conditions (dirt, sweat, moisture). To make them robust against skin conditions, touchless fingerprint technologies are emerging. Two classes exist: reflection - based touchless finger imaging (RTFI) and transmission-based touchless finger imaging (TTFI). In the case of RTFI there are 2 light sources illuminating the fingerprint [12]. The finger must absorb only a small portion of the incident light, while the majority of light is reflected back to the optical detector. The device must be designed to allow different light quantity absorbed by the fingerprint's valleys compared to the light absorbed by the ridges to assure a good contrast. The other parameters such as the depth-of-focus and field-of-view of the camera, the irradiation and the frequency of the light sources are also crucial for reliable performance when the skin condition changes from dry to wet. The light sources has to be placed as close as possible to detector to minimize the shadowing effect and the emitted light should be in the blue spectrum (around 500 nm wavelength). The design is very complex and acquiring an optimum image contrast is not an easy task, leading to expensive devices compared to the touch-based fingerprint devices. The other approach, TTFI is similar to the optical coherence tomography principle where the light is transmitting through the finger [13] and the light that is back-scattered from the skin tissue is captured. The finger is placed between the light source and detector so that the light illuminates the nails side of the finger while the opposite finger part is oriented towards the detector. A red light with wavelength of 660 nm is used here because this wavelength corresponds to the maximum transmittance ratio to the skin tissue. The light penetrate the finger and then collected by the detector. Apart from high cost for the touchless fingerprint recognition technology, the curvature of the finger represents another limitation of this technology resulting in a relatively low interest for commercial adoption. The latter issue can be solved by employing a multi-vision system consisting of several cameras located on a semicircle and pointing out to the center of the finger. Such device may contain five cameras along with a set of green LED arrays to illuminate the finger [14]. Once the finger is in the correct position, each LED array is set to a specific light intensity and the five cameras start capturing a picture of the finger simultaneously. Using five cameras a enlarged (180 degree) field-of-view is obtained and the views are combined together to form a 3D finger reconstruction.

**Hand Geometry based Recognition**

Hand geometry based recognition systems consider the measurement of length, width, thickness, and surface area of the fingers and hand [15]. This biometric offers low security level because it is not scalable, i.e. those measurements do not tend to be unique for large-scale identification systems [16]. One important inconvenient is that such biometric systems require complex hardware to capture the hand image and may not be appropriate for computer-based login [17].

**Iris Recognition**

Iris recognition is the most reliable type of biometric identification. It is considered to be the ideal biometric in terms of uniqueness and stability (its features do not vary over time) leading to massive deployment for large-scale systems that proved to be very effective [18]. The iris is the colored portion of the eye surrounding the pupil and the biometric system searches for its specific intricate patterns composed of many furrows and ridges. The basic steps are: image acquisition, iris localization using landmark features and segmentation, biometric template generation and biometric template matching. The acquisition factors are resolution, signal/noise ratio, contrast and illumination wavelength. Once the iris is segmented, it may suffer a pseudo-polar coordinate transformation operation to take into account variations in pupil size. To capture the iris image, the conventional iris recognition technology requires a very short focal length, increasing the intrusiveness of this approach. However, iris recognition systems where the iris image is captured at longer distance exist nowadays. While for short focal length the image resolution is not an issue, this becomes very challenging with increasing distance, leading to significant drop in accuracy. Iris biometric technologies operating at long distance (beyond 1 m) are developed by various vendors. For instance, AOptix has implemented a system able to operate within a range of 1.5 - 2.5 m [19]. They have also developed a system having onboard coaxial imaging and adaptive optics to facilitate the capture of iris image at up to 18 m. Another vendor, Honeywell [20] has designed a combined face and iris recognition system that is capable of acquiring face and iris images at distances from 1 m and beyond 4 m. Carnegie Mellon University's CyLab Biometrics Center have been developing an iris recognition solution for the past several years that can successfully identify subjects from up to 12 meters away [21]. However, regardless of technology, one important aspect with the iris recognition systems is that the approach is not applicable when the user has contact lens.

**Retina Recognition**

In order to obtain retinal images, an infrared camera is used to capture the unique pattern of veins located at the back of the eye. Similarly to iris recognition, this modality also suffers from the problem of user inconvenience, which is even more inconvenient as the user is asked to carefully present their eyes to the camera at very close proximity. Another inconvenient is that this approach requires complex and expensive dedicated hardware, making such solution to be limited to applications with very high security demands [22]. On a positive side, unlike face, iris or fingerprint biometrics, retina based patterns are very difficult to spoof.

**Vascular Pattern Recognition**

This approach uses the subcutaneous vascular network on the back of the hand for specific individual patterns which are distinctive even for identical twins. A near-infrared light is emitted toward the back or palm of the hand. The reflected light prints an image on the sensor, image representing the encoded absorbance of blood vessels [23]. Due to the hemoglobin presented

in the blood, the veins appear as dark areas pattern and clearly delimited. The image is next digitized and specific features including vessel branching points, thickness, or branching angles are extracted as distinct features.

## 2.2   Behavioural Biometrics

The behavioural biometrics typically measures the behaviour of the user over time. This biometric type usually does not explicitly ask the user to be cooperative and thus, it is more transparent, user-friendly, less intrusive and more convenient than their physiological counter-parts. On the downside, the behavioural biometrics suffers from low level of uniqueness and permanence, compared to the physical biometrics. Moreover, their accuracy for authentication is lower and are rather more suitable for verification. The approaches can be split into the following classes:

- gait recognition

- keystroke analysis based authentication

- mouse dynamics

- speaker recognition

### Gait recognition

Analyzing the way an individual walks is the key issue for the gait recognition systems. The main advantage is the fact that this approach has no physical contact being ideal for acquiring data at long distance with low resolution. The fine details are not crucial here, rather the movement time patterns are considered. Such systems are influenced by external factors such as footwear walking surface or clothing. The gait recognition systems can be classified either as model based or appearance based [24]. Model based approaches fit a model representing time pattern of the human anatomy against video data then extracting and analyzing its parameters. Appearance model based approaches analyze the silhouette shape and motion of an individual and the way this vary in time. The images are recorded while the individual walks in a plane normal to the camera view. The performance of these biometric systems are highly dependent on the camera viewpoint. A change in the walking direction can negatively influence their performance. By using geometric cues, some systems improve viewpoint invariance when dealing with 2D imagery. Another alternative is to use 3D human figure capturing to have viewpoint independence. Both 2D and 3D approaches are described in great details in [24].

### Keystroke analysis based authentication

Keystroke analysis based authentication is defined as the process of recognizing an individual from his typing characteristics. The verification can be performed either static (text-dependent) or dynamic (text-independent) mode. The characteristics are typically composed of the time between successive keystrokes, more precisely the inter-stroke latency, time durations between the keystrokes, dwell times (i.e. the time a key is pressed down), overall typing speed, frequency of errors (use of backspace), use of numpad, etc. For a large scale application, these characteristics are not unique amongst too many users. Therefore this analysis cannot be reliable used as recognition feature (although some report indicate this could also be possible [25]), but they can be suitable for verification systems. Aside from relative low accuracy, the enrollment procedure is the major drawback of such behavioural biometric systems. To generate representative biometric

templates the user might be asked to repeat the enroll procedure by providing a username, password or a specific text for a large number of times. An interesting application is presented in [26] where the keystroke dynamics based authentication has been analyzed in the context of collaborative systems.

**Mouse dynamics**

A behavioural profile can be also constructed using mouse actions performed by an user. Mouse derived features are easy to handle without user's knowledge. The mouse authentication involves registration phase and login phase. A template is built using the mouse features captured at the time of registration. The same template is compared with login details which are captured by the mouse task. In case of laptop, touchpad helps to extract the mouse features. The mouse's sensitivity affects the performance. The mouse features include general movement, drag and drop, stillness, point and click (single or double) actions, [27], [28].

**Speaker recognition**

Speaker recognition is the most researched behavioural biometric. Although the voice production considers the physical aspects of the mouth, nose and throat, this biometric is considered as behavioural type because the pronunciation and the manner of speech is intrinsically behavioural. The specific voice features refer to various analysis such as amplitude spectrum, localization of spectral peaks related to the vocal tract shape or pitch striations related to the user's glottal source. Similar to keystroke analysis, the speaker recognition can be performed either in static (text-dependent) or dynamic mode (text-independent) mode [29]. In the text-dependent mode the use is asked by the biometric system to pronounce a particular phrase, while, in the case of the text-independent mode the user is free to speak any phrase. In the latter case the verification accuracy usually improves as the text length increases. In between, a pseudo-dynamic mode exists where the user is requested to say two numbers randomly previously enrolled in a database. As principle, the normalized amplitude of the input signal is decomposed into several band-pass frequency channels with the purpose of feature extraction. The type of the extracted feature may vary. Typical features are the Fourier transform of the voice signal for each channel, along with some extra information consisting in pith, tone, cadence or shape of the larynx. Amongst behavioral biometric systems, the speaker recognition is the most accurate behavioral approach. Nevertheless, the voice might be perturbed by various factors such as illness, emotional or mental state or even age, conducting to inaccurate results.

## 3 Mobile and Web-based Biometrics Technology

According to Acuity Market Intelligence, the mobile biometric market will technically explode from $1.6 billion in 2014 to $34.6 billion in 2020 [30]. This prediction is foreseen for all biometric sensors (modalities) embedded in smart mobile devices (smart phones, tablets, and intelligent wearables. Another mobile biometrics considered also refer to biometric applications offered by vendors or mobile service providers, including retailers, payment procedures or banks. A third identified biometric sector is given by payment or non-payment transactions using secure web (cloud)-based services augmented with biometric authentication option. The report claimed that 100% of smart mobile devices will include embedded biometric sensors as a standard feature by 2020. According to the report, each year, more than 800 billion transactions requiring different level of biometric authentication will be processed, while more than 5.5 billion biometric applications are foreseen to be downloaded.

The aforementioned statistics come with no surprise. Millions of internet users experience a malware or hacker attack each year. The situation is even more critical with the use of mobile access where losses to fraud or identity theft are measured in the hundred of billions of dollars. Thus, implementing more authentication modalities by replacing the conventional ways with biometrics for mobile devices seems to be a reliable solution. Mobile biometrics solutions are implemented by device manufacturers as well as independent vendors as third-parties which offer software solutions. Intel Security Division has developed a biometric authentication application relying either on face or fingerprint named $TrueKey^{TM}$ [31], application available for various platforms either server-based or mobile. Another company, Sensory, released an authentication application named $TrulySecure^{TM}$ that combines voice and vision (face-based) authentication for mobile phones, tablets, and PCs [32]. Fingerprints, face, iris palm print or voice biometric authentication and verification solutions are developed by Neurotechnology [33].

Mobile technology also incorporates various biometric modalities. Devices with built-in fingerprint sensors exist on the market. One example is TouchID fingerprint technology developed for iPhone 5S by Apple, that incorporates a fingerprint module. Samsung also came up with fingerprint solution for its Samsung's Galaxy Tab S model as well as Samsung Galaxy S6 model. Vision based authentication solutions are allowed by all smartphones which integrate high resolution cameras into their hardware, facilitating third-parties to easily develop such software based authentication options. Other mobile or web-based biometric technology vendors include Applied Recognition with Ver-ID for various applications [34]. Notable, a facial biometric application has been recently released by IsItYou augmented with a unique anti-spoofing mechanism [35].

To address the interoperability among authentication devices a Fast IDentity Online (FIDO) Alliance was formed in 2012 [36], including powerful partners such as Google, Paypal, Miscrofsot, MasterCard, GitHub or DropBox. The alliance works towards creating secure interfaces between FIDO-enabled biometric devices and cloud-based website by developing dedicated plugins. FIDO is very active in defining web-based related biometric standards and a great impact is foreseen for macroeconomic application. Recently (November 2015), FIDO submitted to the World Wide Web Consortium three technical specifications with the purpose of defining a web-based API to be integrated into all web browsers and platform to facilitate a strong and secure authentication option.

## 4 Biometrics Attack

Similar to hacking a conventional authentication modality (password, token, etc), efforts have been made to hack or break a biometric authentication systems. A potential attack against a biometric system is possible for any component of the system. The network distributed (web-based) systems are more vulnerable to the attacks compared to the stand-alone biometric systems. This is due to the fact that, for a stand-alone biometric system, all processes are performed into a single processing unit. On the contrary, for physically disparate biometric systems, the attack may also occur in the transmission path, or any server performing the authentication.

The most common attack is the one against the sensor. When the samples acquisition process is fully automated (i.e. no watching guard exists to monitor the acquisition process) an impostor can easily bypass the system by simply presenting a copy of biometric data of a legitimate user in front of the sensor. The attempt of breaking the biometric system using such method is named spoofing attack. To date, there is no commercial biometric technology that is robust against such attacks.

The copy may come in various formats, depending on the biometric modality. In the case of facial biometric, the impostor may present a still image, video sequence playback, or even a 3D silica or rubber mask of the genuine user. A demonstration carried out by the Security

and Vulnerability Research Team of the University of Hanoi drawn attention regarding this issue by bringing evidence on how easy is to bypass the biometric systems namely Lenovo's Veriface III, Asus' SmartLogon V1.0.0005, or Toshibas Face Recognition version 2.0.2.32 - each set to its highest security level, using fake facial images of the valid user and thus gaining illegitimate access to the laptops [37]. This vulnerability was also tested in the spoofing challenge competition organized as special session at ICB 2013 [38]. These examples clearly point out the weaknesses of such systems and emphasize the necessity of incorporating reliable anti-spoofing mechanisms into the FA systems. Hence, not surprisingly, many research works were devoted to find robust solutions for detecting spoofing attacks. Within the same framework, a competition on counter measures to 2D facial spoofing attacks was also settled at ICB 2013 where anti-spoofing methods were evaluated [39]. The spoofing attack issue for various biometrics (face, iris, fingerprint, gait, etc) is a theme for the FP7 funded project TABULA RASA, where the topic was intensively and specifically addressed and analyzed [40]. Various solutions have been proposed to detect spoofing attacks. The spoof detection approaches may fall into four categories: a) challenge response based methods requiring user interaction, b) behavioral involuntary movements detection for parts of the face and head, c) data - driven characterization, and d) presence of special anti-spoofing devices. Google proposed a blinking based antispoofing mechanism [41].

The fingerprint modality can also be easily spoofed, as fingerprints are left behind on many objects the user touches. An impostor can use the same approach deployed by law enforcement agencies for lifting the fingerprints. Once lifted, a duplicate can be easily constructed from silicon or gelatin material. By so doing, in 2002, Matsumoto successfully fooled eleven different commercial fingerprint readers, with both optical and capacitive sensors, and some with live finger detection option, with a rate of success of 80% [42]. Matsumoto created a copy of a live finger as well as an artificial finger using a latent fingerprint left on a glass also accepted as genuine. Eleven years later (i.e. 2013), a biometrics hacking team of the Chaos Computer Club (CCC) has successfully bypassed the biometric security of Apple's TouchID implemented on iPhone 5S and Samsung Galaxy S5 [43]. Regarding Samsung's S5 biometric authentication system, the team claimed that not only it was possible to spoof the fingerprint authentication system, even after the device has been turned off, but the system also allows for seemingly unlimited authentication attempts without ever requiring a password, which was unacceptable. Two more years later, the vulnerability remains as it was reported at the Blackhat hacking conference in Las Vegas by Zhang et al. [44]. Similar to facial spoofing challenge competition, an iris and fingerprint based live detection competition is open [45]. The most recent report (2015) confirms the issue is still not solved, although some improvements exist [46].

Spoofing a real iris with a good quality image is also possible. Gupta et al. [47] used a commercial SDK, VeriEye [48] and successfully spoofed the system with printed images of iris.

Finally, voice impersonation can be applied to trick both automated and human verification for voice authentication systems [49]. A legitime user's voice can be recorded in various ways, including close proximity between the attacker and user, throughout a spam call or searching for audio-video recordings over the Internet. With the help of a voice morphing program, the attacker may synthesize the user's voice by using just a few samples. The cloned voice "borrowed" the features of the authentic voice and the authors successfully fooled the speaker authentication system that was based on the Bob Spear Speaker Verification System [50]. Their findings were alarming, i.e. the system was able to reject only 20 % of fake voices.

## 5 Attributes of Biometric Technology

The biometric systems and technologies is expected to posses several characteristics to be practically usable, as follows:

- Universality. This is the ability for a specific biometric system to be applied to a whole population of users. This is directly connected to Failure to Enroll (FTE) condition that refers to the case when a part of the population may not be enrolled for whatever reason. On particular reason is when the individual does not have the required biometric, leading to Failure to Enroll (FTA) error. A person suffering from mutism can not be enrolled with a speaker recognition technology; a fingerprint system can not be used for persons with missing fingers, etc.

- Uniqueness. The ability to successfully discriminate people. The biometric features must be as distinct as possible from one individual to another. The biometric features must convey large differences between individuals (large inter-class variability) while having small difference between samples taken from the same individual (small intra-class variability).

- Permanence. The ability of biometric features not to change over time. Some features do not change (iris, fingerprint patterns, vascular system, etc.) while others do (facial features). For time varying features a periodic biometric update is required.

- Collectibility. The ability of the system to perform the acquisition for any occasion (regardless of environment change, such as change in illumination, etc). There are cases where the acquisition process can not be performed for the same individual previously enrolled. For example, if the person suffers some skin condition destroying the epidermis or gets a serious scar on his finger, the fingerprint biometric authentication system will more likely output a false reject due to significant difference between the enroll and test biometric features. Similar scenario is possible for people suffering from cataract when tested with an iris authentication system, or people undergoing facial plastic surgery recovering from accidents or facial injury, when tested against a facial biometric system.

- Simplicity. Recording and transmission should be easy to use and not error-prone.

- Cost-efficiency. The whole process should be cost-efficient.

- Acceptability. The degree to which a biometric technology is found acceptable by the society. Typically, gross invasive biometric technologies (such as retina based systems) are tend to be less acceptable than those using non-invasive approaches (such as vision based or touchless sensors). Another aspect to be considered is the access to privacy.

- Scalability. This attribute refers to the ability of the system to accommodate a large number of enrollment individuals while providing a reasonable accuracy. The degree of scalability is application dependent. For instance, when using a biometric-based lock option for a mobile device with the intent to lock some specific applications inside the device, only one (device's owner) or a few individuals (perhaps family's members) would enroll. The matching is then either one-to-one or one-to-few type and the scalability is not an issue. On the contrary, for a network distributed system (such as bank application or decision systems) the number of enrolled individuals might easily reach millions and the system should cope with this overwhelming data. For such large-scale biometric application its performance (accuracy, FRR and FAR) is more critical. More exactly, one false rejection a month might be acceptable, but hundreds false rejection a day would be disastrous. The same rationale applies to FAR. Just to give a simple example, let us suppose a biometric system is 99.9% accurate. That is, if someone is an attacker, there is a 1-in-1000 chance that the biometric system fails to detect the attacker (outputs a false accept), while the same chance would be for a legitimate user to be denied as false attacker.

- Resilience. The ability of the system to handle exceptions. An example would be an individual whose biometric features might not be easily acquired. If a user has a broken arm, he may need human intervention to use a hand or fingerprint based biometric system.

- Circumventable. The ability of the system to detect attacks. An important role has the sensor that should be tamper-proof.

## 6    Biometric Standards

As noted throughout the chapter, a network distributed biometric technology involves several components, including the sensor, the communication channel, the web-based decisional server, components that rely on different hardware architecture. Not only the hardware is different but also the integrated software is different for each hardware configuration. Moreover, a fully operational system working on a specific operating system is not compatible with another operating system. Another representative example is provided by the multi-modal biometric systems relying on two or multiple biometric modalities (face, fingerprint, voice, as an example) that yield individual scores which are finally fused to output a single matching score. Without a common format that has to be shared among these modalities, the multi-modal biometric system can not operate. Finding mechanisms for each component of the biometric system to communicate has leaded to standardization. There are several working groups concerning biometric standards. At international level, the International Standard Organisation (ISO) and International Electrotechnical Commission (IEC) play a significant role. ISO and IEC have established a Joint Technical Committee 1 JTC 1/SC 37 [51] to ensure a high priority, focused, and comprehensive approach worldwide for the rapid development and approval of formal international biometric standards. There are several aspects to consider, including Data Interchange Formats, Data Structure Standard and Technical Interface Standards.

- *Data Interchange Format* represents the lowest level of interoperability between systems using the same modality and addresses the actual representation of the biometric data itself. The number and type of features can vary considerable depending upon the matching algorithm. There is a need to format these features so that the other components of the system may properly interpret the transmitted information.

- Once the data is formatted it needs to be transmitted. *Data Structure Standard* addresses this by providing the necessary wrapper around the biometric data within the so called *Common Biometric Exchange File Format* to facilitate interoperability between different systems or system components, forward compatibility for technology improvement, and software hardware integration. Data Interchange Format Standards provide the mechanism for extraction, matching and decision modules of the biometric system. The main component of this standard is the *Biometric Information Record* composed of three parts. The first part named the *Standard Biometric Header* contains information to an application regarding the format of and other properties of the next part named the *Biometric Data Block* that contains the biometric data conforming to a defined format. The third part named the *Security Block* provides information related to the encryption protocol and the integrity of the Biometric Information Record.

- *Technical Interface Standards* provide an Application Programming Interface (API) by defining the format for the Biometric Information Record so that components can understand and interpret records. A representative standard is BioAPI [52] that defines

a framework for installing the components, making them compliant with plug-and-play concept. BioAPI tries to hide as much as of unique attributes of individual biometric technologies, vendor implementations, products and devices. A *Biometric Service Provider* could then plug the components throughout a *Service Provider Interface*. An application can use biometric services using two fundamental ways: either through primitive functions or through abstract functions. Primitive functions are the most basic functions and relates to *BioAPI_Capture*, *BioAPI_Process*, *BioAPI_VerifyMatch* and *BioAPI_IdentifyMatch*. The abstract functions are defined by *BioAPI_Enroll*, *BioAPI_Verify* and *BioAPI_Identify*.

The standardization of biometric technology leaded to proper interoperability between and within biometric systems, ensuring a cost-effective technology implementation.

# 7 Conclusions

This paper only briefly touches the main issues of biometric systems and technologies, pointing out their differences, modalities, open problems and standardization. Their performance greatly vary upon the operating and external conditions as no universal biometric technology exists. The best performance is obtained where the technology is designed for strict controlled conditions and where data acquisition is accomplished under human supervision. Not mentioning a possible accuracy drop, when no human guard is present, a biometric system can be easily attacked and spoofed, a critical open issue yet to be solved. Intensive work is still undergoing to improve their performance while protecting them against various attacks.

# Bibliography

[1] S. K. Zhou, R. Chellappa, Ramalingam, W. Zhao (2006), *Unconstrained Face Recognition*, Springer.

[2] K. Delac, M. Grgic (Eds.) (2007), *Face Recognition*, I-Tech Education and Publishing, Vienna, Austria.

[3] K. Delac, M. Grgic, M. S. Bartlett (Eds.) (2008), *Recent Advances in Face Recognition*, IN-TECH, Vienna, Austria.

[4] M. Tistarelli, S. Z. Li, R. Chellappa (Eds.)(2009), *Handbook of Remote Biometrics for Surveillance and Security*, Springer.

[5] S. Z. Li, Stan, A. Jain (Eds.)(2011), *Handbook of Face Recognition*, Springer.

[6] M. D. Marsico, M. Nappi, M. Tistarelli (Eds.)(2014), *Face Recognition in Adverse Conditions*, IGI-Global.

[7] X. Chen, P. J. Flynn, K. W. Bowyer (2005), IR and Visible Light Face Recognition, *Computer Image and Vision Understanding*, 99(3): 332–358.

[8] S. G. Kong, J. Heo, B. R. Abidi, J. K. Paik, M. A. Abidi (2005), Recent Advances in Visual and Infrared Face Recognition: A Review, *Computer Image and Vision Understanding*, 97(1): 103–135.

[9] D. Socolinsky, L. Wolff, J. Neuheisel, C. Eveland (2001), Illumination Invariant Face Recognition Using Thermal Infrared Imagery, *Proc. of 2001 IEEE Conf. on Computer Vision and Pattern Recognition*, 1: 527-534.

[10] D. Socolinsky, A. Salgian, J. D. Neuheisel (2003), Face recogniton with visible and thermal infrared imagery, *Computer Image and Vision Understanding*, 91(1): 72–114.

[11] D. Socolinsky, A. Selinger (2004), Thermal face recognition in an operational scenario, *Proc. of 2004 IEEE Conf. on Computer Vision and Pattern Recognition*, 1012-1019.

[12] Y. Song, C. Lee, J. Kim (2004), A New Scheme for Touchless Fingerprint Recognition System, *Proc. of 2004 Intl Symposium on Intelligent Signal Processing and Communication Systems*, 524-527.

[13] E. Sano, T. Maeda, T. Nakamura, M. Shikai, M. Sakata, M. Matshusita, K. Sasakawa (2006), Fingerprint Authentication Device Based on Optical Characteristics Inside a Finger, *Proc. of 2004 IEEE Conf. on Computer Vision and Pattern Recognition Workshop*, DOI:10.1109/CVPRW.2006.83.

[14] G. Parziale, E. Diaz-Santana, R. Hauke (2006), The surround Imager: a multi-camera touchless device to acquire 3d rolled-equivalent fingerprints, *Proc. of the 2006 Intl Conf. on Advances in Biometrics*, 244-250.

[15] R. Smith (2002), *Authentication: From Passwords to Public Keys*, Addison and Wesley, Boston.

[16] J. Ashbourn (2000), *Biometrics: Advanced Identity Verification: The Complete Guide*, Springer, London.

[17] http://us.allegion.com/Products/biometrics/Pages/default.aspx

[18] J. Daugman (1994), *Biometric personal identification system based on Iris Recognition*, U.S. Patent 5,291,560.

[19] M. J. Northcott, J. E. Graves (2008), *Iris Imaging Using Reflection from the Eyes*, U.S. Patent Application 200800002863.

[20] G. Geterman, V. Jacobsen, J. Jelinek, T. Phinney, R. Jmza, T. Ahrens, G. Kilgore, R. Whillock, S. Bedros (2008), *Combined Face and Iris Recognition*, U.S. Patent Application 20080075334.

[21] http://www.cmu-biometrics.org/

[22] R. Das (2014), *Biometric Technology: Authentication, Biocryptography, and Cloud-Based Architecture*, CRC Press.

[23] N. Miura, A. Nagasaka, T. Miyatake (2004), Feature extraction of finger-vein patterns based on repeated line tracking and its application to personal identification, *Machine Vision and Applications*, 15(4): 194-203.

[24] R. D. Seely , M. Goffredo, J. N. Carter, M. S. Nixon (2009), View Invariant Gait Recognition, *Handbook of Remote Biometrics for Surveillance and Security*, 61-81.

[25] J. Ilonen (2003), Keystroke dynamics, http://www2.it.lut.fi/kurssit/03-04/010970000/seminars/Ilonen.pdf.

[26] R. Giot, M. El-Abed, C. Rosenberger (2009), Keystroke dynamics authentication for collaborative systems, *Intl. Symposium on Collaborative Technologies and Systems*, 172-179.

[27] P. Bours (2012), Continuous keystroke dynamics: A different perspective towards biometric evaluation, *Information Security Techn. Report Volume* 17(1-2): 36-43.

[28] C. Shen, Z. Cai, X. Guan, Y. Du, T. Yu (2013), User Authentication Through Mouse Dynamics, *IEEE Trans. on Information Forensics and Security* 8(1): 16-30.

[29] Z. Saquib, N. Salam, R. P. Nair, N. Pandey, A. Joshi (2010), A Survey on Automatic Speaker Recognition Systems, *Signal Processing and Multimedia*,134-145.

[30] The Global Biometrics and Mobility Report: The Convergence of Commerce and Privacy Market Analysis and Forecasts 2014 to 2020, Available at: http://www.acuity-mi.com/GBMR_Report.php, Accessed on 12 Dec. 2015.

[31] `https://www.truekey.com/` Accessed on 14 Dec. 2015.

[32] `http://www.sensory.com/products/technologies/trulysecure/`, Accessed on 14 Dec. 2015.

[33] `http://www.neurotechnology.com/`

[34] `http://appliedrec.com/`

[35] `http://www.isityou.biz/`

[36] `https://fidoalliance.org/`

[37] N. M. Duc and B. Q. Minh (2009), Your face is NOT your password, *Black Hat Conference.*

[38] `http://www.tabularasa-euproject.org/evaluations/tabula-rasa-spoofing-challenge-2013/`

[39] `http://www.biometrics-center.ch/testing/tabula-rasa-spoofing-challenge-2013`

[40] `http://www.tabularasa-euproject.org/`

[41] `http://www.google.com/patents/US8437513`, Accessed on 17 Dec. 2015.

[42] T. Matsumoto, H. Matsumoto, K. Yamada, S. Hoshino (2002), Impact of Artificial Gummy Fingers on Fingerprint Systems, *Proc. of SPIE*, Vol. 4677, Optical Security and Counterfeit Deterrence Techniques IV, 2002.

[43] `https://www.ccc.de/en/updates/2013/ccc-breaks-apple-touchid`

[44] Y. Zhang,Z. Chen, H. Xue, T. Wei (2015), Fingerprints On Mobile Devices: Abusing and Leaking, *Black Hat Conference.*

[45] `http://livdet.org/`

[46] V. Mura, L. Ghiani, G. L. Marcialis, F. Roli, D. A. Yambay, S. A. Schuckers (2015), LivDet 2015 Fingerprint Liveness Detection Competition 2015, Available at: `http://livdet.org/reports.php`

[47] P. Gupta, S. Behera, M. Vatsa, R. Singh (2014), On Iris Spoofing Using Print Attack, *Proc. of the 2014 22nd Intl Conf. on Pattern Recognition*, 1681-1686.

[48] VeriEye, Iris recognition software, `http://www.neurotechnology.com/verieye.html`

[49] D. Mukhopadhyay, M. Shirvanian and N. Saxena (2015), All Your Voices Are Belong to Us: Stealing Voices to Fool Humans and Machines, *European Symposium on Research in Computer Security.*

[50] E. Khoury, L. El Shafey, S. Marcel (2014), Spear: An open source toolbox for speaker recognition based on Bob, *IEEE Intl. Conf. on Acoustics, Speech and Signal Processing (ICASSP).*

[51] `http://www.iso.org/iso/home/store/catalogue_tc/catalogue_tc_browse.htm?commid=313770&published=on`

[52] `http://www.iso.org/iso/catalogue_detail.htm?csnumber=33922`

# Biomedical Image Registration by Means of Bacterial Foraging Paradigm

H. Costin, S. Bejinariu, D. Costin

**Hariton Costin**
[1]Faculty of Medical Bioengineering Grigore T. Popa University of Medicine and Pharmacy, Iaşi, Romania
[2]Institute of Computer Science of Romanian Academy Iaşi Branch, Romania
hncostin@mail.umfiasi.ro

**Silviu Bejinariu**
[2]Institute of Computer Science of Romanian Academy Iaşi Branch, Romania
silviu.bejinariu@iit.academiaromana-is.ro

**Diana Costin\***
[3]Faculty of Medicine, Grigore T. Popa University of Medicine and Pharmacy, Iaşi, Romania
*Corresponding author: diana.costin@umfiasi.ro

**Abstract:** Image registration (IR) is the process of geometric overlaying or alignment of two or more 2D/3D images of the same scene (unimodal registration), taken or not at different time slots, from different angles, and/or by different image acquisition systems (multimodal registration). Technically, image registration implies a complex optimization of different parameters, performed at local or/and global level. Local optimization methods often fail because functions of the involved metrics with respect to transformation parameters are generally nonconvex and irregular, and global methods are required, at least at the beginning of the procedure. This paper presents a new evolutionary and bio-inspired robust approach for IR, Bacterial Foraging Optimization Algorithm (BFOA), which is adapted for PET-CT multimodal and magnetic resonance image rigid registration. Results of optimizing the normalized mutual information and normalized cross correlation similarity metrics validated the efficacy and precision of the proposed method by using a freely available medical image database.

**Keywords:** medical imaging, image registration, soft computing, evolutionary strategies, bacterial foraging algorithm, global optimization.

## 1 About Multimodal Image Registration

Image registration (IR) is a fundamental task in computer vision used to find either a spatial *transformation* (e.g., rotation, translation, etc.) or a correspondence (matching of similar image entities) among two (or more) images taken under different conditions (at different times, using different sensors, from different viewpoints, or a combination of them), with the aim of overlaying such images into a common one [1], [2], [3], [4]. Over the years, IR has been applied to a broad range of situations from remote sensing to medical images or artificial vision and CAD systems, and different techniques have been independently studied resulting in a large body of research.

IR methods can be classified in two groups according to the nature of images: *pixel/voxel-*based IR methods (also called *intensity*-based), where the whole image is considered for the registration process; and, on the other side, *feature*-based methods, which consider prominent information extracted from the images, being a reduced subset of them. The latter methods take advantage of the lesser amount of information managed in order to overcome the problems found in the former when the images present some inconsistences to deal with, for example,

regardless of changes in the geometry of the images, radiometric conditions, and appearance of noise and occlusion. These features correspond to *geometric primitives* (points, lines, surfaces, etc.) which are invariant to the transformation to be considered between the input images. Moreover, the latter methods perform faster than the former ones due to the reduced amount of data they take into account, at the expense of achieving *coarse* results. Likewise, IR is the process of finding the optimal spatial transformation (e.g., rigid, similarity, affine, etc.) achieving the best overlaying between two (or more) different images named *scene and model images* (Figure 1). They both are related with the specific transformation, measured by a *similarity metric function.* Such transformation estimation is interpreted into an iterative optimization procedure in order to properly explore the search space. Two search approaches have been considered in the IR literature: *matching-based*, where the optimization problem is intended to look for a set of correspondences of pairs of those more similar image entities in both the scene and the model images, from which the registration transformation is derived; and the *transformation parameter-based*, where the strategy is to directly explore inside each range of the transformation parameters. Both strategies can be used with either a voxel-based or a feature-based approach.

Specific aspects such as the presence of noise, image discretization, different amplitudes in the scale of the IR transformation parameters, the magnitude of the transformation to be estimated cause difficulties for traditional local optimizers (gradient- and nongradient-based) and they become prone to be trapped in local minima. As a consequence, global methods are preferred, at least at the beginning of the IR process. As for image segmentation procedure, there is not a universal design for an IR method that could be applicable to all registration tasks, since various considerations on the particular application must be taken into account.

In recent years a lot of studies and papers were dedicated to medical IR, with more or less good results [5], [6], [7], [8], [9], [10], [11], [12], [13], [14], [15], [16], [15], [16], [17]. Thus, e.g. rigid 3D transformations were performed, e.g., by Alpert [18] using the images principal axes and center of gravity. Affine registration was obtained by Wahl [21], employing user identified anatomical landmarks and external markers, and Maguire et al. [22], who optimized cross-correlation around such user identified anatomical landmarks and external markers. In [11] a robust surface registration using a Gaussian-weighted distance map (GWDM) for PET-CT brain fusion was proposed. A similarity measure was evaluated repeatedly by weighted cross-correlation (WCC).

## 1.1  Transformations

The IR methods can also be classified according to the registration transformation used to relate both the scene and the model images. The first category of transformation models includes *linear transformations*, which preserves the operations of vector addition and scalar multiplication, being a combination of translation, rotation, global scaling, and shear components. The most common linear transformations are rigid, similarity, affine, projective, and curved. Linear transformations are global in nature, thus not being able to model local deformations. The second category of transformation models includes *elastic* and *nonrigid* transformations, which allow local warping of image features, thus providing support for local deformations.

## 1.2   Similarity Metric

The similarity metric is a function $F$ that measures the goodness of a given registration solution, that is, of a registration transformation $f$. The final performance of any IR method strongly depends on its accurate estimation. Each solution is evaluated by $F$ applying such transformation f on one of the two images, usually to the scene image ($f(I_s)$). Next, the degree of closeness or fitting between the transformed scene and the model images, $\Psi(\cdot)$ must be determined

$$F(I_s, I_m, f) = \Psi(f(I_s), I_m) \tag{1}$$

The main approaches trying to estimate the function $\Psi(\cdot)$ depend on the dimensionality (2D or 3D) and the nature of the considered images. There are: (a) voxel-based approach: sum of squared differences, normalized cross-correlation (i.e., correlation coefficient or phase correlation), and mutual information; (b) feature-based approach: feature values-based metrics (i.e., registration based on the curvature) and distance between corresponding geometric primitives.

Unfortunately, the $F$ function is affected by both the discretization of images and the presence of noise, yielding worse estimations and favoring the IR to get trapped in local minima.

## 1.3   Search Space Strategies

The IR process performs an iterative exploration to obtain that optimal transformation $f$. So, the closer $f$ to the unknown global optimum, the better the fitting (measured by the similarity metric $F$) between scene and model. The optimization process considered to obtain those solutions can be deterministic or stochastic (either a global or a local one).

Although the final registration problem solution consists of the right values for the parameters which determine f, we can distinguish two different strategies to solve the problem, each of them working in a different solution space: (i) the first searches in the *matching space* to obtain a set of correspondences of pairs of the most similar image entities in both the scene and the model images, from which the registration transformation is derived; (ii) the second directly makes a search in the space of the f parameters guided by the F function, called *transformation parameters* space. The matching-based search space exploration usually consists of the two following stages: first, a set of correspondences with those more similar regions of pixels (voxel-based) or geometric primitives (feature-based) in both the scene and the model images must be computed; second, the transformation f is assessed by numerical methods considering the previous matching.

On the contrary, transformation parameters-based search space involves directly searching for the solution in the space of parameters of the transformation $f$. In this respect, each solution to the IR problem is encoded as a vector composed of the values for the parameters of $f$, and the IR method generates possible vectors of parameter values, that is, possible registration transformations. As a consequence, the search space exploration is guided by the similarity metric $F$. In this way, each solution vector is evaluated by the chosen metric, and the IR problem becomes a parameter optimization procedure of finding the best values of $f$ that maximize the similarity metric $F$. Other classification divides search strategies in *local* and *global* ones. Local optimization techniques frequently fail because functions of these metrics with respect to transformation parameters are generally nonconvex and irregular and, therefore, global methods – such as those based on evolutionary algorithms – are often required.

# 2   Optimization using BFOA

In recent years, the application of several well-known *evolutionary algorithms* (*EAs*) [23] to the IR optimization process has introduced an outstanding interest in order to solve those

problems due to their global optimization techniques nature. The first attempts to solve IR using evolutionary computation can be found in the early eighties, when Fitzpatrick et al. [24] proposed such approach based on a genetic algorithm for the 2D case and applied it to angiographic images. Since then, several evolutionary approaches have been proposed to solve the IR problem, mainly in connection with the transformation parameters-based search space, as shown e.g. in [25], [1], [26], [27], [28], [29], [30]. The main reason of using global optimization techniques, such as EAs-based algorithms for IR, is that they may not require an optimum solution to achieve high accuracy of registration.

Introduced by Passino [31], [32], bacterial foraging paradigm is a bio-inspired optimization method based on the foraging model. This paradigm belongs to the broader class of distributed nongradient global optimization. A foraging animal takes actions to maximize the energy obtained per unit time spent foraging, E/T, in the face of constraints presented by its own physiology (e.g., sensing and cognitive capabilities) and environment (e.g., density of prey, risks from predators, physical characteristics of the search area). In other words, these social animals, like E. coli – a bacterium, try to maximize their long-term average rate of energy intake.

Prominent applications in medical image processing are related to edge detection [33], image segmentation [19], [20], but also for image registration [36], [37], knowing that these procedures may be viewed as optimization tasks.

## 2.1 BFO Algorithm

The bacterial foraging paradigm is suitable as model for optimization algorithms because animals/bacteria behavior is to search for nutrients and avoid noxious substances to maximize their energy. As in all evolutionary models, individuals with a good strategy to find nutrients are replicated and those having poor foraging strategy are eliminated. In contrast to genetic algorithms and evolutionary strategies, which exploit the competitive characteristics of biological evolution (e.g., survival of the fittest), bacterial foraging (BF) exploits cooperative and social aspects of animal colonies (like E. coli bacterium) in their attempts to obtain nutrients that maximizes energy intake per unit time spent for foraging.

Each member of the bacteria colony is characterized by its position in the $n$-dimensional space which is a possible solution of the optimization problem. The solution is computed as the position in which a bacterium is in the best healthy state or has the lowest cost value. During foraging, the bacteria colony (swarm) proceeds through four foraging steps: chemotaxis, swarming, reproduction and elimination-dispersal.

Let's consider a bacteria colony with $S$ individuals; $P(j, k, l) = \{\theta^t(j, k, l), i = 1...S\}$ is the position of colony members in the $j^{th}$ chemotactic step, $k^{th}$ is the $k$-th reproduction step and $l^{th}$ – the $l$-th elimination-dispersal step; $J(i, j, k, l)$ denotes the cost of the $i^{th}$ bacterium in position $\theta^t(j, k, l)$.

- *Chemotaxis*: E. Coli bacteria have two types of movements: tumble and swim. The chemotactic step is defined as a tumble followed by a tumble or a tumble followed by a run. In the chemotactic step each bacterium changes its position to: $\theta^t(j + 1, k, l) = \theta^i(j, k, l) + C(i)\varphi(i)$, where $C(i)$ is the size of the chemotactic step and is a unit length random generated direction [4]. If the cost computed in the new position is lower than in the previous position, then the swim is continued in the same direction as long as the cost is reduced but not more than a maximum number of steps.

- *Swarming*: In case the bacteria have the ability to signal to others the existence of a favorable or poisonous environment, they will tend to swarm together in the direction of nutrients. The cell to cell attraction or rejection is modeled by adding to the cost function $J(i, j, k, l)$ computed for a specific bacterium, components computed as function of the status of all the other bacteria in the colony.

- *Reproduction*: All bacteria reach the reproduction state after a number of chemotactic steps. The healthy state is computed for all bacteria and it may be expressed as the total quantity of accumulated nutrients or simply by the value of the cost function in the current position. The least healthy bacteria die while and to keep constant the size of the colony, an equal number of healthier bacteria split into two bacteria without mutation.
- *Elimination and Dispersal*: After a number of reproduction steps, some bacteria are dispersed into the environment (moved in a random position) with a specified probability, without taking into account their healthy state.

BFOA starts with a colony of $S$ bacteria placed in randomly generated positions. The evolutionary process goes through $N_{ed}$ elimination/dispersal steps, each of these consists of $N_{re}$ reproduction steps. Each reproduction step consists of $N_c$ chemotactic steps. In each chemotactic step a bacterium may do at most $N_s$ swimming steps if the value of the cost function decreases. The position in which a bacterium has the greatest healthy status is the solution of the optimization problem. In case of image registration, the size of the search space is equal to the number of parameters of the geometric transform and as healthy status is used the value of a measure that evaluates the similarity between the transformed source image and the model image.

## 2.2 Parallel Version of BFO Algorithm

A closer look at BFOA reveals that it contains 4 nested loops: elimination/dispersal, reproduction and chemotaxis for each bacterium in the colony. The body of the inner loop is executed $N_{ed} \times N_{re} \times N_C \times S$ times, which may be a fairly large number. In the examples presented in the next sections, it is executed 256000 times, but the cost function evaluation is performed about 600000 times due to the fact that each bacterium may perform more swim steps in a single chemotactic step.

We propose a parallelization based on the shared memory model that is suitable for multi-core processor based systems. It must be noticed that in this case the number of available processors is reduced $(2, 4$ or $8)$. An excessive tasks partitioning obviously leads to poor performances due to the large number of synchronization operations.

If we consider to not use the attractant/repellant effect in the optimization algorithm, then the calculations performed for each individual bacterium in the inner loop are independent excepting the test in which the best value of the cost function is checked. So, we can execute in parallel a chemotactic step for all bacteria, taking care to not simultaneously call the function to check for the best value of the cost function.

# 3 Pixel Based Image Registration

The proposed IR procedures use the Normalized Mutual Information and Normalized Cross Correlation as measures to evaluate the quality of the registration process.

Our study approaches the *rigid body image registration*, which initially determines global alignment, followed by local elastic registration. Let $\mathbf{T}$ denote the spatial transformation that maps features or coordinates (spatial locations) from one image or coordinate space to another image or coordinate space. Let $\mathbf{p}_A$ and $\mathbf{p}_B$ denote coordinate points (pixel locations) in images $A$ and $B$, respectively. The image registration problem is to determine $T$ so that the mapping $\mathbf{T} : \mathbf{p}_A \to \mathbf{p}_B \Leftrightarrow \mathbf{T}(\mathbf{p}_A) = \mathbf{p}_B$ results in the "best" alignment of $A$ and $B$. For 3-D rigid body registration, the mapping of coordinates $\mathbf{p} = [x, y, z]^T$ into $\mathbf{p'} = [x', y', z']^T$ can be formulated as a matrix multiplication in homogeneous coordinates, as shown in equation (2) in an explicit manner. That is, the goal of the optimization is to determine the parameters $t_x, t_y, t_z, \alpha, \beta,$ and

$\gamma$ in (2). Usually, optimization in image registration means to maximize similarity. Similarity metric values, as functions of transformation parameters, refer to the *objective function*, denoted as $f(\mathbf{x})$. Alternatively, one may formulate the image registration as a minimization problem and, thus, the goal is to minimize $-f(\mathbf{x})$. Although there is yet no proof for its optimality, because of its robustness (usually it attains its maximum at correct alignment) and good results in previous works, normalized mutual information was selected as the similarity measure in our study. Moreover, it is still generally non-smooth and prone to local optima. For this reason, global optimization approaches are preferred.

$$\begin{bmatrix} p' \\ 1 \end{bmatrix} = \mathbf{T} \begin{bmatrix} p \\ 1 \end{bmatrix} \Leftrightarrow$$

$$\begin{bmatrix} x' \\ y' \\ z' \\ 1 \end{bmatrix} = \begin{bmatrix} \cos\beta\cos\gamma & \cos\alpha\sin\gamma + \sin\alpha\sin\beta\cos\gamma & \sin\alpha\sin\gamma - \cos\alpha\sin\beta\cos\gamma & t_x \\ -\cos\beta\sin\gamma & \cos\alpha\cos\gamma - \sin\alpha\sin\beta\sin\gamma & \sin\alpha\cos\gamma - \cos\alpha\sin\beta\sin\gamma & t_y \\ \sin\beta & -\sin\alpha\cos\beta & \cos\alpha\cos\beta & t_z \\ 0 & 0 & 0 & 1 \end{bmatrix} \begin{bmatrix} x \\ y \\ z \\ 1 \end{bmatrix} \quad (2)$$

## 3.1 Normalized Mutual Information

Mutual Information ($MI$) and Normalized Mutual Information ($NMI$) evaluate the relative independence of two images and do not depend on the specific dynamic range or intensity scaling of the images [1], [10]:

$$MI(A, B) = H(A) + H(B) - H(A, B) \tag{3}$$
$$NMI(A, B) = (H(A) + H(B))/H(A, B), \tag{4}$$

where $H(A)$, $H(B)$ are the image entropies and $H(A, B)$ is the joint entropy of the two images. High values of mutual information indicate high dependence between images. Because the goal of the optimization algorithms is to minimize a cost function, the value of $(-1) * NMI$ will be used to evaluate the quality of a certain solution. In the cost function evaluation, the geometric transform corresponding to the current solution is applied to the source image and then the $NMI$ value is computed for the model image and the transformed source image. The area based IR implementations are time consuming because each cost evaluation requires a geometric transform to be applied and also image and matrix operations to compute $NMI$.

## 3.2 Normalized Cross Correlation

Cross correlation is used for estimating the degree to which two series are correlated. One of the most encountered applications of the normalized cross correlation is to determine the position of a template sub-image $B$ in a source image $A$. The normalized cross correlation (NCC) is computed by

$$NCC(i, j) = \frac{\Sigma_{\bar{i}}\Sigma_{\bar{j}} A(i + \bar{i}, j + \bar{j}) \cdot B(\bar{i}, \bar{j})}{\sqrt{\Sigma_{\bar{i}}\Sigma_{\bar{j}} B(\bar{i}, \bar{j})^2} \cdot \sqrt{\Sigma_{\bar{i}}\Sigma_{\bar{j}} A(i + \bar{i}, j + \bar{j})^2}}. \tag{5}$$

The problem is to determine the position of a given pattern in a two dimensional image $f$. Let $f(x, y)$ denote the intensity value of the image $f$ of size $M_x \times M_y$ at the point $(x, y)$, $x \in \{0, \ldots, M_x - 1\}$, $y \in \{0, \ldots, M_y - 1\}$. The pattern is represented by a given template $t$ of size $N_x \times N_y$. A common way to calculate the position $(u_{pos}, v_{pos})$ of the pattern in the image $f$ is to evaluate the normalized cross correlation value $\gamma$ at each point $(u, v)$ for $f$ and template

$t$, which has been shifted by $u$ steps in the $x$ direction and by $v$ steps in the $y$ direction. The following equation gives a basic definition for the normalized cross correlation coefficient

$$\gamma = \frac{\Sigma_{x,y}(f(x,y) - \overline{f_{u,v}})(t(x-u,y-v) - \bar{t})}{\sqrt{\Sigma_{x,y}(f(x,y) - \overline{f_{u,v}})^2 \Sigma_{x,y}(t(x-u,y-v) - \bar{t})^2}}, \tag{6}$$

where $(\overline{f_{u,v}})$ denotes the mean value of $f(x,y)$ within the area of the template t shifted to $(u,v)$, which is computed by:

$$(\overline{f_{u,v}}) = \frac{1}{N_x N_y} \sum_{x=u}^{u+N_x-1} \sum_{y=v}^{v+N_y-1} f(x,y). \tag{7}$$

With similar notation, $\bar{t}$ is the mean value of the template $t$. The denominator in (6) is the variance of the zero mean image function $f(x,y) - \overline{fu,v}$ and the shifted zero mean template function $t(x-u, y-v) - \bar{t}$. Due to this normalization, $\gamma(u,v)$ is independent to changes in brightness or contrast of the image, which are related to the mean value and the standard deviation.

## 4 Experiments and Results

The BFOA based image registration procedure was tested on a large set of DICOM medical images from a database at the address `http://www.osirix-viewer.com/datasets/` [39]. In Figure 1 below, information about some test images are shown.
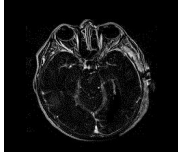
| Image | Description: | |
|---|---|---|
| | File : | img_1.tif |
| | Size : | $256 \times 256 \times 8b$ |
| | Name : | PETCETIX |
| | Modality : | PET-CT |
| | Description: | Whole body FDG PET-CT study |
| | | in a patient with abdominal lymphoma. |
| | File: | img_2.tif |
| | Size: | 256 x 256 x 8b |
| | Name: | BRAINIX |
| | Modality: | MR |
| | Description: | Brain tumor. |
| | File: | img_3.tif |
| | Size: | 256 x 256 x 8b |
| | Name: | WRIX |
| | Modality: | MRI |
| | Description: | Scaphoid fracture. T1 / STIR fusion. |

Figure 1: Test images used in the experiment

In the experiment, 4 images were used: $\text{img}\_1, \text{img}\_2, \text{img}\_2{}_{\text{H}}\text{istEq}$ (that was obtained by applying the histogram equalization to img_2 having low contrast), and img_3.

The source images were obtained by applying a rotation (angle $\theta = 10°$) against the rotation center ($c_x = -20$ and $c_y = 20$) followed by an isotropic scaling ($scale = 1.2$). The transform matrix is:

$$T = \begin{bmatrix} \alpha & \beta & (1-\alpha)c_x - \beta c_y \\ -\beta & \alpha & \beta c_x + (1-\alpha)c_y \\ 0 & 0 & 1 \end{bmatrix} \tag{8}$$

where $\alpha = \text{scale} \cdot \cos\theta$ and $\beta = \text{scale} \cdot \sin\theta$. The actual value of the transform matrix is

$$T = \begin{bmatrix} 1.1818 & 0.2084 & -0.5322 \\ -0.2084 & 1.1818 & -7.8029 \\ 0 & 0 & 1 \end{bmatrix} \tag{9}$$

The inverse transform matrix is $T^{-1} = \begin{bmatrix} 0.8207 & -1.1477 & -0.6924 \\ 1.1447 & 0.8207 & 6.4807 \\ 0 & 0 & 1 \end{bmatrix}$ that corresponds to an

affine transform with the following parameters: $\theta' = -10°$, $c_x' = -20$, $c_y' = 20$ and $scale' = 0.8333$. The search space for the optimization problem is $R^4$.

The BFO parameters values used in the experiment are:

Colony size, $S = 400$; Number of chemotactic steps, $N_c = 20$; Maximum number of swim steps, $N_s = 10$; Number of reproduction steps, $N_{re} = 16$; Number of elimination/dispersal steps, $N_{ed} = 2$; Probability of dispersal, $P_{ed} = 0.25$; Length of the move $step = 0.001$.

As it can be observed in Figure 1 the test images have the same size but are different in terms of contrast. It was expected that the image contrast affects the quality of the registration process, and this assumption was found to be true.

In vision, *contrast* is the difference in luminance that makes an object distinguishable. The test images we used in this paper were not analyzed for their content (i.e., it is a context-free registration), so the contrast and his evaluation was performed by means of the histogram of the images.

Root *mean square contrast* is computed as standard deviation of pixel values. It does not depend on the spatial frequency or spatial distribution in the image.

$$Contrast_{RMS} = \sqrt{\tfrac{1}{MN}\sum_{i=1}^{N}\sum_{j=1}^{M}(I(i,j) - I_{avg})^2}, \tag{10}$$

where $M, N$ are the image dimensions, $I(i,j)$ is the image pixel at $(i,j)$ coordinates and $I_{avg}$ is the average of pixel values in image $I$.

*Visibility (Michelson contrast)* is represented by formula

$$Contrast_{Michelson} = \frac{I_{\max} - I_{\min}}{I_{\max} + I_{\min}}, \tag{11}$$

where $I_{\min}$ and $I_{\max}$ are the lowest and highest pixel values in image $I$, respectively.

Contrast values computed for the tested model images are described in Table 1.

Table 1: Contrast values computed for the test images

| Image | Gray values | | | Contrast | |
|---|---|---|---|---|---|
| | min | max | average | Michelson | RMS |
| img_1 | 0 | 255 | 56.7 | 1.0 | 0.27 |
| img_2 | 0 | 146 | 6.0 | 1.0 | 0.05 |
| img_2_HistEq | 0 | 255 | 74.7 | 1.0 | 0.35 |
| img_3 | 19 | 238 | 39.7 | 0.85 | 0.15 |

For image_2.tif with initial low contrast a histogram equalization procedure was performed and image named img_2_HistEq was obtained. The source images were obtained by applying the affine transform specified above followed by salt-and-pepper and Gaussian noise alteration.

The Signal-To-Noise Ratio was computed using the formula below and is shown in Table 2.

$$SNR = 10 \log \frac{\sum_{i=1}^{N} \sum_{j=1}^{M} I(i,j)^2}{\sum_{i=1}^{N} \sum_{j=1}^{M} (I(i,j) - I_{noise}(i,j))^2} dB, \qquad (12)$$

Table 2: Signal-to-Noise Ratio (SNR) values for testimages with noise

| | Gray values | | | Contrast | |
|---|---|---|---|---|---|
| Image | min | max | average | Michelson | RMS |
| img_1 | 0 | 255 | 56.7 | 1.0 | 0.27 |
| img_2 | 0 | 146 | 6.0 | 1.0 | 0.05 |
| img_2_HistEq | 0 | 255 | 74.7 | 1.0 | 0.35 |
| img_3 | 19 | 238 | 39.7 | 0.85 | 0.15 |

The registered images for test image img_1 are shown in Figure 2.
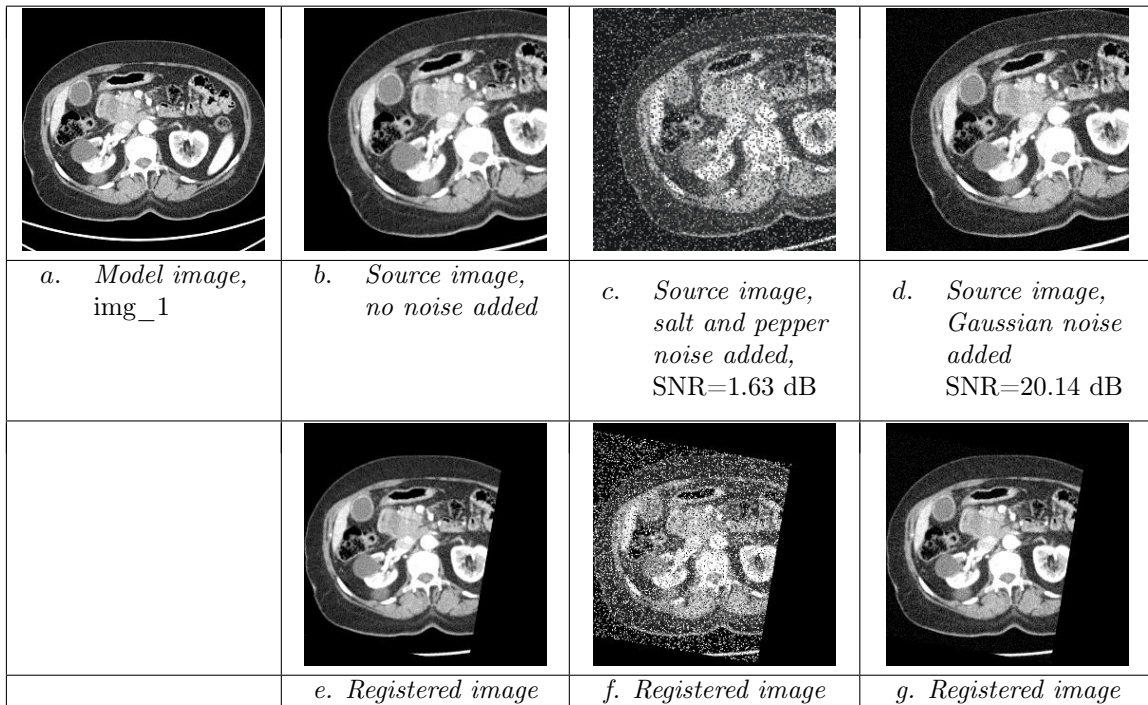


Figure 2: Registered images for test image img_1

In Table 3, the columns NMI/Expected and NCC/Expected contain respectively the values of Mutual Information and Normalized Cross Correlation computed for the model image and the image obtained by applying the inverse affine transform on the source images. The NMI/Computed and NCC/Computed contain respectively the Mutual Information and Normalized Cross Correlation computed for the model image and the registered image obtained by applying the approximated affine transform. The first 3 rows in Table 3 contain the values obtained using MI as similarity measure while the last 3 rows contain the results obtained by using NCC as similarity measure in the registration evaluation.

Table 3: Image registration results obtained for test image img_1

| Similarity | Added Noise, SNR | NMI | | NCC | | Computed inverse transform | | | |
|---|---|---|---|---|---|---|---|---|---|
| | | Expected | Computed | Expected | Computed | $c_x$ | $c_y$ | $\theta$ | scale |
| NMI | - | 1.255 | 1.215 | 0.896 | 0.893 | -24.963 | 20.101 | -9.708 | 0.834 |
| | S&P, 1.63 dB | 1.129 | 1.119 | 0.782 | 0.780 | -25.270 | 19.444 | -9.657 | 0.834 |
| | Gaussian, 20.14 dB | 1.199 | 1.188 | 0.894 | 0.892 | -23.730 | 19.062 | -9.783 | 0.835 |
| NCC | - | 1.255 | 1.205 | 0.896 | 0.892 | -26.209 | 19.702 | -9.625 | 0.835 |
| | S&P, 1.63 dB | 1.128 | 1.119 | 0.784 | 0.783 | -25.773 | 20.007 | -9.630 | 0.834 |
| | Gaussian, 20.14 dB | 1.199 | 1.182 | 0.894 | 0.891 | -25.538 | 21.529 | -9.597 | 0.834 |

In the case of the image drawn in Figure 2, it must be noticed that in all cases the value of the similarity measure computed for the registered image does not exceed the expected value. This happens because the image histogram is uniform (the gray levels are more uniformly distributed in the image), even if there does exist a considerable number of black pixels. Accordingly, the results obtained using the two similarity measures are quite similar.

Similarly, registered images for test image img_2 are depicted in Figure 3.



| a. Model image, img_2 | b. Source image, no noise added | c. Source image, salt and pepper noise added, SNR=-15.04 dB | d. Source image, Gaussian noise added SNR=5.76 |
|---|---|---|---|
| | e. Registered image | f. Registered image | g. Registered image |
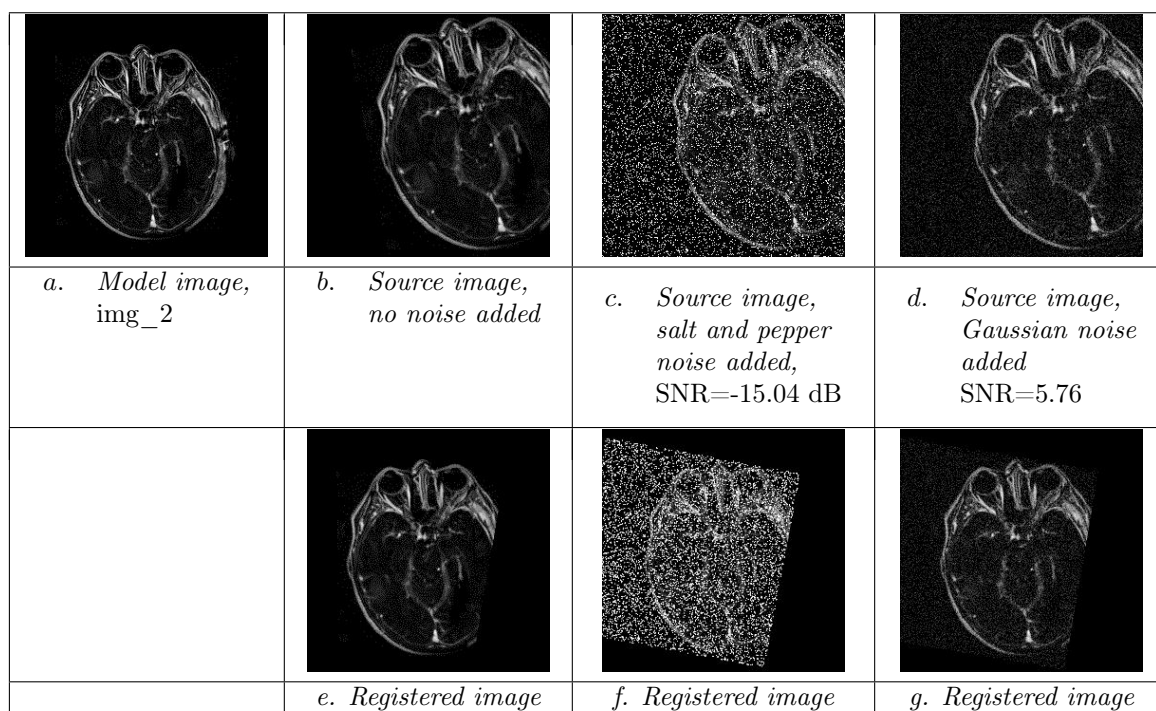
Figure 3: Registered images for test image img_2

In the case of test image img_2, even if the image has a low contrast, the IR result is also good. The image contrast is $Contrast_{RMS} = 0.05$ (a very low value) and in all cases the similarity measure error is less than $1/1000$, so the proposed BFOA-based IR method works well in case of low contrast images. Moreover, for very noisy images (SNR as low as $-15.04dB$) this method also works very well, as shown in Figures 3 $(f, g)$.

Table 4: Image registration results obtained for test image img_2

| Similarity | Added Noise, SNR | NMI Expected | NMI Computed | NCC Expected | NCC Computed | Computed inverse transform $c_x$ | $c_y$ | $\theta$ | scale |
|---|---|---|---|---|---|---|---|---|---|
| NMI | - | 1.226 | 1.187 | 0.923 | 0.916 | -25.026 | 19.450 | -9.684 | 0.835 |
| | S&P, -15.04 dB | 1.110 | 1.101 | 0.849 | 0.845 | -24.837 | 20.368 | -9.668 | 0.834 |
| | Gaussian, 5.76 | 1.198 | 1.174 | 0.922 | 0.917 | -24.008 | 18.941 | -9.771 | 0.835 |
| NCC | - | 1.226 | 1.176 | 0.923 | 0.914 | -26.053 | 19.905 | -9.607 | 0.836 |
| | S&P, -15.04 dB | 1.111 | 1.101 | 0.850 | 0.846 | -24.638 | 21.124 | -9.677 | 0.834 |
| | Gaussian, 5.76 | 1.198 | 1.196 | 0.922 | 0.922 | -20.056 | 19.796 | -9.991 | 0.834 |



a.   Model image, img_3
b.   Source image, no noise added
c.   Source image, salt and pepper noise added, SNR=-2.28 dB
d.   Source image, Gaussian noise added SNR=15.80

e. Registered image
f. Registered image
g. Registered image
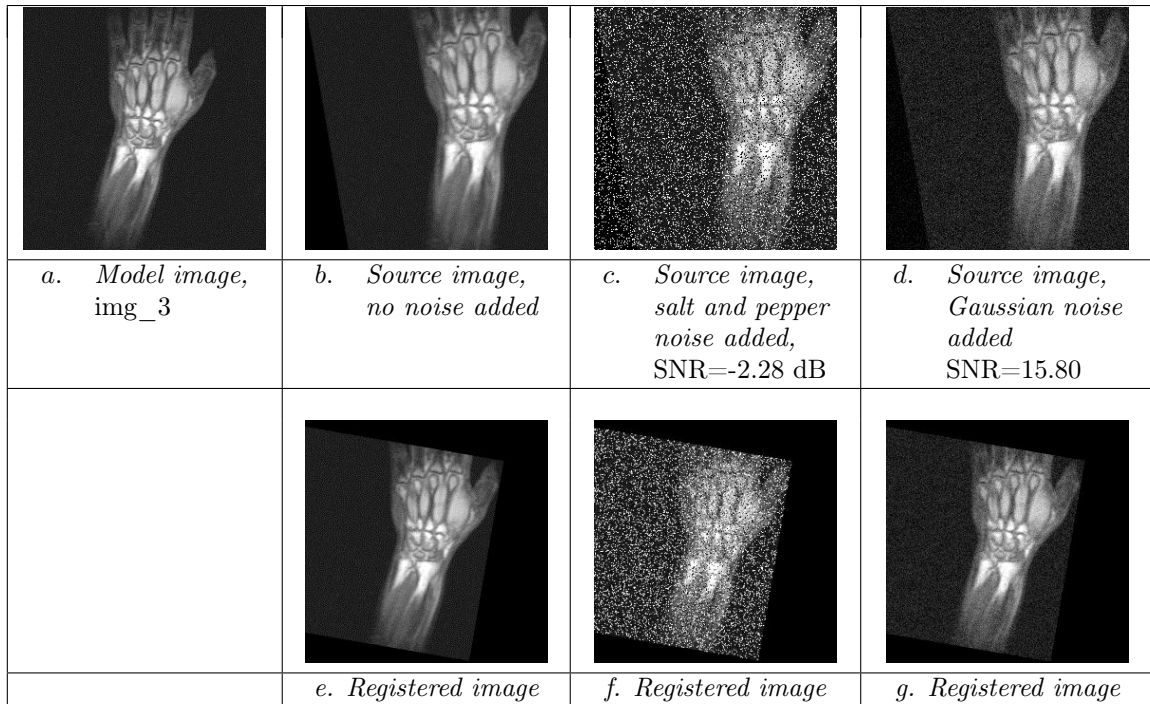
Figure 4: Registered images for test image img_3

Table 5: Image registration results obtained for test image img_3

| Similarity | Added Noise, SNR | NMI Expected | NMI Computed | NCC Expected | NCC Computed | Computed inverse transform $c_x$ | $c_y$ | $\theta$ | scale |
|---|---|---|---|---|---|---|---|---|---|
| NMI | - | 1.351 | 1.302 | 0.854 | 0.954 | -22.549 | 18.654 | -9.873 | 0.835 |
| | S&P, -2.28 | 1.122 | 1.102 | 0.772 | 0.773 | -25.759 | 18.014 | -9.633 | 0.837 |
| | Gaussian, 15.80 | 1.159 | 1.155 | 0.949 | 0.949 | -25.641 | 16.334 | -9.750 | 0.838 |
| NCC | - | 1.351 | 1.225 | 0.954 | 0.955 | -26.621 | 15.157 | -9.677 | 0.840 |
| | S&P, -2.28 | 1.123 | 1.084 | 0.773 | 0.778 | -26.407 | -37.414 | -10.042 | 0.886 |
| | Gaussian, 15.80 | 1.159 | 1.152 | 0.949 | 0.949 | -26.876 | 13.791 | -9.657 | 0.842 |

In case of the test image img_3 (Table 5), it must be noticed that in all experimental situations the computed NCC value is very slightly greater than the expected value. This may be explained by: (1) the low contrast of model and source images, (2) the images have a high portion of dark background and (3) the black areas inserted (as a necessity, from experimental reasons) in the transformed and registered images after the affine transforms application. But also in these conditions the values of MI seem to be more relevant and give a real evaluation of the registration

process.



| a.   Model image | b.   Source image, no noise added | c.   Source image, salt and pepper noise added, SNR=4.12 dB | d.   Source image, Gaussian noise added SNR=22.49 |
| | e. Registered image | f. Registered image | g. Registered image |
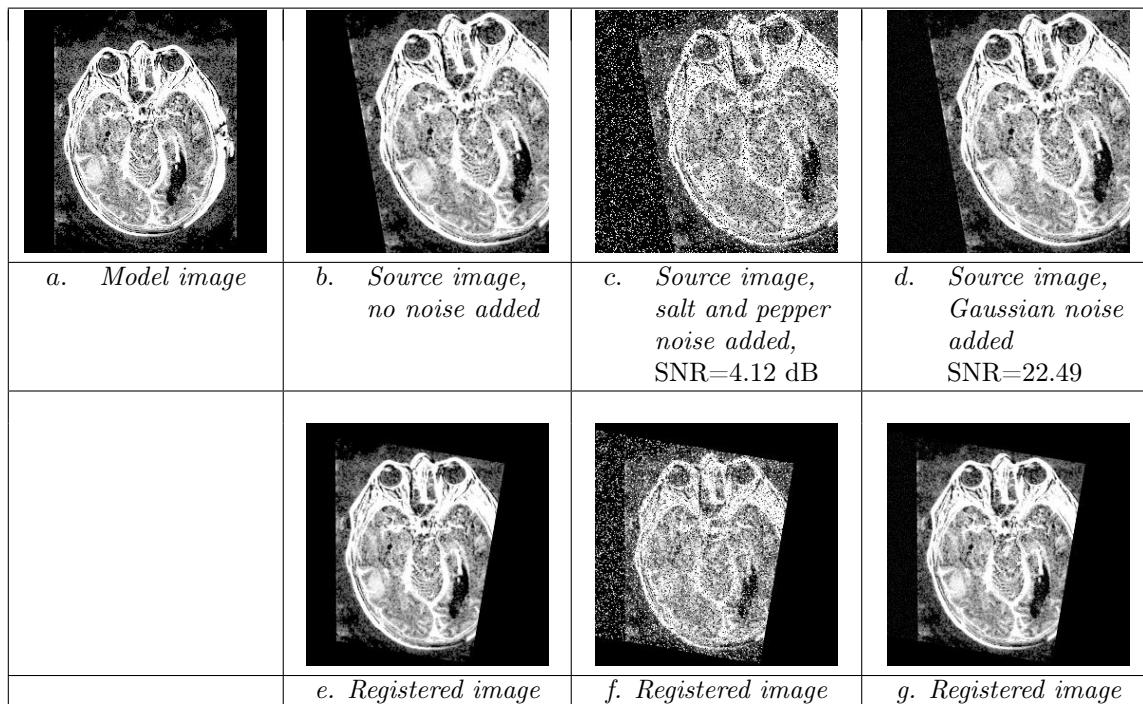
Figure 5: Registered images for test image img_2_HistEq

The proposed IR procedure was also applied to the low contrast image img_2, processed by applying the histogram equalization (Figure 5). In this way the contrast value was increased from 0.05 to 0.35. It must be noticed that in this case the registration results are similar to the case of the original image, img_2 (Table 6).

Table 6: Image registration results obtained for test image img_2_HistEq

| | | NMI | | NCC | | Computed inverse transform | | | |
| Similarity | Added Noise, SNR | Expected | Computed | Expected | Computed | $c_x$ | $c_y$ | $\theta$ | scale |
|---|---|---|---|---|---|---|---|---|---|
| NMI | - | 1.226 | 1.181 | 0.923 | 0.915 | -24.543 | 17.356 | -9.710 | 0.837 |
| | S&P, 4.12 dB | 1.110 | 1.096 | 0.849 | 0.842 | -26.152 | 18.808 | -9.604 | 0.836 |
| | Gaussian, 22.49 dB | 1.198 | 1.166 | 0.922 | 0.914 | -25.166 | 21.608 | -9.624 | 0.833 |
| NCC | - | 1.226 | 1.169 | 0.923 | 0.912 | -26.339 | 18.247 | -9.615 | 0.837 |
| | S&P, 4.12 dB | 1.111 | 1.109 | 0.850 | 0.850 | -18.283 | 19.322 | 10.118 | 0.834 |
| | Gaussian, 22.49 dB | 1.198 | 1.175 | 0.922 | 0.918 | -24.136 | 20.753 | -9.718 | 0.834 |

## 4.1   Execution Time and Parallel Approach of the Algorithm

The following tables contain for each test image the execution time in seconds, the number of cost function evaluations for sequential and parallel executions and also the *parallel efficiency* ($Eff$). The most common evaluation of parallel algorithms is performed using the parallel efficiency $Eff = \frac{t_s}{t_p \times n}$, where $t_s$ is the time used by the sequential version of the algorithm, $t_p$ is the processing time for the parallel version and $n$ is the number of used processors [38].

When comparing these values, the following issues must be considered:

– The parallel implementation was evaluated on Intel Core i5 3.10 GHz processor, with 4 cores. The system has 4 GB RAM and uses Windows 7 (64 bits) as operating system. The application was compiled as a 32 bits application;

– The execution times have to be considered as approximations, because the application was executed in Windows OS without obtaining the exclusive access of processor. The processor allocation during parallel execution was made by the operating system;
– In all executions of BFOA, the random number string was the same (the generator was initialized using the same value).

In Table 7 and Table 8 below the execution time (in seconds), the number of cost function evaluations and parallel efficiency are presented.

Table 7: Parallel efficiency obtained for images img_1 and img_3

| Image | | img_1 | | | | | img_3 | | | | |
| --- | --- | --- | --- | --- | --- | --- | --- | --- | --- | --- | --- |
| | | Sequential | | Parallel | | | Sequential | | Parallel | | |
| Similarity | Added Noise | Time (s) | #cost | Time (s) | #cost | Eff | Time (s) | #cost | Time (s) | #cost | Eff |
| NMI | - | 839.769 | 570692 | 244.220 | 568823 | 0.86 | 694.267 | 586892 | 218.744 | 589716 | 0.79 |
| | S&P | 859.737 | 535249 | 248.010 | 532361 | 0.87 | 718.868 | 535803 | 220.960 | 532431 | 0.81 |
| | Gaussian | 838.271 | 565463 | 244.094 | 567932 | 0.86 | 695.468 | 573242 | 219.478 | 572184 | 0.79 |
| NCC | - | 2173.749 | 653157 | 647.888 | 654266 | 0.84 | 2312.044 | 686083 | 685.157 | 686872 | 0.84 |
| | S&P | 2032.006 | 606303 | 602.491 | 609533 | 0.84 | 1927.860 | 571561 | 580.043 | 575190 | 0.83 |
| | Gaussian | 2061.705 | 650318 | 646.531 | 653771 | 0.80 | 2269.206 | 671327 | 687.808 | 674931 | 0.82 |

Table 8: Parallel efficiency obtained for images img_2 and img_2_HistEq

| Image | | img_2 | | | | | img_2_HistEq | | | | |
| --- | --- | --- | --- | --- | --- | --- | --- | --- | --- | --- | --- |
| | | Sequential | | Parallel | | | Sequential | | Parallel | | |
| Similarity | Added Noise | Time (s) | #cost | Time (s) | #cost | Eff | Time (s) | #cost | Time (s) | #cost | Eff |
| NMI | - | 685.63 | 567856 | 218.67 | 569872 | 0.78 | 691.07 | 567856 | 221.71 | 570865 | 0.78 |
| | S&P | 667.93 | 537816 | 210.76 | 539742 | 0.79 | 671.09 | 537816 | 210.49 | 535776 | 0.80 |
| | Gaussian | 682.24 | 569109 | 216.31 | 568918 | 0.79 | 689.23 | 569109 | 218.71 | 568197 | 0.79 |
| NCC | - | 2295.84 | 678710 | 665.08 | 673911 | 0.86 | 2306.49 | 678710 | 674.81 | 677368 | 0.85 |
| | S&P | 2110.49 | 623178 | 617.76 | 624415 | 0.85 | 2120.18 | 623178 | 617.97 | 625897 | 0.86 |
| | Gaussian | 2296.54 | 676781 | 682.82 | 680036 | 0.84 | 2307.30 | 676781 | 680.80 | 675274 | 0.85 |

Also, Figures 6 and 7 show parallel versus sequential execution time for img_2 and img_2_HistEq respectively, for clean and different added noise.
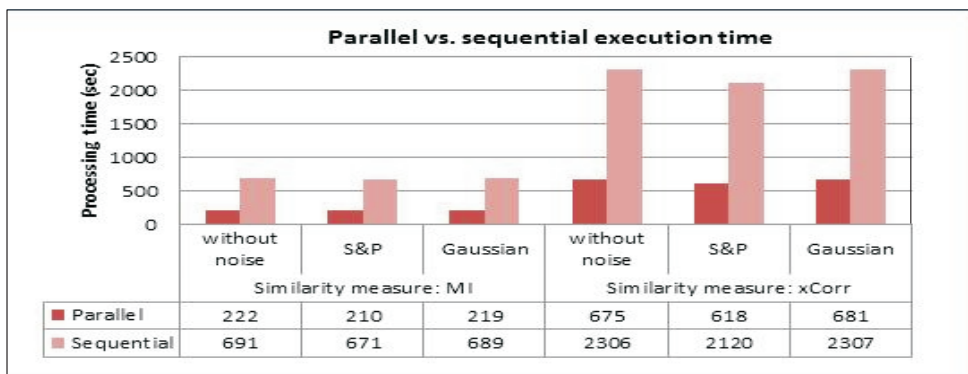


Figure 6: Parallel and sequential execution time in case of image img_2_HistEq

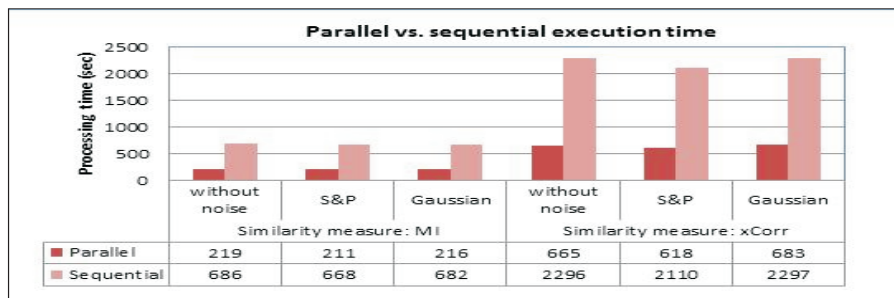| | without noise | S&P | Gaussian | without noise | S&P | Gaussian |
|---|---|---|---|---|---|---|
| | Similarity measure: MI | | | Similarity measure: xCorr | | |
| Parallel | 219 | 211 | 216 | 665 | 618 | 683 |
| Sequential | 686 | 668 | 682 | 2296 | 2110 | 2297 |

Figure 7: Parallel and sequential execution time in case of image img_2

As is depicted in Table 7 and Table 8, the parallel efficiency value is between 0.78 and 0.86. Higher values of efficiency are obtained for longer tasks, when normalized cross correlation is used for image similarity evaluation. It must be noticed that in this case, the parallel version execution time is similar to the sequential version execution time when NMI is used for similarity evaluation. Considering that also the registration precision is higher in case of NMI usage, it can be concluded that NMI is recommended as evaluation measure. The obtained parallel efficiency value is high, considering the time required for synchronization tasks and critical sections which cannot be parallelized. It must be noticed that in case of images img_2 and img_2_HistEq, for the sequential image registration, the cost function is called the same number of times. The execution time is different because in Windows operating system the processor is also used for other tasks. In case of parallel image registration, the number of cost function evaluation is different for the different allocation of the processor cores. Figures 6 and 7 show processing time for different added noise and the two similarity measures considered, for sequential and parallel versions of the proposed algorithm, when registering images img_2_HistEq and img_2, respectively.

## 5 Conclusions

This study proved the feasibility of rigid and mono-modal image registration by using a new optimization approach - Bacterial Foraging Optimization Algorithm (BFOA), a bio-inspired technique that belongs to the large family of evolutionary computing and metaheuristic methods. As similarity measures between two images performing registration process, we used the normalized mutual information and normalized cross correlation which had to be optimized by BFOA. The obtained results are encouraging, i.e. the accuracy of registration process as high even in the case of noisy images, with very low signal-to-noise ratios. In this way our method might be considered as a robust registration technique. Yet, the maximum expected value of the IR evaluation measure was not reached because when processing images from the used database two technical details have limited the overall registration:

– after the affine transform applied to obtain the source image and inverse transform is applied to obtain the registered image, some black areas are inserted in some images due to geometrical experimental reasons;

– the pixels values are changed because during the direct and inverse affine transform the pixels values are approximated using interpolation methods. In this experiment the bilinear interpolation is used.

Concerning the possibility to accelerate the execution time of the registration process, it is noteworthy that the proposed algorithm is suited to parallelization, as shown above. In this respect runtimes at least 3 times lower of the parallel version than of sequential approach were obtained, so the parameter named "speedup" equals 3. When computing parallel efficiency, it is worth mentioning that values of 0.78–0.86 were obtained when using the Intel Core i5 processor (4 cores), that meaning a good efficiency of the parallel approach.

# Bibliography

[1] Cordon, O.; Damas, S.; Santamaria, J. (2006); Feature-based Image Registration by Means of the CHC Evolutionary Algorithm, *Image and Vision Computing*, 24(5): 525-533.

[2] Gonzales, R.C.; Woods, R.E. (2002); *Digital Image Processing* (2nd ed.), Prentice Hall, New Jersey.

[3] Pratt, W.K. (2001); *Digital Image Processing*, John Wiley & Sons, New York.

[4] Rangayyan, R.M. (2005); *Biomedical Image Analysis*, CRC Press, Boca Raton, 2005.

[5] Alterovitz, R., et al. (2006); Registration of MR Prostate Images with Biomechanical Modeling and Nonlinear Parameter Estimation, *Medical Physics*, 33(2): 446-454.

[6] Cooper, J. (2003); Optical Flow for Validating Medical Image Registration, *Proc. of the 9th IASTED Int. Conference on Signal and Image Processing*, IASTED/ACTA Press: 502-506.

[7] He, R.; Narayana, P.A. (2002); Global Optimization of Mutual Information: Application to Three Dimensional Retrospective Registration of Magnetic Resonance Images, *Computerized Medical Imaging and Graphics*, 26(4): 277-292.

[8] Hill, D.; Studholme, C.; Hawkes, D. (1994); Voxel Similarity Measures for Automated Image Registration, *Proceedings of the Third SPIE Conference on Visualization in Biomedical Computing*: 205-216.

[9] Lavavely, W.C.; Scarfone, C. et al. (2004); Phantom Validation of Co-Registration of PET and CT for Image-Guided Radiotherapy, *Medical Physics*, 31(5): 1083-92.

[10] Levin, D.N.; Pelizzari, C.A. et al. (1988); Retrospective Geometric Correlation of MR, CT, and PET Images, *Radiology*, 169(3): 817-823.

[11] Lee, H.; Hong, H. (2006); Robust Surface Registration for Brain PET-CT Fusion, *Medical Imaging 2006: Visualization, Image-Guided Procedures, and Display*, Ed. by Cleary, Kevin R.; Galloway, Robert L., Jr., *Proceedings of the SPIE*, 6141: 684-693.

[12] Maintz, B.A.; van den Elsen, P.A.; Viergever, M.A. (1996); Registration of SPECT and MR Brain Images Using a Fuzzy Surface, in Loew, M.H. and Hanson, K.M. (eds), *Medical Imaging: Image processing*, Bellingham, WA. SPIE, 2710: 821-829.

[13] Maintz, B.A.; Viergever, M.A. (1998); *A Survey of Medical Image Registration, Medical Image Analysis*, Oxford University Press, 2(1): 1-37.

[14] Pluim, J.P.; Maintz, J.B.A.; Viergever, M.A. (2003); Mutual Information-based Registration of Medical Images: A Survey, *IEEE Transactions on Medical Imaging*, 22(8): 986-1004.

[15] Pietrzyk, U., Herholz, K. et al., (1996); Clinical Applications of Registration and Fusion of Multimodality Brain Images from PET, SPECT, CT, and MRI, *European Journal of Radiology*, 21: 174-182.

[16] Chen, Qin-Sheng (1993); *Image Registration and Its Applications in Medical Imaging*, PhD thesis, Vrije Universiteit Brussel.

[17] Zibaeifard, M.; Rahmati, M. (2001); An Improved Multi-stage Method for Medical Image Registration Based on Mutual Information, *Proceedings of the 8-th International Conference on Computer Vision*: 718-725.

[18] Xuan, J.; Wang,Y. et al.(2006); Nonrigid Medical Image Registration by Finite-element Deformable Sheet-curve Models, *Int. Journal of Biomedical Imaging*, 2006, Article ID 73430: 1-9, Hindawi Publishing Corporation.

[19] Zitova, B., Flusser, J. (2003); Image Registration Methods: A Survey, *Image and Vision Computing*, 21, Elsevier, 977-1000.

[20] Alpert, N.M.; Bradshaw, J.F.; Kennedy, D.; Correia, J.A. (1990); The Principal Axis Transformation – A Method for Image Registration, *Journal of Nuclear Medicine*, 31, 1717-1722.

[21] Wahl, R.L.; Quint, L.E.; et al. (1993); "Anametabolic" Tumor Imaging: Fusion of FDG PET with CT or MRI to Localize Foci of Increased Activity. *Journal of Nuclear Medicine*, 34: 1190-1197.

[22] Maguire, G.Q. Noz, M. et al. (1991); Graphics Applied to Medical Image Registration. *IEEE Computer Graphics and Applications*, 11(2): 20-28.

[23] Back, T.; Fogel, D.B.; Michalewicz, Z. (Eds.) (1997); *Handbook of Evolutionary Computation*, IOP, Bristol, UK; Oxford University Press, Oxford, UK.

[24] Fitzpatrick, J.M.; Grefenstette, J.J.; Van Gucht, D. (1984); Image Registration by Genetic Search, *Proc. of the IEEE Southeast Conference*, Louisville, USA, 460-464.

[25] Chow, C. K.; Tsui, H.T.; Lee, T. (2004); Surface Registration Using a Dynamic Genetic Algorithm, *Pattern Recognition*, 37(1): 105-117.

[26] Cordon, O.; Damas, S.; Santamaria, J. (2007); A Practical Review on the Applicability of Different Evolutionary Algorithms to 3D Feature-based Image Registration, in *Genetic and Evolutionary Computation for Image Processing and Analysis*, Eds.: S. Cagnoni, E. Lutton, G. Olague, Hindawi Publishing Corporation, 241-264.

[27] Etienne, E.K.; Nachtegael, M. (2000) (eds.). *Fuzzy Techniques in Image Processing*, Physica-Verlag, N.Y.

[28] Reyes-Sierra, M.; Coello C.A. (2006); Multi-objective Particle Swarm Optimizers: A Survey of the State-of-the-art, *International Journal of Computational Intelligence Research*, 2(3): 287-308.

[29] Rouet, J.-M.; Jacq, J.-J.; Roux, C. (2000); Genetic Algorithms for a Robust 3-D MR-CT Registration, *IEEE Trans. on Information Technology in Biomedicine*, 4(2): 126-136.

[30] Wachowiak, M. P.; Smolíková, R. et al. (2004); An Approach to Multimodal Biomedical Image Registration Utilizing Particle Swarm Optimization, *IEEE Transactions on Evolutionary Computation*, 8(3): 289-301.

[31] Passino, K.M. (2002); Biomimicry of Bacterial Foraging for Distributed Optimization and Control, *IEEE Control Systems Magazine*, 52-67.

[32] Liu, Y.; Passino, K.M. (2002); Biomimicry of Social Foraging Bacteria for Distributed Optimization: Models, Principles, and Emergent Behaviors, *Journal of Optimization Theory and Applications*, 115(3): 603-628.

[33] Verma, O. P.; Hanmandlu, M.; Kumar, P.; Chhabra, S.; Jindal, A. (2011); A Novel Bacterial Foraging Technique for Edge Detection, *Pattern Recognition Letters*, Elsevier, 32: 1187-1196.

[34] N. Sanyal, A. Chatterjee, S. Munshi (2011); "An Adaptive Bacterial Foraging Algorithm for Fuzzy Entropy Based Image Segmentation", *Expert Systems with Applications*, Elsevier, 38: 15489-15498.

[35] Sathya, P.D.; Kayalvizhi, R. (2011); Modified Bacterial Foraging Algorithm Based Multi-level Thresholding for Image Segmentation, *Engineering Applications of Artificial Intelligence*, Elsevier, 24: 595-615.

[36] Yudong, Z.; Lenan, W. (2008); Multi-resolution Rigid Image Registration Using Bacterial Multiple Colony Chemotaxis, *5th Int. Conf. on Visual Information Engineering*, VIE 2008, 528-532.

[37] Bejinariu, S. I.; Costin, H., Rotaru, F.; Niţă, C.; Luca, R.; Lazăr, C. (2014); Parallel Processing and Bioinspired Computing for Biomedical Image Registration, *The Computer Science Journal of Moldova*, 22(2): 253-277.

[38] Campbell, C.; Miller, A. (2012); *Parallel Programming with Microsoft Visual* C++, Microsoft Corporation.

[39] DICOM Sample Image Sets (http://www.osirix-viewer.com/datasets/), accessed on 1.09.2014

# Dynamic Secure Interconnection for Security Enhancement in Cloud Computing

L. He, F. Huang, J. Zhang, B. Liu, C. Chen, Z. Zhang, Y. Yang, W. Lu

**Liwen He\*, Feiyi Huang, Jie Zhang, Bin Liu,**
**Chunling Chen, Weifeng Lu**

Nanjing University of Posts and Telecommunications
66 New Mofan Road (P. Code:210003), Nanjing, China
helw@njupt.edu.cn, feiyi.huang@gmail.com, zhangjie@njupt.edu.cn,
clchen@njupt.edu.cn, luwf@njupt.edu.cn
\*Corresponding author: helw@njupt.edu.cn

**Zonghua Zhang**

Institut Mines-Télécom of France
Rue Guglielmo Marconi, 59650, Villeneuve-d'Ascq, France
zonghua.zhang@ifl.fr

**Yang Yang**

ShanghaiTech University, Chinese Academy of Sciences
Information Building No 1, 280 Linhong Road, 200335, Shanghai, China
yang.yang@shrcwc.org

**Abstract:** Cloud computing brings efficiency improvement on resource utilization and other benefits such as on-demand service provisioning, location independence and ubiquitous access, elastic resource pooling, pay as usage pricing mode, etc. However, it also introduces new security issues because the data management and ownership are separated, and the management is operated on a virtualized platform. In this paper, a novel dynamic secure interconnection (DSI) mechanism is proposed to isolate the cloud computing system into a couple of dynamic virtual trust zones with different security policies implemented for different customers so as to enhance security. Experimental results are presented to demonstrate the feasibility and effectiveness of the DSI mechanism.
**Keywords:** Cloud Computing, virtualization management, security, dynamic secure interconnection

## 1 Introduction

In recent years, cloud computing is drawing more and more attention with its capabilities of efficient resource utilization, virtual machine live migration and multi-tenancy operational mode. Virtualization is the fundamental technology for both public and private cloud, virtual machine is expected to be dynamically allocated according to the requirements of customers, to be seamlessly migrated from one physical machine to another, and to be managed appropriately to prevent illegal access. However, cloud computing brings unprecedented challenges on security issues. As long as customers upload their sensitive data into a cloud computing system, the cloud computing service provider (CSP) is responsible for managing the data. Customers will lose the control of the data, who is using them, and when it is deleted.

And in a cloud computing environment, virtualization cannot be protected by conventional network security solution, such as Ą°security zoneĄą separation, firewall, VPN, intrusion detection/prevention system, anti-DDoS solution, deep packet inspection technology [1].

In this paper, we propose a security enhanced virtual machine management mechanism named dynamic secure interconnection (DSI) for cloud computing system. A Ą°dynamic virtual trust

zonesĄą is established to enhance information and virtualization security. In section 2, backgrounds about the cloud computing and virtualization security issues are reviewed. Section 3 provides a typical cloud computing model and states the typical security problems and requirements, and Section 4 proposes the DSI mechanism and operational procedure in details. A testbed and some experimental results are presented in Section 5. The paper is concluded in Section 6.

## 2    Related Work

The security issues are the major concerns for enterprise to adopt cloud computing [2] [3] [4]. Seven cloud computing security risks are identified by Gartner [5], i.e. privileged use access, regulatory compliance, data location, data segregation, recovery, investigation support, long-term viability. The root cause of these security risks is data storage, management and computation are performed on a shared and virtualized environment.

Since VMs work over hypervisor, malicious VMs cannot gain access to other VMs or launch cross-VM attacks when security countermeasures are implemented on hypervisors. However, this security boundary can be broken and malicious VMs can get full access to the physical host so as to get access to other VMs located on the same host illegally [6] [7]. Virtualization security has been studied from many aspects. In [8], an out-of-VM monitoring mechanism is proposed by using a trust VM to monitor the statues of guest VMs which deliver services to customers. The solution assumes the trust VM can prevent a variety of security threats. However, there is a large performance overhead associated with this solution when traffic is switched between the guest VMs and the trust VM. In order to provide a trusted VM on untrusted computing OS, a secure virtualization architecture is proposed to provide a secure execution environment [9]. The architecture includes a secure run-time environment, secure network interface and a secure secondary storage. Apart from the secure architecture, trust platform module has be used to establish the root of trust for VMs [10]. In [11], a virtual layer management framework is presented to ensure that cloud providers properly isolate VMs that run in the same physical platform, a cloud computing system is divided into a number of domains on the virtualization layer. Corresponding protocols are also proposed to manage the domain creation, interaction and termination. The interaction among the domains is based on secure channels [12] to establish trustworthy self-management foundation.

Data protection is another critical issue. Service providers such as Foursquare which provides a location based service and Reddit which supplies social news voting services use Amazon EC2 (Elastic Cloud Computing platform). In 2011, the crash of Amazon EC2 service takes down the service of Foursquare, Reddit, Cydia, Discovr and Scvngr [13]. Also, application (software) service provider can only rely on the infrastructure service provider to ensure the business continuity under the umbrella of SLA (service level agreement). They can implement their own security policies to achieve data security, preventing data loss or leakage. In [14], Hwang and Li propose a data coloring and software watermarking technique to establish trust among cloud service providers. In particular, if data objects and software modules are shared over multiple data centres, the trust-overlay network can establish a reputation system to protect data security and integrity.

Cloud privacy is to ensure the personal or sensitive information only be accessed by intended and authorized person or applications. The privacy issue originates from the lack of user access control and information transparency. That is when adopting a cloud storage service, e.g. the Dropbox [15], the customers are difficult to implement mechanisms to protect their information from unauthorized access or misuses. Promising privacy preservation solutions include minimizing personal information stored in the cloud, maximizing use control, allowing user to

choose, specify and limit the data usage [16]. In addition, data encryption is always a popular way, despite the extra overhead and complexity resulting from encryption algorithms and key management issues. In [17], a data secure sharing mechanism is proposed to enforce data access control, strengthening data encryption and improving the key sharing process when cloud customers store their data in a public cloud platform. The solution can protect the cloud storage providers from unauthorized access, ensuring data confidentiality and privacy. In [18], a privacy-preserving public auditing supported secure cloud storage system is proposed, which enables that data privacy of cloud storage to be publicly audited by a third party auditor. In particular, the homomorphic liner authenticator and random masking techniques are utilized to guarantee that the third party auditor would not learn any knowledge about the data content stored on the cloud server during the auditing process.

## 3  Problem Description

A number of open source cloud computing platform is based on the policies configured such as user authentication, authorization and accounting, VM allocation, drifting and state management, host machine management, service provision management. In the model, the security issues become much more complicated. First, the conventional network security solutions become less effective since they are usually deployed at the edge of a physical network to control and protect the incoming or outgoing traffic of a LAN. Second, new virtualization security countermeasures should be implemented on the virtualized perimeters where the physical network perimeter does not exist. Third, in the multi-tenancy environment, customers who share the same local network should have logically or physically separated computing, storage and networking resources, especially when customers come from different enterprises. That means cloud service provider should allocate each customer and their resources within a same virtualized trust group, permitting the interconnection within the same group and control the communication among different groups. Finally, when customers are on travel, the VMs related to them will be drifted and migrated from one physical machine to another, the security policies that implemented by the customer and on related VMs are expected to move along with migration.

## 4  Dynamic Secure Interconnection Mechanism

In this section, a novel mechanism, DSI-VM management mechanism is proposed to enhance security in a cloud computing system. A new concept of Ą°virtual trust zoneĄą is also introduced.

### 4.1  Definitions and Assumptions

**Virtual Trust Zone:** VMs are the basic operation unit to implement management and security policies. When customers login and get service from a cloud computing system, they are allocated with virtualized resources in terms of VMs according to their requirements. VMs that assigned to the same customer should be aggregated in a same group and implemented with the unified management and security policies. Thus, the VMs that stay in the same group have basic trust among each other, and this group is defined as a Ą°virtual trust zoneĄą.

**Virtual Bridge:**VMs that operate over a physical machine share the same physical MAC and IP addresses when the physical machine have only one NIC card. Each VM has its own virtual MAC and virtual IP addresses. A virtual bridge is a function module implemented on the hypervisor. It forwards packets with virtual MAC and IP address to their destination. A virtual bridge can serve all VMs on a hypervisor as well as a single VM.

## 4.2   The DSI Components

The DSI components include a DSI server, several virtual bridges and DSI clients. The DSI server works at a centralized mode while virtual bridge and DSI clients works at a peer-to-peer mode.
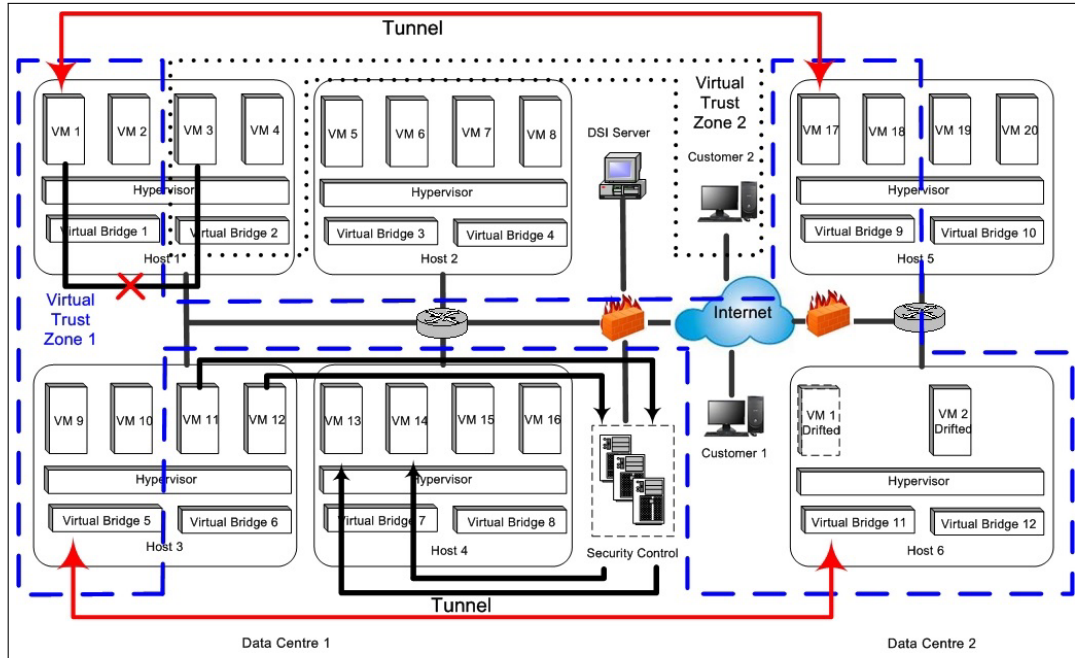


Figure 1: Overview of Dynamic Secure Interconnection Mechanism

### DSI Server

The DSI server is the central controller for handling the management and security policies. When a VM is initialized, it is connected with the DSI server to register and start to operate in the system. When the VM state changes, e.g. suspend, restart, drift or phase out, it will inform DSI server to update the VM state. Thus, the DSI server maintains all VM properties and states, such as the virtual MAC (vMAC) and virtual IP (vIP) addresses of VMs, the VM owner, the corresponding virtual bridge, the real-time VM state, etc.

In addition, DSI server maintains the VM communication protocols, policies and activities. If VMs stay within a same local network, they can talk with each other using vMAC and vIP. If VMs stay in different local network, especially behind NAT devices, vIP based tunnels will be established to connect VMs. Meanwhile, appropriate traffic control policies will be implemented during the connection bootstrapping stage, such as encryption algorithms, key management protocol and traffic redirection.

### DSI client and virtual bridge

The DSI clients are a large number of VMs. The properties of each DSI client includes vMAC and vIP addresses, VM state, VM owner, corresponding virtual bridge, host and its own virtual trust zone ID. Virtual bridges are in charge of performing and implementing the communication protocols and policies. The communication between two DSI clients is performed at a peer-to-peer mode. As shown in the Fig. 1, virtual bridge 1 and 5 can establish a direct connection between VM 1 and VM 9 based on virtual MAC addresses since they belong to the same local

network and can communicate with each other via vMAC and vIP. However, virtual bridge 1 and 9 have to establish VPN tunnels to transit through the NAT device based on the vIP to connect VM 1 and VM 17.

## 4.3    DSI Operation

The DSI operation refers to the interactions among DSI server, several DSI clients and virtual bridges. More specifically, the system administrator specifies the management policy on the DSI server, which then allocates the corresponding communication control policies to individual virtual bridges. Virtual bridges control the communication among DSI clients by relaying, blocking or rate-limiting packets to establish virtual trust zones.

### Policy Configuration

The system management and security policies are configured on the DSI server according to the administrative requirements. That includes the DSI client initialization procedures, DSI client state change procedures, virtual bridge switching protocols and some other traffic management and security protection policies such as client registration, VM state management, access control, network isolation, transmission encryption, traffic redirection, etc.

### Client Initialization and State Maintenance

A new user registration or additional resource request from existing users will incur the creation of VMs (DSI clients). This process is managed by the cloud computing platform based on policies such as load balancing, energy efficiency. After that, the newly generated VMs (DSI clients) will be registered on the DSI server, and provide the DSI server with information such as vMAC and vIP addresses, virtual bridge, VM owner and host machine name. Then the DSI server instructs the DSI clients and corresponding virtual bridges to perform bootstrapping process. That includes the notification of virtual trust zone ID, other clients within the same virtual trust zone, communication protocols and policies.

When the VMs (DSI clients) start to change their states, e.g. suspended, drifted or terminated, the DSI server will be notified with the change. The related communication protocols and policies will then be updated by the DSI server and reconfigured on each virtual bridge. For example, the VM 1 and VM 2 are suspended when their owners travel to other cities. The VMs are drifted and migrated into another data centre and will be allocated on virtual bridge 11 and 12 respectively, with their previous virtual MAC and IP addresses inherited. Previous and existing virtual bridges (virtual bridge 1, 11 and 12) will then report DSI server about the update and new tenant. DSI server will then update the related information in all virtual bridges to make sure the drifted VM 1 and drifted VM 2 can be connected seamlessly.

### Virtual Bridge Communication Management

Virtual bridge is responsible for managing VM interconnection, traffic flow and virtual network topology. In Fig. 1, the VM 1 and VM 2 reside on the same virtual bridge 1 and serve the same customer. Thus, by allowing the interconnection between the VM 1 and VM 2, these two DSI clients are allocated into a same virtual trust zone. On the other hand, if VM 1 and VM 3 are serving customers from different enterprises, the interconnection between them will be blocked by virtual bridge 1 and 2. Thus, the VM 1 and VM 3 are regarded as staying in different virtual trust zone. Virtual bridges configure and maintain ACL (access control list) to authenticate vMAC addresses to start interconnection between DSI clients. Therefore, vMAC

based communication management is more suitable between VMs within the same local network where the virtual MAC addresses can be recognized.

If the two clients stay in different networks or behind NAT devices, the vIP address of a DSI client registered on the DSI server may be meaningless for another DSI client. The virtual IP addresses based tunnelling among VMs is performed by establishing peer-to-peer tunnels between virtual bridges, e.g. VM 1 and VM 17 in Fig. 1. The DSI server configures the virtual bridges to create tunnels with proper parameters such as the vIP address of the destination, the tunnelling protocols and encapsulation options. By doing that, access control and virtual network isolation can be further extended between VMs that stay in different local network.

## 4.4   Security

The dynamic security interconnection mechanism enhances cloud computing security by implementing access control mechanisms among VMs. In particular, virtual trust zones can be established by building the tunnels among virtual bridges.

### Virtual Trust Zone Establishment

A virtual trust zone is a group of DSI clients (VMs) that interconnected by virtual bridges with some interconnection policies. A DSI client (e.g. VM 1) will be generated when a customer first login the system and request for computing and storage resources. When the customer requests for additional resources, a virtual trust zone is established to include the newly generated DSI client and the original one. The clients are trusted with each other and thus the interconnection between them is permitted. When the newly generated clients share the same physical host (e.g. VM 2) or local network (e.g. VM 9) with the original client, the virtual MAC address based access control mechanism and corresponding policies are implemented. If a new client resides in a remote data centre (e.g. VM 17), the IP tunnels based interconnection will be implemented. The IP tunnels based interconnection is also operational between VMs within a data centre (e.g. between VM 1 and VM 9). The virtual bridges will select the light-weighted vMAC based protocol in order to reduce the operation overhead and the management complexity of IP tunnelling protocol.

### Encrypted Tunnel Establishment

When the customer travels from one city to another, the drifted DSI clients (e.g. VM 1 and VM 2) will migrate into a different network. The communication within a virtual trust zone, e.g. between the drifted VM 1 and VM 9, may go through an insecure public network. The encrypted tunnel will be established to protect the information exchange against various attacks such as eavesdropping. The DSI server may provide additional information to facilitate tunnel setup authentication, e.g. the certificate fingerprint [19]. In that case, DSI server presents an IKE/IPsec tunnel for NAT traversal, e.g. the UDP encapsulation of IPsec tunnelling [20].

### Traffic Redirection

The virtual bridges can redirect the outgoing traffic of VMs to a dedicated traffic analysis and cleaning device before relaying them to their destination when the customers require them or when the system is under attacks. The dedicated device may be a secure VM or conventional security system such as anti-DDoS solution [1]. As an example in Fig. 1, the traffic from VM 11 and VM 12 are redirected to a traffic cleaning centre before it is forwarded to their destination, VM 13 and VM 14. The cost of this kind of security solution is performance degradation and operation overhead.

**Security Policy Consistency**

Since the network is separated into several virtual trust zones, security countermeasures can be implemented on a per-trust-zone basis. When the VMs in a virtual trust zone migrated from one host to another, e.g. VM 1 and 2, virtual bridge 1, 11 and 12 will then update DSI server about this information. And the DSI server will then reconfigure the tunnels among the virtual bridges accordingly. As a result, DSI server maintains the information about the dynamic trust zone no matter where the VMs migrate. The security policies can also be shifted along with the VM movement.

**Comparison and Discussion**

With the DSI mechanism, the traffic among VMs in the same trust zone is permitted while the traffic among VMs in different trust zones is controlled. Thus the trust zones are separated by simply managing the interconnection among VMs. This mechanism has several advantages.

- First, compared with the virtual layer management framework proposed in [11], our solution is relatively simple. In [11], several domains and complicated management mechanisms are introduced to manage the virtual layer. The DSI maintains virtual trust zones based only on the interconnection control mechanism.

- Second, DSI is very practical to make full use of all existing protocols, hypervisors and platforms to ensure the compatibility with most of existing cloud computing system.

# 5   Testbed and Experiment Results

A proof-of-concept testbed is constructed for demonstration of the DSI mechanism,and a simple Cloud computing platform named Ą°VM Management platformĄą is implemented to perform the virtualized resource management, as shown in Fig.2.

**Configurations.**  Libvirt toolkit and its virtualization APIs are utilized to construct the platform based on hypervisors of KVM, Xen Server or Virtual Box. Several VM management functionalities and policies are established written by C programs. VM initialization policies include VM instant created on host whose CPU/RAM is most idle; VM instant created on hosts already power on as far as possible; VM instant created on all hosts in average. Apart from that, VM management policies also include the VM suspend, migration, error control and disaster recovery policies. The VM management platform manages all VMs on host 2, 3 and 4.

**Hardware settings.**  The testbed is composed of a Cisco Catalyst 2960PD-8TT-L switch and four PCs, host 1 is used for management, host 2, 3 and 4 are used for resource provision. Each PCs has a Intel CORE i5 four core 3.3GHz CPU, 4G RAM and 320G hard disk, and is able to accommodate 4 VMs. On host 1, 2, 3 and 4, hypervisor is installed on Linux Redhat Enterprise 5.6. In the experiment, three typical open source hypervisors of KVM, Xen Server and Virtual Box are selected to operate on the OS. The KVM and Virtual Box are type 2 hypervisors, while the Xen Server belongs to the type 1.

Virtual bridge functionality is implemented on host 2, 3, and 4. It is enabled based on the tun/tap device of Linux. Apart from switching, protocols of traffic filtering, traffic redirection, tunnel establishment are achieved by a set of C programs. The DSI server functionality is enabled by running a set of C program on the OS of host 1. The DSI functionalities include a management user interface (UI) and maintenance on DSI client information database.

In the experiment, the DSI mechanism operates normally on each of the three hypervisors, no matter whether it is type 1 or type 2. First, four VMs are configured on host 2, four on host
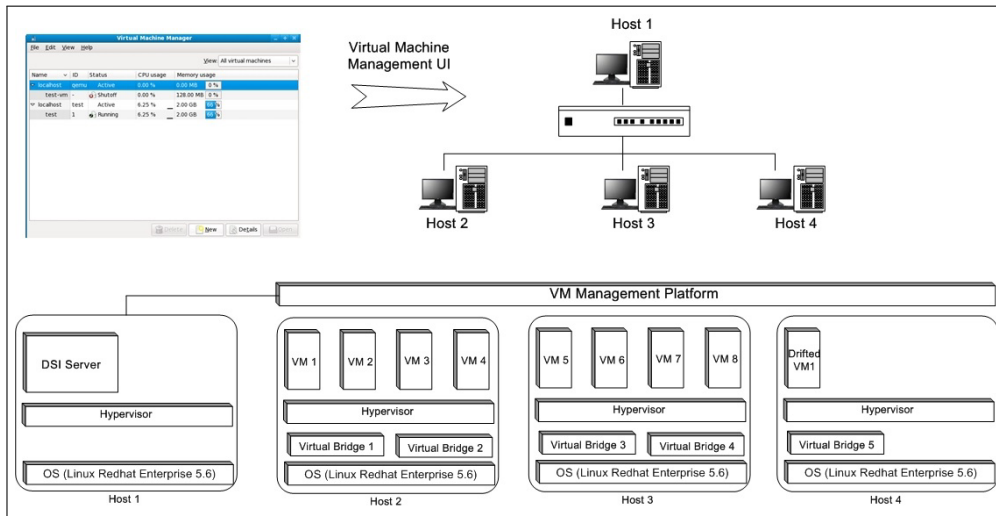
Figure 2: Testbed and Experiment

3 and IP addresses are assigned from 10.0.0.1 to 10.0.0.8. VM 1, 2, 5, 6 are configured in the same virtual trust zone and VM 3, 4, 7, 8 in the same zone. That can be achieved by permitting the interconnection between virtual bridge 1 and 3, and between virtual bridge 2 and 4. Ping command is used to check the interconnection control within and among virtual trust zones. The ĄˇpingĄą between VM 1 and 5 is successful and between VM 1 to 3 is failed. In the second test case, VM 1 drifts from host 2 to 4, the virtual bridges on hosts inform the DSI server about this change, and DSI server updates the DSI client information database and informs related virtual bridge to update their interconnection configuration accordingly. In the test, the database is updated as expected. The ĄˇpingĄą command from drifted VM 1 to VM 5 and 3 get the same result with the first test case. It is shown that the drifted VMs still stay within the same virtual trust zone and security policies keep the same after the migration.

## 6    Conclusion and Future Work

In this paper, dynamic secure interconnection (DSI) mechanism is proposed, analyzed and tested. By managing the VM interconnection and traffic direction of a cloud computing system, the virtualized network can be isolated into a couple of virtual trust zones. Direct connection within the same zone is established regardless the VM location while the traffic among different virtual trust zones will be carefully controlled. Coped with corresponding security service level agreement, security can be enhanced for customers to adopt cloud computing platform. Our proposed mechanism can protect sensitive data and information against various attacks such as eavesdropping to enhance cloud computing security.

As stated in section 4.4, traffic redirection is an important security feature of the DSI mechanism. It can release the working load of traffic scanning and monitoring on VMs and potentially facilitate the deployment of conventional security mechanisms such as anti-DDoS, virus, malware systems. However, this solution may consume extra amount of bandwidth when the traffic is redirected to a monitoring centre. More studies on this issue will be conducted in the future. In addition, the testbed with the VM management functionality is currently implemented only for concept proof, so a real-life cloud computing platform will be established by using open source tools such as Openstack or Eucalyptus to create more practical scenarios. Furthermore, our current experiments only selected some primary open source hypervisors to prove the compatibility

of the DSI mechanism, and the future experiments will involve more commercial hypervisors such as VMware or Hyper-V. DSI performance comparison on type 1 and type 2 hypervisors will also be studied.

# Bibliography

[1] Xiaoming Lu, Weihua Cao, Xusheng Huang, Feiyi Huang, Liwen He, Wenhong Yang, Shaobin Wang, Xiaotong Zhang and Hongsong Chen (2010); A Real Implementation of DPI in 3G Network, *Proceedings of 2010 IEEE Global Telecommunications Conference (GLOBECOM 2010)*, 1-5.

[2] Cloud Computing Survey, IDC Enterprise Panel, [Online] Available: http://blogs.idc.com/ie/?p=210, Aug. 2008.

[3] S. Pearson and A. Benameur, Privacy (2010); Security and Trust Issues Arising from Cloud Computing, *Proceedings of 2010 IEEE Second International Conference on Cloud Computing Technology and Science (CloudCom)*, 693-702.

[4] S. Pearson (2009); Taking account of privacy when designing cloud computing services, *Proceedings of ICSE Workshop on Software Engineering Challenges of Cloud Computing, CLOUD '09*, 44-52.

[5] Jon Brodkin (2008); Gartner: Seven Cloud Computing Security Risks, July 2008, Available at http://www.infoworld.com/article/2652198/security/gartner–seven-cloud-computing-security-risks.html.

[6] K. Kortchinsky (2009); *CLOUDBURST: A VMware Guest to Host Escape Story*, BlackHat, USA, 2009.

[7] T. Ristenpart, E. Tromer, H. Shacham and S. Savage (2009); Hey, You, Get Off of My Cloud: Exploring Information Leakage in Third-party Compute Clouds, *CCS'09, ACM*, Chicago, Illiois, November 2009.

[8] B. Payne et al. (2008); Lares: An Architecture for Secure Active Monitoring Using Virtualization, *Proceedings of IEEE Symposium of Security and Privacy*, IEEE Press, 233-247.

[9] C. Li, A. Raghunathan and N. Jha (2011); A trusted virtual machine in an untrusted management environment, *IEEE Transactions on Services Computing* , 5(4): 472 - 483.

[10] M. Achemlal, S. Gharout and C. Gaber (2011); Trusted Platform Module as an Enabler for Security in Cloud Computing, *2011 Conference on Network and Information Systems Security (SAR-SSI)*, 1-6.

[11] Imad M. Abbadi, Muntaha Alawneh and Andrew Martin (2011); Secure Virtual Layer Management in Clouds, *Proceedings of IEEE 10th International Conference on Trust, Security and Privacy in Computing and Communications (TrustCom), 2011*, 99-110.

[12] Muntaha Alawneh and Imad M. Abbadi (2008); Preventing information Leakage between Collaborating Organizations, *Proceedings of the 10th International Conference on Electronic Commerce, ACM Press, August 2008*, 185-194.

[13] Amazon EC2 cloud outage downs Reddit, Quora, CNN News, [Online] Available: http://money.cnn.com/2011/04/21/technology/amazon _server_outage/index.htm

[14]  Kai Hwang and Deyi Li (2010); Trusted Cloud Computing with Secure Resources and Data Coloring, *IEEE Internet Computing*, 14(5); 14-22.

[15]  http://www.dropbox.com/.

[16]  S. Pearson, (2009); Taking account of privacy when designing cloud computing services', *Proceedings of ICSE Workshop on Software Engineering Challenges of Cloud Computing, May 2009*, 44-52.

[17]  Gansen Zhao, Chunming Rong, Jin Li, Feng Zhang and Yong Tang (2010); Trusted Data Sharing over Untrusted Cloud Storage Providers, *Proceedings of 2010 IEEE Second International Conference on Cloud Computing Technology and Science (CloudCom), 2010*, 97-103.

[18]  C. Wang, S. Chow, Q. Wang, K. Ren and W. Lou (2011); Privacy-Preserving Public Auditing for Secure Cloud Storage, *IEEE Transactions on Computers*, 1-14.

[19]  J. Lennox (2006); RFC 4572: Connection-Oriented Media Transport over the Transport Layer Security (TLS) Protocol in the Session Description Protocol (SDP), July 2006.

[20]  A. Huttunen, B. Swander, V. Volpe, L. DiBurro and M. Stenberg (2005); RFC 3948 UDP Encapsulation of IPsec ESP Packets, January 2005.

# Extended EDAS Method for Fuzzy Multi-criteria Decision-making: An Application to Supplier Selection

M. Keshavarz Ghorabaee, E.K. Zavadskas, M. Amiri, Z. Turskis

**Mehdi Keshavarz Ghorabaee**
Department of Industrial Management,
Faculty of Management and Accounting,
Allameh Tabataba'i University,
Tehran, Iran
m.keshavarzv_gh@yahoo.com

**Edmundas Kazimieras Zavadskas\***
Research Institute of Smart Building Technologies,
Vilnius Gediminas Technical University,
Sauletekio al. 11, LT-10223 Vilnius, Lithuania
*Corresponding author: edmundas.zavadskas@vgtu.lt

**Maghsoud Amiri**
Department of Industrial Management,
Faculty of Management and Accounting,
Allameh Tabataba'i University,
Tehran, Iran
amiri@atu.ac.ir

**Zenonas Turskis**
Research Institute of Smart Building Technologies,
Vilnius Gediminas Technical University,
Sauletekio al. 11, LT-10223 Vilnius, Lithuania
zenonas.turskis@vgtu.lt

**Abstract:**
In the real-world problems, we are likely confronted with some alternatives that need to be evaluated with respect to multiple conflicting criteria. Multi-criteria decision-making (MCDM) refers to making decisions in such a situation. There are many methods and techniques available for solving MCDM problems. The evaluation based on distance from average solution (EDAS) method is an efficient multi-criteria decision-making method. Because the uncertainty is usually an inevitable part of the MCDM problems, fuzzy MCDM methods can be very useful for dealing with the real-world decision-making problems. In this study, we extend the EDAS method to handle the MCDM problems in the fuzzy environment. A case study of supplier selection is used to show the procedure of the proposed method and applicability of it. Also, we perform a sensitivity analysis by using simulated weights for criteria to examine the stability and validity of the results of the proposed method. The results of this study show that the extended fuzzy EDAS method is efficient and has good stability for solving MCDM problems.

**Keywords:** Multi-criteria decision-making, Fuzzy sets, Fuzzy MCDM, EDAS method, Fuzzy EDAS, Supplier selection.

## 1 Introduction

Usually, the real-world decision-making problems are very complex and could not be considered as single-criterion problems. In other words, using only one dimension for the decision-making process could lead to an unrealistic decision [7], [9], [10], [33], [34]. To obtain more

comprehensive models for these problems, we need to involve multiple factors or criteria. Multi-criteria decision-making (MCDM) comprises efficient methods and techniques to deal with problems that include more than one criterion in the decision-making process [4], [13] [19], [25], [35].

The information about the real-world problems is usually not known accurately. This uncertainty makes the decision-making process complex and challenging. Fuzzy set theory was proposed by Zadeh [31] to deal with this kind of subjective and imprecise information. This theory is a very efficient modeling tool for the MCDM problems in an uncertain environment. Linguistic terms defined by fuzzy sets are usually used to represent uncertain information in the fuzzy decision-making process [18].

Many researchers have applied and extended fuzzy MCDM methods in real-world problems [5], [26], [27]. Nieto-Morote and Ruz-Vila [20] proposed an MCDM approach based on the fuzzy AHP and linguistic terms to evaluate combined cooling, heat, and power production systems. Cagri Tolga et al. [6] developed a fuzzy MCDM approach based on the analytic network process for retail location selection problem. Sedaghat [23] presented a fuzzy MCDM approach based on AHP, TOPSIS, VIKOR and SAW methods for evaluation of productivity improvement of private banks. Wan and Dong [28] developed a new method for solving the multi-criteria group decision-making problems with the trapezoidal intuitionistic fuzzy number and incomplete criteria weight information, and used it for stock selection problem. Stanujkic [24] developed an extended version of ARAS method with interval-valued triangular fuzzy numbers and utilized it for evaluating the performance of websites. Baležentis et al. [3] extended the MULTIMOORA method with intuitionistic fuzzy numbers and applied it for personnel selection problem. Keshavarz Ghorabaee [14] proposed an extended VIKOR method with interval type-2 fuzzy sets and applied it to a problem of evaluation and selection of the industrial robots.

Due to involvement of many factors in evaluation and selection of the suppliers, this problem is usually considered as an MCDM problem [12]. Like many other MCDM problems, supplier selection problem is usually handled in an uncertain environment. Therefore, fuzzy MCDM methods and techniques are very useful to deal with this problem. Many researchers have studied supplier selection problem using fuzzy set theory. Yücenur et al. [30] developed a model for selecting the global supplier using the fuzzy analytic hierarchy process and analytic network process. Baležentis and Baležentis [2] developed an innovative MCDM approach based on MULTIMOORA method and 2-tuple linguistics for supplier evaluation and selection. Pitchipoo et al. [22] proposed a structured and integrated decision-making approach for evaluating suppliers by combining the fuzzy analytic hierarchy process and grey relational analysis (GRA). Keshavarz Ghorabaee et al. [15] extended a multi-criteria group decision-making based on the COPRAS method with type-2 fuzzy sets, and applied it to supplier selection process. Kar [16] developed a hybrid group decision support system for supplier selection using analytic hierarchy process, fuzzy set theory and neural network.

The evaluation based on distance from average solution (EDAS) method was introduced by Keshavarz Ghorabaee et al. [17] for inventory ABC classification. It was presented that the EDAS method has good efficiency and needs fewer computations in comparison with other ABC classification methods. Moreover, the efficiency of the EDAS method as an MCDM method was demonstrated by comparing it with some commonly used methods. The evaluation of alternatives in this method is based on distances of each alternative from the average solution with respect to each criterion. In this study, the EDAS method is extended to deal with the fuzzy MCDM problems. In this paper, these linguistic terms are defined by trapezoidal fuzzy numbers to extend the EDAS method in fuzzy environment. A case study of supplier selection is employed to describe the process and demonstrate the effectiveness of the proposed extended method. We also perform a sensitivity analysis with different sets of simulated criteria weights to represent the validity and stability of the ranking results when the weights of criteria are changed. The

results of sensitivity analysis show that the proposed fuzzy method is stable in different weights of criteria and has a good efficiency in a fuzzy environment.

The rest of this paper is organized as follows. In Section 2, we summarize some basic concepts and definitions about the fuzzy set theory and arithmetic operation of fuzzy numbers. In Section 3, an extended EDAS method is presented to deal with MCDM problems under fuzzy environment. In Section 4, we use a case study of supplier selection to illustrate the procedure and application of the extended EDAS method. In Section 5, a sensitivity analysis is performed to show the validity and stability of the results of the proposed method. The conclusions are discussed in Section 6.

## 2 Basic Concepts and Definitions

Fuzzy set theory was developed by Zadeh [31] for handling problems in which information is imprecise, vague, and uncertain. The term "fuzzy" is related to the situation that we have not well-defined boundaries of the set of activities or observations. Some of the definitions related to fuzzy sets and fuzzy numbers, which are used in this research to extend the EDAS method, are stated as follows:

**Definition 1.** A fuzzy subset $\widetilde{A}$ of a universal set $X$ can be defined by its membership function $\mu_{\widetilde{A}}(x)$ as [36]:

$$\widetilde{A} = \left(x, \mu_{\widetilde{A}}(x)\right)|x \in X \tag{1}$$

where $x \in X$ denotes the elements belonging to the universal set, and $\mu_{\widetilde{A}}(x) : X \mapsto [0, 1]$.

**Definition 2.** A fuzzy number is a special case of a convex, normalized fuzzy subset ($\sup \mu_{\widetilde{A}}(x) = 1$) of the real line $\mathbb{R}(\mu_{\widetilde{A}}(x) : \mathbb{R} \mapsto [0, 1])$ [29].

**Definition 3.** A fuzzy number $\widetilde{A}$ is a trapezoidal fuzzy number (TFN) if its membership function is [21]:

$$\mu_{\widetilde{A}}(x) = \begin{cases} (x - a_1)/(a_2 - a_1) & a_1 \leqslant x \leqslant a_2 \\ 1 & a_2 \leqslant x \leqslant a_3 \\ (a_4 - x)/(a_4 - a_3) & a_3 \leqslant x \leqslant a_4 \\ 0 & otherwise \end{cases} \tag{2}$$

This fuzzy number can also be defined by a quadruplet $\widetilde{A} = (a_1, a_2, a_3, a_4)$. An example of this type of fuzzy numbers is shown in Figure 1.

**Definition 4.** A crisp number $k$ can be represented by a trapezoidal fuzzy number $\widetilde{k} = (k, k, k, k)$.

**Definition 5.** Suppose that $\widetilde{A} = (a_1, a_2, a_3, a_4)$ and $\widetilde{B} = (b_1, b_2, b_3, b_4)$ be two positive trapezoidal fuzzy numbers ($a_1 \geqslant 0$ and $b_1 > 0$) and $k$ is a crisp number. The arithmetic operations with these fuzzy numbers are defined as follows [8]:

- Addition:

$$\widetilde{A} \oplus \widetilde{B} = (a_1 + b_1, a_2 + b_2, a_3 + b_3, a_4 + b_4) \tag{3}$$

$$\widetilde{A} + k = (a_1 + k, a_2 + k, a_3 + k, a_4 + k) \tag{4}$$

- Subtraction:

$$\widetilde{A} \ominus \widetilde{B} = (a_1 - b_4, a_2 - b_3, a_3 - b_2, a_4 - b_1) \tag{5}$$

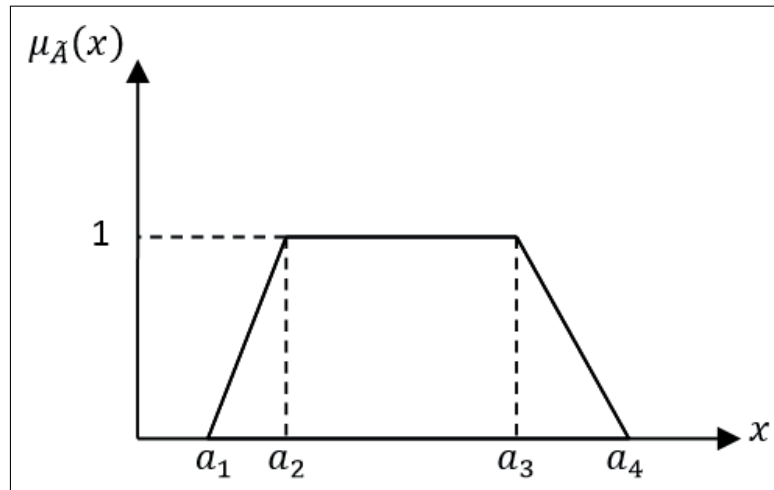$$\widetilde{A} - k = (a_1 - k, a_2 - k, a_3 - k, a_4 - k) \tag{6}$$

Figure 1: A trapezoidal fuzzy number

- Multiplication:

$$\widetilde{A} \otimes \widetilde{B} = (a_1 \times b_1, a_2 \times b_2, a_3 \times b_3, a_4 \times b_4) \tag{7}$$

$$\widetilde{A} \times k = \begin{cases} (a_1 \times k, a_2 \times k, a_3 \times k, a_4 \times k) & \text{if } k \geq 0 \\ (a_4 \times k, a_3 \times k, a_2 \times k, a_1 \times k) & \text{if } k < 0 \end{cases} \tag{8}$$

- Division:

$$\widetilde{A} \oslash \widetilde{B} = (a_1/b_4, a_2/b_3, a_3/b_2, a_4/b_1) \tag{9}$$

$$\widetilde{A}/k = \begin{cases} (a_1/k, a_2/k, a_3/k, a_4/k) & \text{if } k > 0 \\ (a_4/k, a_3/k, a_2/k, a_1/k) & \text{if } k < 0 \end{cases} \tag{10}$$

**Definition 6.** Let $\widetilde{A} = (a_1, a_2, a_3, a_4)$ be a trapezoidal fuzzy number. Then, the defuzzified (crisp) value of this fuzzy number can be defined as follows [15]:

$$\kappa(\widetilde{A}) = \frac{1}{3}\left(a_1 + a_2 + a_3 + a_4 - \frac{a_3 a_4 - a_1 a_2}{(a_3 + a_4) - (a_1 + a_2)}\right) \tag{11}$$

**Definition 7.** Suppose that $\widetilde{A} = (a_1, a_2, a_3, a_4)$ be a trapezoidal fuzzy number. A function, called psi ($\psi$), is defined in the following to find the maximum between a trapezoidal fuzzy number and zero.

$$\psi(\widetilde{A}) = \begin{cases} \widetilde{A} & \text{if } \kappa(\widetilde{A}) > 0 \\ \widetilde{0} & \text{if } \kappa(\widetilde{A}) \leqslant 0 \end{cases} \tag{12}$$

where $\widetilde{0} = (0, 0, 0, 0)$.

## 3  An Extended EDAS Method

As previously stated, the EDAS method was developed by Keshavarz Ghorabaee et al. [17] for multi-criteria inventory classification. It was also demonstrated that the EDAS method is an efficient method to handle MCDM problems. In this section, an extended version of the EDAS

method is proposed to deal with multi-criteria group decision-making problems in the fuzzy environment. In this study, the decision-makers express the weights of criteria and the rating of alternatives with respect to each criterion by linguistic terms. These linguistic terms are quantified by positive trapezoidal fuzzy numbers. Therefore, the concepts and arithmetic operations of the trapezoidal fuzzy numbers are utilized for extending the EDAS method. Suppose that we have a set of $n$ alternatives ($A = \{A_1, A_2, \ldots, A_n\}$), a set of m criteria ($C = \{c_1, c_2, \ldots, c_m\}$) and $k$ decision-makers ($D = \{D_1, D_2, \ldots, D_k\}$). The steps of the extended fuzzy EDAS method are presented as follows:

**Step 1:** Construct the average decision matrix ($X$), shown as follows:

$$X = [\widetilde{x}_{ij}]_{n \times m} \tag{13}$$

$$\widetilde{x}_{ij} = \frac{1}{k} \bigoplus_{p=1}^{k} \widetilde{x}_{ij}^{p} \tag{14}$$

where $\widetilde{x}_{ij}^{p}$ denotes the performance value of alternative $A_i$ ($1 \le i \le n$) with respect to criterion $c_j$ ($1 \le j \le m$) assigned by the $p$th decision-maker ($1 \le p \le k$).

**Step 2:** Construct the matrix of criteria weights, shown as follows:

$$W = [\widetilde{w}_j]_{1 \times m} \tag{15}$$

$$\widetilde{w}_j = \frac{1}{k} \bigoplus_{p=1}^{k} \widetilde{w}_j^{p} \tag{16}$$

where $\widetilde{w}_j^{p}$ denotes the weight of criterion $c_j$ ($1 \le j \le m$) assigned by the $p$th decision-maker ($1 \le p \le k$).

**Step 3:** Construct the matrix of criteria weights, shown as follows:

$$AV = [\widetilde{av}_j]_{1 \times m} \tag{17}$$

$$\widetilde{av}_j = \frac{1}{n} \bigoplus_{i=1}^{n} \widetilde{x}_{ij} \tag{18}$$

The elements of this matrix $\widetilde{av}_j$ represents the average solutions with respect to each criterion. Therefore, the dimension of the matrix is equal to the dimension of criteria weights matrix.

**Step 4:** Suppose that $B$ is the set of beneficial criteria and $N$ is the set of non-beneficial criteria. In this step the matrices of positive distance from average ($PDA$) and negative distance from average ($NDA$) are calculated according to the type of criteria (beneficial and non-beneficial), shown as follows:

$$PDA = [\widetilde{pda}_{ij}]_{n \times m} \tag{19}$$

$$NDA = [\widetilde{nda}_{ij}]_{n \times m} \tag{20}$$

$$\widetilde{pda}_{ij} = \begin{cases} \dfrac{\psi(\widetilde{x}_{ij} \ominus \widetilde{av}_j)}{\kappa(\widetilde{av}_j)} & \text{if } j \in B \\[2mm] \dfrac{\psi(\widetilde{av}_j \ominus \widetilde{x}_{ij})}{\kappa(\widetilde{av}_j)} & \text{if } j \in N \end{cases} \tag{21}$$

$$\widetilde{nda}_{ij} = \begin{cases} \dfrac{\psi(\widetilde{av}_j \ominus \widetilde{x}_{ij})}{\kappa(\widetilde{av}_j)} & \text{if } j \in B \\[2mm] \dfrac{\psi(\widetilde{x}_{ij} \ominus \widetilde{av}_j)}{\kappa(\widetilde{av}_j)} & \text{if } j \in N \end{cases} \tag{22}$$

where $\widetilde{pda}_{ij}$ and $\widetilde{nda}_{ij}$ denote the positive and negative distance of performance value of $i$th alternative from the average solution in terms of $j$th criterion, respectively.

**Step 5:** Calculate the weighted sum of positive and negative distances for all alternatives, shown as follows:

$$\widetilde{sp}_i = \bigoplus_{j=1}^{m} (\widetilde{w}_j \otimes \widetilde{pda}_{ij}) \tag{23}$$

$$\widetilde{sn}_i = \bigoplus_{j=1}^{m} (\widetilde{w}_j \otimes \widetilde{nda}_{ij}) \tag{24}$$

**Step 6:** The normalize values of $\widetilde{sp}_i$ and $\widetilde{sn}_i$ for all alternatives are calculated as follows:

$$\widetilde{nsp}_i = \frac{\widetilde{sp}_i}{\max_i(\kappa(\widetilde{sp}_i))} \tag{25}$$

$$\widetilde{nsn}_i = 1 - \frac{\widetilde{sn}_i}{\max_i(\kappa(\widetilde{sn}_i))} \tag{26}$$

**Step 7:** Calculate the appraisal score $(\widetilde{as}_i)$ for all alternatives, shown as follows:

$$\widetilde{as}_i = \frac{1}{2}(\widetilde{nsp}_i \oplus \widetilde{nsn}_i) \tag{27}$$

**Step 8:** Rank the alternatives according to the decreasing values of appraisal scores $(\widetilde{as}_i)$. In other words, the alternative with the highest appraisal score is the best choice among the candidate alternatives.

## 4 Case Study of Supplier Selection

In this section, we use the proposed fuzzy MCDM method for a real supplier selection case study. The case study is related to a detergent manufacturer. The main product of this company is washing powder. In general, washing powder contains water softeners, bleach, enzymes, surfactants, fragrances, brighteners and many other agents. The company needs to supply the chemical materials of these components from an appropriate supplier for the future of its production. For this aim, the chief executive officer of the company formed a group of five experts from the company's employees. We consider the members of this group as the decision-makers ($DM_1$ to $DM_5$). After a basic assessment performed by this group, five candidates (Supplier 1 to Supplier 5) are remained for further evaluation. These candidates are considered as the alternatives of the MCDM problem ($A_1$ to $A_5$). Six criteria with some sub-criteria are selected by decision-makers for evaluation of suppliers. Figure 2 shows the criteria, sub-criteria and the hierarchical structure of the case study problem.

In this structure, "Total cost" and "Distance" are non-beneficial sub-criteria, and the other sub-criteria are beneficial. The linguistic terms are utilized by decision-makers for evaluation of criteria importance and rating the alternatives on each criterion. These linguistic terms and their corresponding trapezoidal fuzzy numbers are represented in Table 1.

The importance weights of the criteria determined by five decision-makers are shown in Table 2 and the ratings of the alternatives (suppliers) given by these decision-makers under the various criteria are presented in Table 3. The process of using the proposed fuzzy method for this problem is summarized as follows:

*Step 1*: Based on Tables 1 and 3 and Eqs. (13) and (14), the average decision matrix is constructed. The elements of this matrix can be found in Table 4.
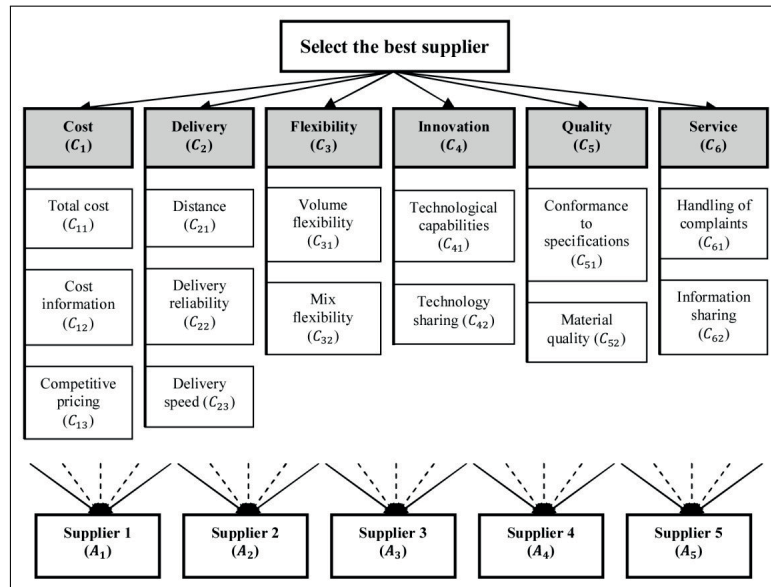
Figure 2: The criteria, sub-criteria and the hierarchical structure of the case study

Table 1: Linguistic terms and their corresponding trapezoidal fuzzy number.

| Terms | TFN for weighting criteria | TFN for rating alternatives |
|---|---|---|
| Very low (VL) | $(0, 0, 0.1, 0.2)$ | $(0, 0, 1, 2)$ |
| Low (L) | $(0.1, 0.2, 0.2, 0.3)$ | $(1, 2, 2, 3)$ |
| Medium low (ML) | $(0.2, 0.3, 0.4, 0.5)$ | $(2, 3, 4, 5)$ |
| Medium (M) | $(0.4, 0.5, 0.5, 0.6)$ | $(4, 5, 5, 6)$ |
| Medium high (MH) | $(0.5, 0.6, 0.7, 0.8)$ | $(5, 6, 7, 8)$ |
| High (H) | $(0.7, 0.8, 0.8, 0.9)$ | $(7, 8, 8, 9)$ |
| Very high (VH) | $(0.8, 0.9, 1, 1)$ | $(8, 9, 10, 10)$ |

*Steps 2 and 3*: Based on Tables 1 and 2 and Eqs. (15) and (16), the average weight of each criterion is calculated (the last column of Table 2), and by using the results of Step 1 and Eqs. (17) and (18) the average solution matrix can be calculated (the last column of Table 4).

*Steps 4 to 8*: Based on the Table 4 and Eqs. (19) to (27), the positive and negative distances are determined and then we calculate the weighted sum of positive and negative distances ($\widetilde{sp}_i$ and $\widetilde{sn}_i$), the normalized values of them ($(\widetilde{nsp}_i$ and $\widetilde{nsn}_i)$) and the appraisal scores for all alternatives. Table 5 shows the selected results of these steps. The defuzzified values of appraisal scores are also represented in the last column of this table. According to Table 5, the ranking order of alternatives is $A_1 \succ A_5 \succ A_2 \succ A_4 \succ A_3$. Therefore, $A_1$ is the best supplier in our assessment.

## 5   Sensitivity Analysis

To show the stability of the results, the aforementioned example is solved using different sets of criteria (sub-criteria) weights. We simulate 14 sets of weights for the 14 sub-criteria of the example. Figure 3 shows the simulated weights in each set. As can be seen in this figure, one sub-criterion has the highest and one sub-criterion has the lowest weight in each set. Figure 4 shows the ranking of each alternative in each set of criteria (sub-criteria) weights. As can be seen in Figure 4, the ranks of all alternatives are relatively stable in different weights of sub-criteria

Table 2: The weight of criteria assigned by decision-makers and the matrix of criteria weights

| **Criteria** | | $DM_1$ | $DM_2$ | $DM_3$ | $DM_4$ | $DM_5$ | $W$ |
|---|---|---|---|---|---|---|---|
| $C_1$ | $C_{11}$ | VH | H | H | VH | VH | $(0.76, 0.86, 0.92, 0.96)$ |
| | $C_{12}$ | ML | M | ML | L | L | $(0.2, 0.3, 0.34, 0.44)$ |
| | $C_{13}$ | M | MH | H | M | M | $(0.48, 0.58, 0.6, 0.7)$ |
| $C_2$ | $C_{21}$ | VH | VH | H | VH | MH | $(0.72, 0.82, 0.9, 0.94)$ |
| | $C_{22}$ | MH | H | MH | MH | M | $(0.52, 0.62, 0.68, 0.78)$ |
| | $C_{23}$ | H | H | H | MH | M | $(0.6, 0.7, 0.72, 0.82)$ |
| $C_3$ | $C_{31}$ | ML | M | ML | M | M | $(0.32, 0.42, 0.46, 0.56)$ |
| | $C_{32}$ | L | VL | VL | L | ML | $(0.08, 0.14, 0.2, 0.3)$ |
| $C_4$ | $C_{41}$ | VL | VL | L | L | VL | $(0.04, 0.08, 0.14, 0.24)$ |
| | $C_{42}$ | VL | VL | VL | VL | L | $(0.02, 0.04, 0.12, 0.22)$ |
| $C_5$ | $C_{51}$ | H | MH | M | M | MH | $(0.5, 0.6, 0.64, 0.74)$ |
| | $C_{52}$ | VH | VH | H | VH | H | $(0.76, 0.86, 0.92, 0.96)$ |
| $C_6$ | $C_{61}$ | ML | M | ML | L | ML | $(0.22, 0.32, 0.38, 0.48)$ |
| | $C_{62}$ | VL | L | ML | ML | L | $(0.12, 0.2, 0.26, 0.36)$ |

Table 3: The ratings of the alternatives with respect to each criterion and each decision-maker

| | | $C_{11}$ | $C_{12}$ | $C_{13}$ | $C_{21}$ | $C_{22}$ | $C_{23}$ | $C_{31}$ | $C_{32}$ | $C_{41}$ | $C_{42}$ | $C_{51}$ | $C_{52}$ | $C_{61}$ | $C_{62}$ |
|---|---|---|---|---|---|---|---|---|---|---|---|---|---|---|---|
| $DM_1$ | $A_1$ | VL | MH | H | M | H | MH | M | H | MH | ML | VH | H | H | MH |
| | $A_2$ | ML | H | H | MH | M | MH | VH | MH | VH | M | L | H | L | MH |
| | $A_3$ | H | M | L | M | L | M | H | MH | L | MH | L | L | M | L |
| | $A_4$ | VH | ML | M | H | H | VH | M | L | L | H | MH | ML | L | H |
| | $A_5$ | M | H | H | L | M | MH | VH | H | H | M | MH | H | L | MH |
| $DM_2$ | $A_1$ | L | MH | MH | M | MH | H | ML | MH | M | L | VH | H | H | H |
| | $A_2$ | M | H | M | M | M | MH | VH | M | H | M | L | MH | VL | M |
| | $A_3$ | H | M | ML | ML | L | M | H | MH | L | MH | L | ML | M | L |
| | $A_4$ | VH | M | M | H | MH | VH | M | L | ML | VH | M | ML | L | H |
| | $A_5$ | M | H | H | VL | M | MH | VH | H | H | M | MH | H | VL | MH |
| $DM_3$ | $A_1$ | L | M | H | ML | H | H | ML | MH | MH | ML | H | MH | MH | VH |
| | $A_2$ | ML | MH | MH | M | MH | MH | H | MH | H | MH | VL | MH | L | M |
| | $A_3$ | MH | ML | ML | M | ML | MH | VH | H | ML | H | VL | ML | MH | L |
| | $A_4$ | H | L | MH | MH | MH | H | ML | VL | ML | VH | M | M | VL | MH |
| | $A_5$ | ML | MH | H | L | ML | H | H | MH | MH | ML | M | VH | VL | M |
| $DM_4$ | $A_1$ | VL | MH | M | ML | H | H | M | H | M | ML | H | H | MH | VH |
| | $A_2$ | ML | H | M | M | MH | H | H | MH | VH | M | VL | H | VL | MH |
| | $A_3$ | H | ML | ML | ML | ML | MH | VH | H | VL | H | VL | L | M | VL |
| | $A_4$ | H | L | MH | MH | MH | VH | ML | ML | ML | VH | M | ML | VL | H |
| | $A_5$ | MH | MH | MH | ML | ML | H | H | MH | H | ML | MH | H | VL | M |
| $DM_5$ | $A_1$ | L | H | MH | M | MH | MH | ML | MH | M | L | VH | MH | H | MH |
| | $A_2$ | M | H | M | MH | M | H | H | M | H | M | L | MH | L | MH |
| | $A_3$ | MH | L | L | M | ML | MH | VH | M | VL | MH | VL | L | MH | L |
| | $A_4$ | VH | L | M | MH | H | VH | ML | L | L | H | MH | ML | VL | MH |
| | $A_5$ | M | H | H | L | M | MH | VH | MH | H | M | H | H | VL | MH |

Table 4: The elements of the average decision-matrix and the average solution matrix

| | $A_1$ | $A_2$ | $A_3$ | $A_4$ | $A_5$ | AV |
|---|---|---|---|---|---|---|
| $C_{11}$ | (0.06, 0.12, 0.16, 0.26) | (0.28, 0.38, 0.44, 0.54) | (0.62, 0.72, 0.76, 0.86) | (0.76, 0.86, 0.92, 0.96) | (0.38, 0.48, 0.52, 0.62) | (0.42, 0.51, 0.56, 0.65) |
| $C_{12}$ | (0.52, 0.62, 0.68, 0.78) | (0.66, 0.76, 0.78, 0.88) | (0.26, 0.36, 0.4, 0.5) | (0.18, 0.28, 0.3, 0.4) | (0.62, 0.72, 0.76, 0.86) | (0.45, 0.55, 0.58, 0.68) |
| $C_{13}$ | (0.56, 0.66, 0.7, 0.8) | (0.48, 0.58, 0.6, 0.7) | (0.16, 0.26, 0.32, 0.42) | (0.44, 0.54, 0.58, 0.68) | (0.66, 0.76, 0.78, 0.88) | (0.46, 0.56, 0.6, 0.7) |
| $C_{21}$ | (0.32, 0.42, 0.46, 0.56) | (0.44, 0.54, 0.58, 0.68) | (0.32, 0.42, 0.46, 0.56) | (0.58, 0.68, 0.74, 0.84) | (0.66, 0.76, 0.78, 0.88) | (0.35, 0.45, 0.49, 0.59) |
| $C_{22}$ | (0.62, 0.72, 0.76, 0.86) | (0.44, 0.54, 0.58, 0.68) | (0.16, 0.26, 0.32, 0.42) | (0.58, 0.68, 0.74, 0.84) | (0.32, 0.42, 0.46, 0.56) | (0.42, 0.52, 0.57, 0.67) |
| $C_{23}$ | (0.62, 0.72, 0.76, 0.86) | (0.58, 0.68, 0.74, 0.84) | (0.46, 0.56, 0.62, 0.72) | (0.78, 0.88, 0.96, 0.98) | (0.58, 0.68, 0.74, 0.84) | (0.6, 0.7, 0.76, 0.85) |
| $C_{31}$ | (0.28, 0.38, 0.44, 0.54) | (0.74, 0.84, 0.88, 0.94) | (0.76, 0.86, 0.92, 0.96) | (0.28, 0.38, 0.44, 0.54) | (0.76, 0.86, 0.92, 0.96) | (0.56, 0.66, 0.72, 0.79) |
| $C_{32}$ | (0.58, 0.68, 0.74, 0.84) | (0.46, 0.56, 0.62, 0.72) | (0.56, 0.66, 0.7, 0.8) | (0.1, 0.18, 0.22, 0.32) | (0.58, 0.68, 0.74, 0.84) | (0.46, 0.55, 0.6, 0.7) |
| $C_{41}$ | (0.44, 0.54, 0.58, 0.68) | (0.74, 0.84, 0.88, 0.94) | (0.08, 0.14, 0.2, 0.3) | (0.16, 0.26, 0.32, 0.42) | (0.66, 0.76, 0.78, 0.88) | (0.42, 0.51, 0.55, 0.64) |
| $C_{42}$ | (0.16, 0.26, 0.32, 0.42) | (0.42, 0.52, 0.54, 0.64) | (0.58, 0.68, 0.74, 0.84) | (0.76, 0.86, 0.92, 0.96) | (0.32, 0.42, 0.46, 0.56) | (0.45, 0.55, 0.6, 0.68) |
| $C_{51}$ | (0.76, 0.86, 0.92, 0.96) | (0.06, 0.12, 0.16, 0.26) | (0.04, 0.08, 0.14, 0.24) | (0.44, 0.54, 0.58, 0.68) | (0.52, 0.62, 0.68, 0.78) | (0.36, 0.44, 0.5, 0.58) |
| $C_{52}$ | (0.62, 0.72, 0.76, 0.86) | (0.58, 0.68, 0.74, 0.84) | (0.14, 0.24, 0.28, 0.38) | (0.24, 0.34, 0.42, 0.52) | (0.72, 0.82, 0.84, 0.92) | (0.46, 0.56, 0.61, 0.7) |
| $C_{61}$ | (0.62, 0.72, 0.76, 0.86) | (0.06, 0.12, 0.16, 0.26) | (0.44, 0.54, 0.58, 0.68) | (0.04, 0.08, 0.14, 0.24) | (0.02, 0.04, 0.12, 0.22) | (0.24, 0.3, 0.35, 0.45) |
| $C_{62}$ | (0.66, 0.76, 0.84, 0.9) | (0.46, 0.56, 0.62, 0.72) | (0.08, 0.16, 0.18, 0.28) | (0.62, 0.72, 0.76, 0.86) | (0.46, 0.56, 0.62, 0.72) | (0.46, 0.55, 0.6, 0.7) |

Table 5: The weighted sum of distances, the normalized values of them and the appraisal scores

| | $\widetilde{sp_i}$ | $\widetilde{sn_i}$ | $\widetilde{nsp_i}$ | $\widetilde{nsn_i}$ | $\widetilde{as_i}$ | $\kappa(\widetilde{sp_i})$ |
|---|---|---|---|---|---|---|
| $A_1$ | (-0.83, 1.8, 3.2, 6.3) | (0.012, 0.15, 0.3, 0.62) | (-0.32, 0.69, 1.2, 2.4) | (0.76, 0.88, 0.94, 1.0) | (0.22, 0.79, 1.1, 1.7) | 0.95 |
| $A_2$ | (-1.3, 0.34, 1.1, 3.1) | (-0.57, 0.54, 1.1, 2.4) | (-0.51, 0.13, 0.44, 1.2) | (0.063, 0.57, 0.79, 1.2) | (-0.22, 0.35, 0.61, 1.2) | 0.49 |
| $A_3$ | (-0.57, 0.26, 0.72, 1.8) | (0.097, 1.9, 3.0, 5.4) | (-0.22, 0.1, 0.27, 0.7) | (-1.1, -0.13, 0.28, 0.96) | (-0.64, -0.018, 0.28, 0.83) | 0.11 |
| $A_4$ | (-0.48, 0.35, 0.88, 2.0) | (-0.19, 1.5, 2.7, 4.9) | (-0.18, 0.13, 0.33, 0.75) | (-0.9, -0.031, 0.41, 1.1) | (-0.54, 0.051, 0.37, 0.91) | 0.20 |
| $A_5$ | (-0.72, 1.2, 2.2, 4.6) | (-0.49, 0.21, 0.66, 1.6) | (-0.27, 0.46, 0.84, 1.8) | (0.4, 0.75, 0.92, 1.2) | (0.064, 0.6, 0.88, 1.5) | 0.76 |
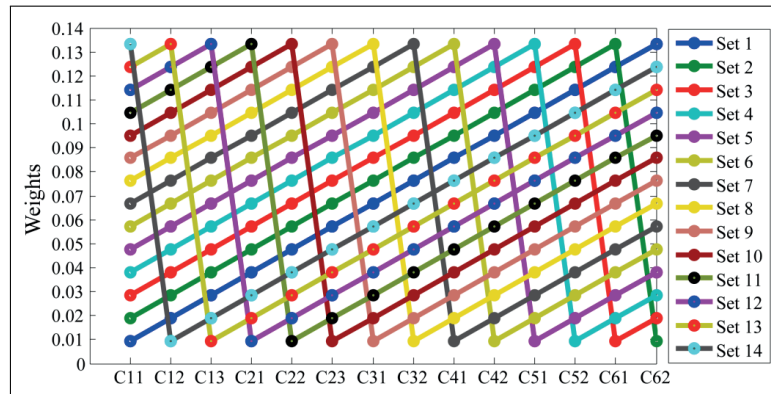
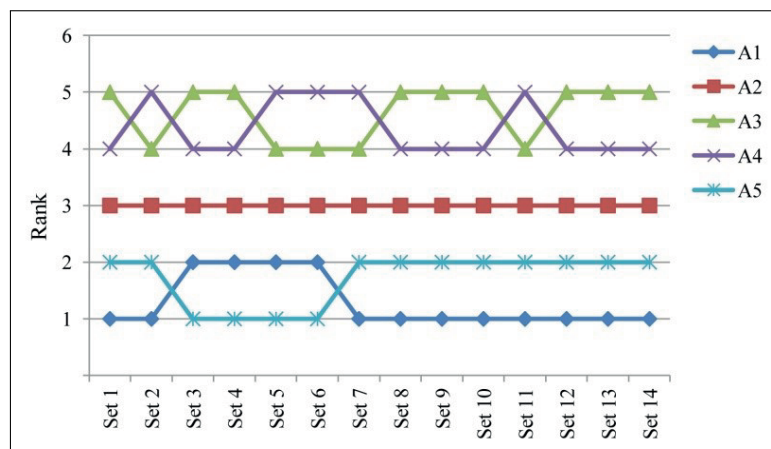Figure 3: The simulated weights for sensitivity analysis



Figure 4: The rank of alternatives in different sets

weights. For example, the best alternative is $A_1$ or $A_5$ and the worst alternative is $A_3$ or $A_4$ in all sets. To show the changes clearly, the shapes of fuzzy appraisal scores are represented in Figure 5. The smooth changes which can be seen in this figure show that the results of the proposed method are stable when the weights of criteria (sub-criteria) are varied. Therefore, we can say that the proposed fuzzy method is efficient for ranking alternatives in an MCDM problem.

## 6 Conclusion

Multi-criteria decision-making is an important sub-discipline of operations research that considers multiple criteria in the decision-making process. Due to uncertainty of data in this process, the problems cannot precisely be modeled by crisp values. Fuzzy MCDM methods are efficient tools to deal with the uncertain decision-making problems and have been used widely because of their ability to solve a broad range of problems in different application fields. These methods can be used in the decision-making software to make some efficient decision support systems [1], [11], [32]. The method presented in this paper will be a basis for development of a novel fuzzy decision-making software or decision support systems, which supports fuzzy data and allows to solve different problems. In this research, the EDAS method, which is an efficient MCDM method, has been developed to handle fuzzy multi-criteria decision-making problems. Linguistic terms determined by trapezoidal fuzzy numbers have been utilized for extending this method. We have used this method in a case study of supplier selection to illustrate the proce-
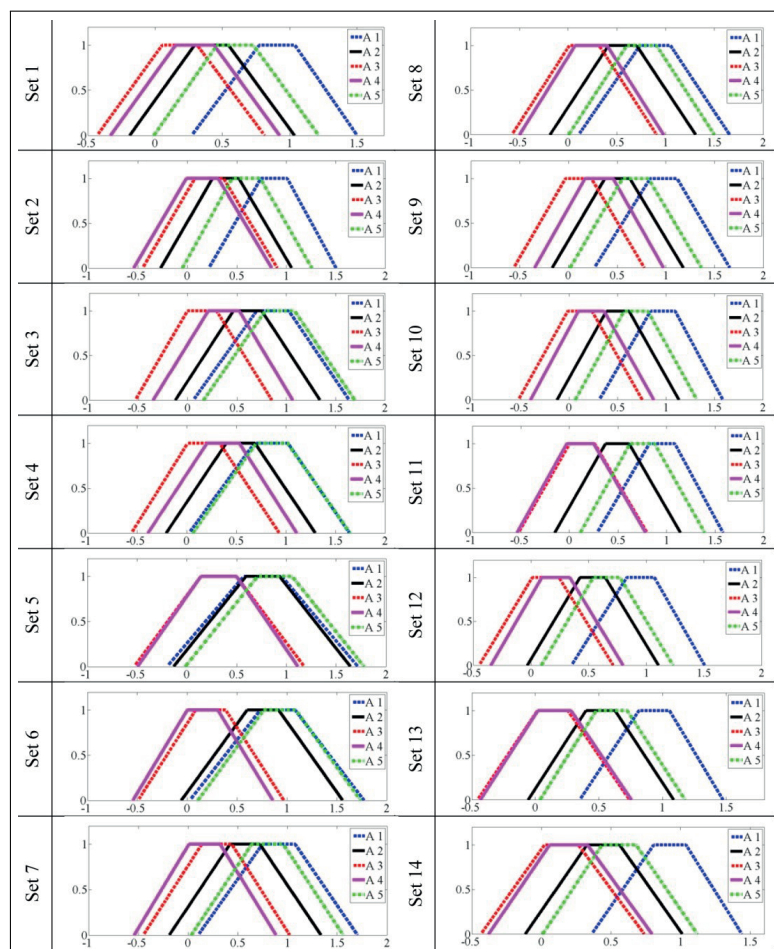
Figure 5: The fuzzy appraisal scores of alternatives in each sets of criteria weight

dure of the proposed method and show the applicability of it in the real-world MCDM problems. A sensitivity analysis has been performed to represent the stability of the results. We have simulated 14 sets of criteria weights to perform this analysis. In each of these sets, one criterion (sub-criterion) has the highest and one criterion (sub-criterion) has the lowest weight. The result of the sensitivity analysis shows the stability of the fuzzy EDAS method in solving multi-criteria decision-making problems.

# Bibliography

[1] Adeli (Ed.), H. (1988); *Expert Systems in Construction and Structural Engineering*, Chapman and Hall, New York.

[2] Baležentis, A.; Baležentis T. (2011); An innovative multi-criteria supplier selection based on two-tuple MULTIMOORA and hybrid data, *Economic Computation and Economic Cybernetics Studies and Research*, 2: 1-20.

[3] Baležentis, T. et al (2014); MULTIMOORA-IFN: A MCDM method based on intuitionistic fuzzy number for performance management, *Economic Computation and Economic Cybernetics Studies and Research*, 48(4): 85-102.

[4] Bogdanovic, D.; Miletic S. (2014); Personnel evaluation and selection by multicriteria decision making method, *Economic Computation and Economic Cybernetics Studies and Research*, 48(3): 179-196.

[5] Brauers, W.K.M. et al (2011); Multimoora for the EU member states updated with fuzzy number theory, *Technological and Economic Development of Economy*, 17(2): 259-290.

[6] Cagri Tolga, A. et al (2013); A fuzzy multi-criteria decision analysis approach for retail location selection, *International Journal of Information Technology and Decision Making*,12(4): 729-755.

[7] Chakraborty, S. et al (2015); Applications of WASPAS method as a multi-criteria decision-making tool, *Economic Computation and Economic Cybernetics Studies and Research*, 49(1): 1-17.

[8] Chen, S.J.; Hwang C.L. (1992); *Fuzzy Multiple Attribute Decision Making: Methods and Applications*, Berlin Heidelberg: Springer.

[9] Dadelo, S. et al (2014); Algorithm of maximizing the set of common solutions for several MCDM problems and it's application for security personnel scheduling, *International Journal of Computers Communications & Control*, 9(2): 151-159.

[10] Elsayed, A. et al (2015); Fuzzy linear physical programming for multiple criteria decision-making under uncertainty, *International Journal of Computers Communications & Control*, 11(1): 26-38.

[11] Filip, F.G. et al (2014); DSS in numbers, *Technological and Economic Development of Economy*, 20(1): 154-164.

[12] Ho, W. et al (2010); Multi-criteria decision making approaches for supplier evaluation and selection: A literature review, *European Journal of Operational Research*, 202(1): 16-24.

[13] Keshavarz Ghorabaee, M. et al (2015); Genetic algorithm for solving bi-objective redundancy allocation problem with k-out-of-n subsystems, *Applied Mathematical Modelling*, 39(20): 6396-6409.

[14] Keshavarz Ghorabaee, M.(2016); Developing an MCDM method for robot selection with interval type-2 fuzzy sets, *Robotics and Computer-Integrated Manufacturing*, 37: 221-232.

[15] Keshavarz Ghorabaee, M. et al (2014); Multiple criteria group decision-making for supplier selection based on COPRAS method with interval type-2 fuzzy sets, *The International Journal of Advanced Manufacturing Technology*, 75(5-8): 1115-1130.

[16] Kar, A.K. (2015); A hybrid group decision support system for supplier selection using analytic hierarchy process, fuzzy set theory and neural network, *Journal of Computational Science*, 6: 23-33.

[17] Keshavarz Ghorabaee, M. et al (2015); Multi-criteria inventory classification using a new method of evaluation based on distance from average solution (EDAS), *Informatica*, 26(3): 435-451.

[18] Keshavarz Ghorabaee, M. et al (2015); Multi-criteria project selection using an extended VIKOR method with interval type-2 fuzzy sets, *International Journal of Information Technology & Decision Making*, 14(5): 993-1016.

[19] Kosareva, N. et al (2015); Personnel ranking and selection problem solution by application of KEMIRA method, *International Journal of Computers Communications & Control*, 11(1): 51-66.

[20] Nieto-Morote, A.; Ruz-Vila F. (2011); A fuzzy AHP multi-criteria decision-making approach applied to combined cooling, heating, and power production systems, *International Journal of Information Technology and Decision Making*, 10(3): 497-517.

[21] Ölçer, A.Y.; Odabaşi A.Y. (2005); A new fuzzy multiple attributive group decision making methodology and its application to propulsion/manoeuvring system selection problem, *European Journal of Operational Research*, 166(1): 93-114.

[22] Pitchipoo, P. et al (2013); Fuzzy hybrid decision model for supplier evaluation and selection, *International Journal of Production Research*, 51(13): 3903-3919.

[23] Sedaghat, M. (2013); A productivity improvement evaluation model by integrating AHP, TOPSIS and VIKOR methods under fuzzy environment (case study: State-owned, partially private and private banks in Iran), *Economic Computation and Economic Cybernetics Studies and Research*, 47(1): 235-258.

[24] Stanujkic, D. (2015); Extension of the ARAS method for decision-making problems with interval-valued triangular fuzzy numbers, *Informatica*, 26(2): 335-355.

[25] Stanujkic, D.; Zavadskas E.K. (2015); A modified weighted sum method based on the decision-maker's preferred levels of performances, *Studies in Informatics and Control*, 24(4): 461-470.

[26] Turskis, Z. et al (2015); A hybrid model based on fuzzy AHP and fuzzy WASPAS for construction site selection, *International Journal of Computers Communications & Control*, 10(6): 113-128.

[27] Turskis, Z.; Zavadskas E.K. (2010); A new fuzzy additive ratio assessment method (ARAS-F). Case study: The analysis of fuzzy multiple criteria in order to select the logistic centers location, *Transport*, 25(4): 423-432.

[28] Wan, S.; Dong J. (2014); Multi-attribute group decision making with trapezoidal intuitionistic fuzzy numbers and application to stock selection, *Informatica*, 25(4): 663-697.

[29] Wang, Y.J.; Lee H.S. (2007); Generalizing TOPSIS for fuzzy multiple-criteria group decision-making, *Computers & Mathematics with Applications*, 53(11): 1762-1772.

[30] Yücenur, G.N. et al (2011); Supplier selection problem in global supply chains by AHP and ANP approaches under fuzzy environment, *The International Journal of Advanced Manufacturing Technology*, 56(5-8): 823-833.

[31] Zadeh, L.A.(1965); Fuzzy sets, *Information and Control*, 8(3): 338-353.

[32] Zavadskas, E.K. et al (1995); *Expert Systems in Construction Industry. Trends, Potential & Applications*, Technika, Vilnius.

[33] Zavadskas, E.K. et al (2013); Multi-criteria assessment model of technologies, *Studies in Informatics and Control*, 22(4): 249-258.

[34] Zavadskas, E.K. et al (2015); Selecting a contractor by using a novel method for multiple attribute analysis: weighted aggregated sum product assessment with grey values (WASPAS-G), *Studies in Informatics and Control*, 24(2): 141-150.

[35] Zavadskas, E.K. et al (2009); Multi-attribute decision-making model by applying grey numbers, *Informatica*, 20(2): 305-320.

[36] Zimmermann, H.J. (2010); Fuzzy set theory, *Wiley Interdisciplinary Reviews: Computational Statistics*, 2(3): 317-332.

# Forecasting Gold Prices Based on Extreme Learning Machine

S. Kumar Chandar, M. Sumathi, S.N. Sivanadam

**S. Kumar Chandar***
Associate Professor,
Christ University, Bangalore, India
*Corresponding author: kumar.chandar@christuniversity.in

**M. Sumathi**
Associate Professor,
Sri Meenakshi Government College For Arts For Women (Autonomous),
Madurai, India
sumathivasagam@gmail.com

**S.N. Sivanandam**
Professor Emeritus,
Karpagam College Of Engineering, Coimbatore, India
sns12.kit@gmail.com

**Abstract:** In recent years, the investors pay major attention to invest in gold market because of huge profits in the future. Gold is the only commodity which maintains its value even in the economic and financial crisis. Also, the gold prices are closely related with other commodities. The future gold price prediction becomes the warning system for the investors due to unforeseen risk in the market. Hence, an accurate gold price forecasting is required to foresee the business trends. This paper concentrates on forecasting the future gold prices from four commodities like historical data's of gold prices, silver prices, Crude oil prices, Standard and Poor's 500 stock index ($S\&P500$) index and foreign exchange rate. The period used for the study is from $1st$ January 2000 to 31st April 2014. In this paper, a learning algorithm for single hidden layered Feed forward neural networks called Extreme Learning Machine (ELM) is used which has good learning ability. Also, this study compares the five models namely Feed forward networks without feedback, Feed forward back propagation networks, Radial basis function, ELMAN networks and ELM learning model. The results prove that the ELM learning performs better than the other methods.
**Keywords:** Feed forward neural networks, Extreme Learning Machine, Gold price forecasting.

## 1 Introduction

Gold is the major commodity in the economic and monetary market. India and china are the major importers among the world and consumes 60 % of the global gold. Every day, the value of the gold increases and cannot be controlled. Nowadays, people tend to invest in gold owing to huge profits in future. The gold prices are closely related with other commodities. A hike in oil prices will have positive impact on gold prices and vice versa. When there is a hike in equities, gold prices goes down. This is because when there is a boom in the stock market, the investors tend to invest the gold money in the equities. Hence, an accurate gold price forecasting is required to foresee the business trends in future.

Soft Computing techniques like Neural Networks, Fuzzy logic, Genetic Algorithms, Particle Swarm Optimization and Simulation Annealing can be used to forecast the gold price. Among the above, Artificial Neural Networks are very accurate and predicts the future very well. Some of the recent studies on gold price forecasting are discussed below.

Gary et al. [1] used neural networks for forecasting Standard & Poor's 500 stock index and gold futures prices. Their forecast was based on the historical prices of the stock index and gold prices. Malliaris et al. [2] used times series techniques and Artificial Neural Networks for forecasting the prices of gold, oil and Euro. They gave an interrelationship among the three and proposed ANN technique to forecast the individual variables. And they concluded that both short term and long term relationship exist between the three variables. Mehdi Bijari et al. [3] proposed a hybrid ARIMA model using Fuzzy logic and Artificial Neural network for forecasting exchange rates and gold prices. Fuzzy logic and ANN was hybridized with the ARIMA model in order to get accurate results. The results explained that the proposed technique predicts the future prices accurately than the other methods. Ali et al. [4] uses Multilayer perceptron neural network model for predicting the changes in stock prices and gold prices. The data used in this study was Tehran's Stock Exchange (T.S.E). The results showed that the ANN models perform better than the traditional statistical techniques. Deepika et al. [5] proposed Autoregressive Integrated Moving Average (ARIMA) models for forecasting the monthly gold price from period 1980 to 2012. This paper also finds the factors influencing the gold price using multiple regression analysis. Lazim Abdullah [6] used Auto-Regressive Integrated Moving Average (ARIMA) model for forecasting the selling prices of gold bullion coins. They forecasted that the selling prices are in the upward direction and the investors can invest money in the gold bullion coins.

Trian et al. [7] explored gold equivalent for forecasting steel prices in pipeline projects. This paper elaborates on how the steel prices depend on the gold price using a regression model of the historical data. Massarrat Ali Khan et al. [8] used Box-Jenkins, ARIMA model for forecasting the gold prices. The period used for the study was from January 2003 to March 2012. They concluded that ARIMA model was the suitable model for forecasting the gold price. Bai Li [9] proposed Improved Artificial Bee colony algorithm (ABC) for forecasting the gold price modelling using Wavelet Neural Networks. The experimental results showed that the Improved ABC algorithm works more effective than the conventional ABC algorithm. Fengyi Zhang et al. [10] proposed the methods for forecasting gold price using Radial Basis Function (RBF) neural networks and hybrid fuzzy clustering algorithm. Principal Component Analysis was used to unite technical indicators namely Moving Average, Receive Operator Characteristics and P-Accuracy rate. The results showed that the hybrid fuzzy clustering algorithm works better than the RBF neural network. Hossein Mombeini et al. [11] developed a defined model for forecasting gold prices. The performance measures are used to access the accuracy of the model. They have presented gold price forecasting using two models namely artificial neural networks and ARIMA models and showed that the ANN model works better than the ARIMA model in terms of performance metrics.

This paper concentrates on forecasting the future gold prices from four commodities like historical data's of gold prices, silver prices, Crude oil prices, Standard & Poor's 500 stock index (S & P 500) index and foreign exchange rate. The period used for the study is from $1st$ January 2000 to $31st$ April 2014. In this paper, a learning algorithm for single hidden layered Feed forward neural networks called Extreme Learning Machine (ELM) is used which has good learning ability. Also, this study compares the three models namely Feed forward networks without feedback, Feed forward back propagation networks and ELM learning model.

The organization of the paper is as follows: Section 1 summarizes on the Introduction and Literature survey. Section 2 illustrate on the research data used in this study, Section 3 explains the ELM algorithm. Section 4 explains on the application of ELM algorithm to gold price forecasting. Section 5 discusses on the results, Section 6 concludes the paper and Section 7 enlighten on the references used in the study.

## 2  Research data

The gold prices are normally related with other commodities like crude oil, stock prices, silver prices etc. The period of the study is from 1st January 2000 to 31$st$ April 2014. The monthly data are used to forecast the future gold prices. In this study, the future gold prices are forecasted from four commodities like historical data's of gold prices, silver prices, Crude oil prices, Standard & Poor's 500 stock index (S & P 500 index and foreign exchange rate.

The gold price and silver price data was gathered from http://www.bullion-rates.com/gold /INR/2014-4-history.htm, crude oil price data was collected from http://www.indexmundi// .com/commodities, Bombay stock exchange data was accumulated from http://bseindia.com website and foreign exchange data was collected from http://fxtop.com/en/historical-exchange-rates.phpMA=1.

In the sample data set, the input attributes contains the average monthly data of gold price per oz, the monthly average data of crude oil, the monthly average data of silver price, the monthly average value of US dollars in terms of Indian rupees the monthly average values of S & P 500 stock data and the target attribute has the actual gold prices.

The summary statistics of the research data is calculated from the input data by finding the minimum, maximum, mean and standard deviation of these values.

**Table 1 Statistics of the research data**

| Input Data | Maximum | Minimum | Mean | Standard Deviation |
|---|---|---|---|---|
| Gold Price | 95,194.24 | 12,100.23 | 39,317.532 | 8,592.43 |
| Crude Oil | 6,928.11 | 887.42 | 3091.0277 | 1716.6898 |
| Silver Price | 1,899.62 | 197.92 | 695.25052 | 517.21883 |
| USD | 63.90 | 39.26 | 47.4437 | 5.037152 |
| S&P 500 stock | 8,592.43 | 850.56 | 4398.487849 | 2500.74607 |

## 3  Extreme Learning Machine

Single layer feed forward network (SLFN) is one of the most common network architecture. It is widely used in many applications like classification and regression. Gradient descent learning methods like SLFN networks are time consuming and have serious issues such as over fitting, local minima problem and some parameters need to be tuned manually. Some researchers have discovered many possibilities for SLFN networks. Among all, Huang et al. [12–14] proposed that randomly chosen input weights and the bias weights in all the iterations with utmost N hidden neurons will bring desirable accuracy. Moore-Penrose generalized pseudo inverse is used for calculating the output weights. The learning algorithm is faster and has good generalization ability. This type of learning is known as 'Extreme Learning Machine' (ELM).

The salient features of ELM are specified in a simple three step algorithm. In contrast to gradient descent methods, ELM need not see the training data before generating the hidden node parameters. ELM algorithm works for all piecewise continuous activation function. ELM tries to find solution for many problems like local minima, time consuming and tuning the parameters. It works easier than other learning algorithms such as neural networks and support vector machine. The brief overview on ELM algorithm is discussed below:

### 3.1  Extreme Learning Machine

A single layer feed forward network with $x_1, x_2, ..., x_m,$ input nodes, $h_1, h_2, ..., h_n,$ hidden nodes and $t_i$ be the target node is shown in Fig.1.
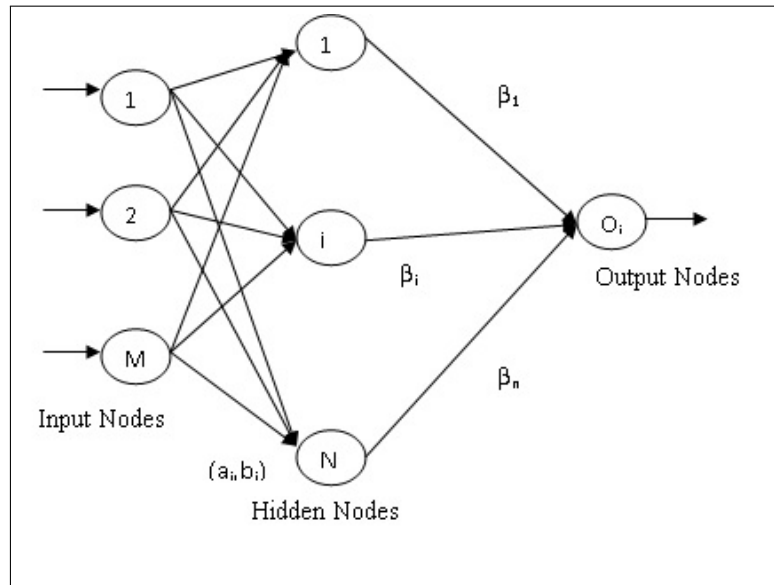
Figure 1:  Single layer feed forward network

Let $(a_i, b_i)$ be the weights connecting from input layer to hidden layer and $\beta_1, \beta_2, ..., \beta_n$ be the weights of the nodes connecting from hidden layer to the output layer. Let 'g' be the piecewise continuous activation function. The hidden layer outputs are given as

$$\sum_{i=1}^{N} [\beta_i g(a_i, b_i, x_j)] = t_j, j = 1, ..., N \tag{1}$$

Equation (1) can be rewritten as $\beta H = T$. Here $H$ is called the hidden layer output matrix , which can be expressed as follows,

$$H(a_1, ..., a_N; b_1, ..., b_N; x_1, ..., x_M) = \tag{2}$$

$$\begin{pmatrix} G(a_1, b_1, x_1) & . & G(a_N, b_N, x_1) \\ . & . & . \\ G(a_1, b_1, x_M) & . & G(a_N, b_N, x_M) \end{pmatrix}$$

$$\beta = [\beta_1 \beta_2 ... \beta_n]^T \text{ and } T = [t_1 t_2 ... t_n]^T \tag{3}$$

In the hidden output matrix, each value represents the hidden output values of their corresponding node. The three step ELM learning algorithm is as follows: In a Single layer feed forward neural network, $(x_i, t_i)$ be the training pair and $g(a, b, x)$ be the hidden node output function.

Step 1: Initially hidden nodes are chosen randomly, $(a_i, b_i)$ where $i = 1, 2, 3, ..., N$

Step 2: Calculate the hidden layer output matrix H

Step 3: Calculate the output weights $\hat{\beta}$ where $\hat{\beta} =$ T. Here represents the Moore-Penrose inverse of hidden layer output matrix H.

# 4   An application of ELM learning to Gold price prediction

In this section, ELM training methodology is applied to gold price prediction. The proposed architecture is shown in Fig.2. The gold prices are normally related with other commodities like crude oil, stock prices, silver prices etc. The period of the study is from $1st$ January 2000 to $31st$ April 2014. In this figure, monthly average price of five parameters like gold price, crude oil, silver price, USD and S&P 500 stock price are taken as inputs for ELM learning network. The output of this network gives the next month's gold average price. All the hidden nodes weights are chosen randomly. First, the hidden node output values are calculated from equation (1). Then the output of this network is calculated by multiplying outputs of the hidden nodes with the weights of the hidden node and the output nodes.
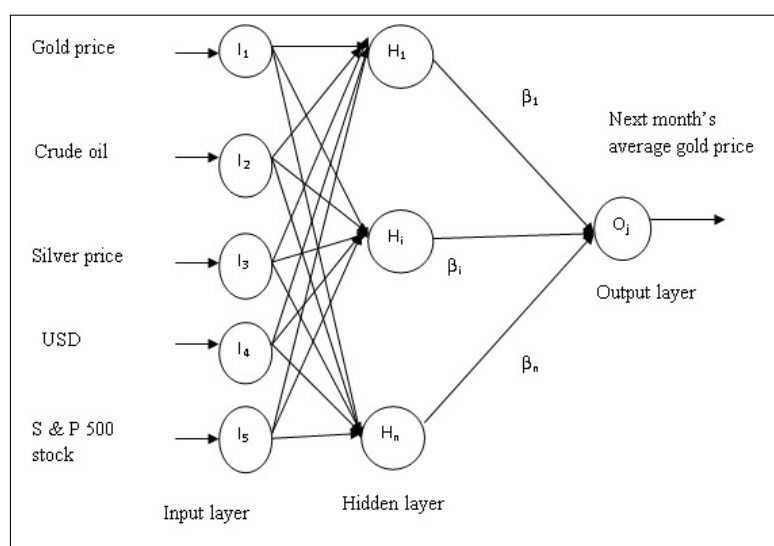


Figure 2:  Architecture of the proposed system

# 5   Results and Discussions

All the implementations are carried out using MATLAB R2009 running in an ordinary PC with Pentium IV processor with 2.40 GHz speed and 256 MB of RAM. . The period of the study is from 1st January 2000 to $31st$ April 2014. The monthly data are used to forecast the future gold prices. In this study, the future gold prices are forecasted from four commodities like historical data's of gold prices, silver prices, Crude oil prices, Standard & Poor's 500 stock index (S & P 500) index and foreign exchange rate. Among the data, 70% of the data is used for training, 15% is used for validation and 15% of the data is used for testing.

The total number of trading days is 86 from ($1st$ Jan 2000 - $31st$ Apr 2014). All the ANN models are predicting next month's average gold value. The details of the historical datasets for all the prediction models are listed in Table 2

**Table 2 Details of Historical dataset**

| Details of the dataset | Total number of trading days | training Sample | validation Sample | Testing Sample |
|---|---|---|---|---|
| Monthly average gold price Monthly average silver price Monthly average Crude oil price Monthly average S&P 500- stock index Monthly average US- dollars in Indian rupees | 172 | 120 | 26 | 26 |

ELM learning algorithm is implemented and compared with other four existing neural networks such as feed forward neural network, back propagation network, Radial basis function and elman networks.

## 5.1 Feed forward networks without feedback

A network is said to be feed forward network when the outputs are not directed back as inputs to the same or preceding layer. In this network, the information moves only in one direction and there is no feedback. All the layers are trained using Levenberg-Marquardt (TRAINLM) function and INITNW and TRAINS functions are used for adaptation of weights. During training process, this network has been given with 1000 epochs. But, it achieves the best performance goal at $13th$ iterations. The training time, training accuracy, testing time and testing accuracy of this network is given in Table 3.

## 5.2 Feed forward back propagation networks

Back propagation networks are multi-layered feed forward networks trained with respect to the back propagation error algorithm. This is the most widely used network. Here, the outputs are directed back as inputs to the same or preceding layer nodes. Hence in this model, the function **'MAPMINMAX'** is used to reduce the noise in the dataset. Training is done with the Levenberg-Marquardt **'TRAINLM'** training function and back propagation weight/bias learning is done using **'LEARNGDM'** function. Adaption is done with **'TRAINS'** which updates weights with the specified learning function. The transfer function **'TANSIG'** function is used for hidden layers and **'PURELIN'** function for output layer. Performance is measured according to the mean square error **'MSE'** performance function. This model runs up to 11 iterations and achieves the best performance goal. The training time, training accuracy, testing time and testing accuracy of this network is given in Table 3.

## 5.3 Radial basis function network

Radial Basis Function Network is a particular type of Feed Forward Network used for approximating the functions and recognizing the patterns. The architecture of the network consists of three layers namely, the input layer, hidden layer and the output layer.

## 5.4 ELMAN networks

The ELMAN networks are a form of recurrent neural networks. A three layer feed forward network where a set of 'Context Units' are attached to the hidden layer. At each time step, a copy of hidden layer unit is copied onto the Context unit having a weight of one. Thus the network is learnt by the current input signals, a copy of previous hidden layer unit's i.e context

units and the output of the network. The context unit can be considered as a one of the inputs to the hidden layer.

## 5.5   ELM learning algorithm

In this study, the weights of the hidden nodes are chosen randomly and the number of hidden nodes is varied from 5 to 20. But the best training and testing accuracy was achieved when the number of hidden nodes was 10. When compared with the other two networks, ELM achieves 97.5% for training and 93.82% for testing. The performance of ELM algorithm with respect to gold price prediction is shown is Table 3.

**Table 3 Performance comparison of different neural networks**

| Algorithm | Training | | Testing | |
|---|---|---|---|---|
| | Training Time | Training Accuracy | Testing Time | Testing Accuracy |
| ELM | 3.1682 | 97.65 % | 0.05272 | 93.82 % |
| Feed forward networks without feedback Zabir Haider Khan et al. [5] | 4.1184 | 93.82 % | 0.3772 | 91.14 % |
| Feed forward Back Propogation networks Malliaris et al. [2] | 7.6752 | 92.41 % | 0.5389 | 90.02 % |
| Radial basis Function Fengyi Zhang et al. [10] | 5.1589 | 95.37 % | 0.1839 | 92.58% |
| Elman Networks | 6.9384 | 94.28% | 0.20915 | 91.67% |
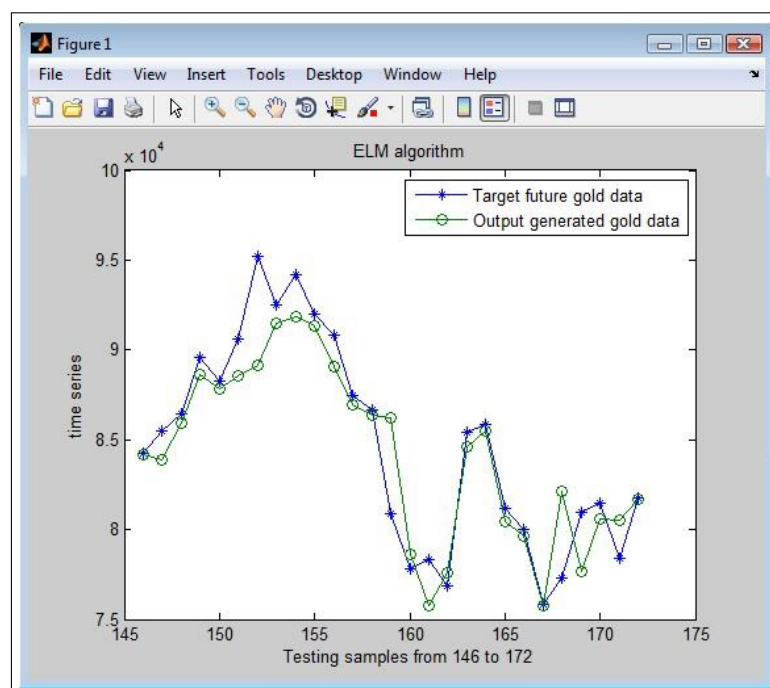


Figure 3:   Comparison graph of Predicted monthly average gold value Vs Target gold price

The graph is drawn between monthly average gold value and time series which is shown in Fig.3. In this graph, the predicted gold prices are mapped and it is compared with the actual gold prices. From the graph, it is understood that this proposed model predicts the future gold prices more accurately with the actual gold prices.

## 6  Conclusions

An accurate gold price forecasting is necessary for predicting the future gold price. Hence in this paper, a new learning algorithm called ELM learning is applied which has good learning ability and generalization capability. The period used for the study is from $1st$ January 2000 to $31st$ April 2014. Since, the gold price is related with other commodities, four commodities like like historical data's of gold prices, silver prices, Crude oil prices, Standard & Poor's 500 stock index (S & P 500) index and foreign exchange rate are given as inputs to the single layer feed forward network Also, this study compares the three models namely Feed forward networks without feedback, Feed forward back propagation networks and ELM learning model. The results clearly explain that the ELM algorithm achieve approximately 3% increase in the training and testing efficiency when compared with the other networks.

## Bibliography

[1] Gary Grudnitski, Larry Osburn, Forecasting S &P and Gold Futures Prices: An Application of Neural Networks, *The Journal of Futures Markets*, 13(6) : 631-643, 1993.

[2] A.G. Malliaris and Mary Malliaris, Time Series and Neural Networks Comparison on Gold, Oil and the Euro, Proceedings of International Joint Conference on Neural Networks, Atlanta, Georgia, USA, June 14-19, 2009.

[3] MehdiBijari, Gholam AliRaissi Ardali, Improvement of Auto-Regressive Integrated Moving Average models using Fuzzy logic and Artificial Neural Networks (ANNs), *Neurocomputing*, 72 : 956-967, 2009.

[4] Ali ghezelbash, Predicting Changes in Stock Index and Gold prices to Neural Network approach, *The Journal of Mathematics and Computer Science*, 4 : 227-236, 2012.

[5] Deepika M G, Gautam Nambiar and Rajkumar M, Forecasting price and analysing factors influencing the price of gold using ARIMA model and multiple regression analysis,*International Journal of Research in Management, Economics and Commerce*, 2(11) : Nov 2012.

[6] Lazim Abdullah, ARIMA model for gold bullion coin selling prices forecasting, *International Journal of Advances in Applied Sciences*, 1(4) : 153-158, 2012.

[7] Trian Hendro Asmoro, Exploring Gold Equivalency for forecasting steel prices on Pipeline projects, 2(5) : 1-22, May 2013.

[8] Dr. M. Massarrat Ali Khan, Forecasting of Gold Prices (Box Jenkins Approach), *International Journal of Emerging Technology and Advanced Engineering*, 3(3) : 2013.

[9] Bai Li, Research on WNN Modelling for Gold Price Forecasting Based on Improved Artificial Bee Colony Algorithm, Hindawi Publishing Corporation Computational Intelligence and Neuroscience Vol. 2014, pp. 1-10, 2014.

[10] Fengyi Zhang and Zhigao Liao, Gold price forecasting based on RBF neural network and hybrid fuzzy clustering algorithm, Proceedings of the seventh International Conference on Mangement Science and Engineering Management, Lecture Notes in Electrical Engineering, Vol. 1, pp. 73-84, 2014.

[11] Hossein Mombeini and Abdolreza Yazdani-Chamzini, Modeling Gold price via Artificial Neural Network, *Journal of Economics, Business and Management*, 3(7) : 2015.

[12] Guang-Bin Huang, Lei Chen, Chee-Kheong Siew, Universal Approximation Using Incremental Networks with Random Hidden Computational Nodes IEEE Transactions on Neural Networks, 17(4) : 879-892, 2006.

[13] Guang-Bin Huang, Qin-Yu Zhu, Chee-Kheong Siew, Extreme Learning Machine: Theory and Applications,*Neurocomputing*, 70 : 489-501, 2006.

[14] Guang-Bin Huanga, Lei Chena, Convex Incremental Extreme Learning Machine, *Neurocomputing*, 70 : 3056-3062, 2007.

# Increasing Face Recognition Rate

B. Lagerwall, S. Viriri

**Brett Lagerwall**
**Serestina Viriri***
School of Mathematics, Statistics and Computer Science
University of KwaZulu-Natal, Westville Campus
Durban, South Africa
*Corresponding author: viriris@ukzn.ac.za

> **Abstract:** This paper describes and discusses a set of algorithms which can im-
> prove face recognition rates. These algorithms include adaptive K-Nearest Neighbour,
> adaptive weighted average, reverse weighted average and exponential weighted aver-
> age. Essentially, the algorithms are extensions to the basic classification algorithm
> used in most face recognition research. Whereas the basic classification algorithm
> selects the subject with the shortest associated distance, the algorithms presented in
> this paper manipulate and extract information from the set of distances between a
> test image and the training image set in order to obtain more accurate classifications.
> The base system to which the algorithms are applied uses the eigenfaces technique
> for recognition with an adapted Viola and Jones algorithm for face extraction. Most
> of the algorithms proposed show a consistent improvement over the baseline test.
> **Keywords:** Face Recognition, Eigenfaces, Classification Algorithms, Weighting Al-
> gorithms.

## 1 Introduction

The process of obtaining the identity of a person from an image can be successfully per-
formed by only looking at his/her face. This typically involves a face detection stage and a face
recognition stage (taking detected faces and classifying them using an already existing database
of faces).

The full potential of face recognition applications has not been realized, since most suffer from
an inability to handle light and pose variations [1]. Yet, face recognition remains an important
topic in computer vision because of the large number of real-world scenarios it can be applied
to. Senior and Bolle [1] state that the three main application domains for face recognition are
access control, identification systems and surveillance. It is evident that face recognition systems
falling into these three domains have in fact become a part of our every day life. Example usage
cases of the three domains are: access control systems in security environments (e.g. banking),
identification systems in websites such as Facebook and surveillance systems which compare faces
against a threat list in sporting events.

Moreover, humans are becoming increasingly reliant on face recognition systems to achieve
day to day tasks. Hence, researchers continue to focus on methods of improving the current
recognition rates.

The rest of the paper is structured as follows: *Section 2* explores the state-of-the-art of face
recognition, *Section 3* gives a brief overview of preprocessing, *Section 4* describes an overall face
recognition system, *Section 5* explores the novel classification techniques, *Section 6* presents
experimental results and discussion; and *Section 7* draws the conclusions and future work.

## 2 Related Work

Lin [2] shows that face recognition is generally broken down into two modules. These are:

- A feature extractor which transforms the pixels of a face into a useful vector representation.

- A pattern recognition module which searches the database to find the best match for the inputted face.

However, it must be noted that the generic face recognition framework shown by Lin [2] is only concerned with classifying a face. A large number of algorithms will pre-process the face images before any classification occurs.

One of the earliest techniques used in face recognition was performed by Turk and Pentland [3]. They used principal component analysis (PCA) to encode facial images in what they call an information theory approach. Basically, all of the faces in a face database are manipulated to form a set of eigenvectors (eigenfaces in face recognition literature [4]). Each of the original faces can be reconstructed via linear combinations of the eigenvectors.

For classification, Turk and Pentland [3] reconstruct the input image by applying weights to each of the eigenvectors. The vector of weights for the input image is compared against the respective weight vectors for each of the images in the database. The subject in the input image is classified to be the subject in the database with the closest match.

Moon and Phillips [4] attempt to improve on the eigenfaces technique by introducing various ideas and optimizations. Most notably, they try using different nearest-neighbour distance classifiers. However, recognition rates for frontal, upright facial images (used in this study) do not seem to dramatically increase from the baseline PCA algorithm developed by Turk and Pentland [3].

Another face recognition system using an information theory approach was created by Liu and Weschler [5]. Their system uses independent component analysis (ICA) instead of PCA, since ICA provides a more powerful data representation. Improvements range between 0 and 4 percent depending on the number of features used [5].

Face recognition algorithms which do not use the information theory (or encoding of information) approach are less common. However, Bronstein et al. [6] attempted to use a 3D model of a face in order to overcome weaknesses suffered by 2D systems (head orientation and facial expressions). Other common methods of performing face recognition involve using physiological biometrics.

Zhang et. al. [15] compared and contrasted the sparse representation [18] and collaborative representation techniques ( [16], [20]) for face recognition. The sparse representation based classification first codes a testing sample as a sparse linear combination of all the training samples, and then classifies the testing sample by evaluating which class leads to the minimum representation error. While the collaborative representation technique is based on the regularized least square. The experimental results show that both collaborative representation and sparse representation achieved accuracy rate of 93.7% on AR database. Furthermore, collaborative representation has significantly less complexity than sparse representation based classification.

Hao et. al. ( [17], [21]) proposed a novel method, called heteroscedastic sparse representation based classification which addresses the complexity problem of sparse representation based classification. In the presence of noises, the sparse representation based classification model exists heteroscedasticity, which makes residual estimation inefficient. Therefore, heteroscedastic correction must be carried out for homoscedasticity by weighting various residuals with heteroscedastic estimation. The experimental results show that heteroscedastic sparse representation based classification has significantly less complexity than sparse representation based classification, while it is more robust.

Robust face recognition via sparse representation [18] considered the problem of automatically recognizing human faces from frontal views with varying expression and illumination, as well as occlusion and disguise. They cast the recognition problem as one of classifying among multiple

linear regression models, and argue that new theory from sparse signal representation offers the key to addressing this problem. This new framework provides new insights into two crucial issues in face recognition: feature extraction and robustness to occlusion.

Furthermore, Wagner et. al. [19] proposed a conceptually simple face recognition system that achieves a high degree of robustness and stability to illumination variation, image misalignment, and partial occlusion. The system uses tools from sparse representation [18] to align a test face image to a set of frontal training images. They demonstrated how to capture a set of training images with enough illumination variation that they span test images taken under uncontrolled illumination. Their system can efficiently and effectively recognize faces under a variety of realistic conditions, using only frontal images under the proposed illuminations as training.

Many of the face recognition methods reviewed used different nearest-neighbour distance classifiers to calculate the distance between a test image and a training image. However, once the distances were calculated, the test image with the smallest distance was always selected to be the best match. This paper takes the classification process one step further by analyzing the results which can be achieved after post-processing the set of calculated distances.

## 3    Preprocessing

Before performing face recognition, a region of interest (ROI) within the image must be extracted. A modified version of the Viola and Jones [7] face detection algorithm was chosen for this purpose. The key points and modifications are mentioned below.

### 3.1    Classifier

A drawback to building a classifier is the sheer amount of training data required (5000 facial images and 10000 non-facial images in Viola and Jones [7]). Thus, an already available classifier is used: the haarcascade_frontalface_default classifier provided with OpenCV [8].

### 3.2    Passing the Classifier

The classifier being used consists of a number of stages and each stage consists of a number of features. At a particular stage, a sub-window can only pass that stage if the sum of the values generated by testing various features (specified in the haarcascade_frontalface_default classifier) is above a certain threshold. For the sub-window to be considered as a face, it must pass all 25 stages.

### 3.3    Merging Detections

Viola and Jones [7] said that they merged all overlapping detections. However, if two faces are close together this could accidentally be counted as a single detection. Instead, a merging algorithm partially based on work done by Rowley et al. [?] was constructed. For each pair of rectangles $i$ and $j$, the rectangles can be said to be detecting the same face if both (1) and (2) hold.

$$euclideanDistance(c_i, c_j) \leq t \times width(i) \tag{1}$$

$$euclideanDistance(c_i, c_j) \leq t \times width(j) \tag{2}$$

where $c_i$ is the centre of rectangle $i$, $c_j$ is the centre of rectangle $j$ and $t$ is a threshold chosen to be 0.2 [9].

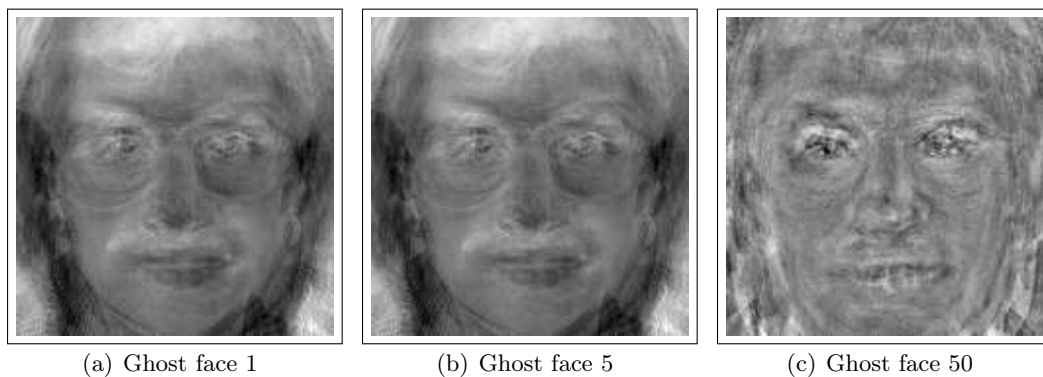| (a) Ghost face 1 | (b) Ghost face 5 | (c) Ghost face 50 |

Figure 1: Showing example ghost faces.

# 4  Face Recognition

The eigenfaces technique is used for face recognition. The key advantages of this algorithm are its quick classification of the probe/test image and its ease of implementation.

## 4.1  Training

Recognition must be performed against a base set of known images. This set is typically called the training set. On each image in the training set, illumination normalization is performed using:

$$image_i = \frac{image_i}{max} \tag{3}$$

where $image_i$ is the $ith$ pixel of the image and $max$ is the largest value of any of the pixels in the image. Then, the basic steps of the eigenfaces algorithm from Turk and Pentland [3] are performed on the training set, involving:

- Mapping the pixel intensities of an image onto a face vector. All of the face vectors from the training set are then placed into a matrix.

- Performing various matrix operations, including eigenvalue decomposition, to obtain eigenfaces or ghost faces (see Figure 1).

- Calculating a weight matrix, where each weight represents the amount to which an eigenface counts towards making up an image.

## 4.2  Classification

When a testing image is inputted, the algorithm must be able to classify the face in the image as one of the subjects in the database. Again, the steps described in Turk and Pentland [3] are performed on the testing image, eventually resulting in a matrix of weights specifying the contribution of each of the eigenfaces in making up the test image.

These weights are then compared to the weights of the training images/database images. A distance classifier (Euclidean distance in this research) is used to determine the distance between the test image and each of the training images. Typically, the person in the test image is classified to be the person in the training set who has the smallest distance between their training image and the testing image.

# 5  Novel Classification Algorithm – Introduction

In traditional face recognition algorithms, a subject in a test image is classified as the subject in an image in the database against which it has the shortest distance. More specifically, if all of the distances calculated between the $n$ training images in the database and the test image are sorted and thus ranked from smallest to biggest, the subject in a test image is classified as the subject in a training image that corresponds to the first distance (or shortest distance) in the sorted list.

If a database contains only one image of each subject, then taking the top match is the only logical classification. However, if a database contains multiple images per subject, then a number of other classification possibilities occur. Described below are some of the classification algorithms proposed which can improve the recognition rates.

Many of the algorithms described rely on the same mathematical foundations. Thus, let us define the following:

| | |
|---|---|
| $n$ | number of images |
| $m$ | number of subjects |
| $k$ | a percentage of the images in the sorted list |
| $k\prime$ | a percentage of the images of a subject |
| $S_x$ | the set of training images of subject $x$ |
| $S_{xk\prime}$ | the set containing the top $k\prime$ percent of training images of subject $x$ |
| $|S_{xk}|$ | the number of images of subject $x$ in the top $k$ percent |
| $I_j$ | the distance between the $j_{th}$ training image and the testing image |
| $w_j$ | the weight applied to the $j_{th}$ training image |

Note that where applicable, the algorithms will use a $k$ percent of images, rather than $k$ images. This is because using a percentage allows for better scaling when subjects in the same database have a different number of images.

# Novel Classification Algorithm – Algorithm Description

## 5.1  Top Match

The test image is classified as the top (or first) image in the sorted list. This algorithm is used as the baseline for comparisons.

## 5.2  Top-k Average

The top $k$ percent of images from the sorted list are chosen. Within the chosen images, the average distance from the images of each subject to the test image is calculated. The subject with the smallest average is selected. More specifically, the subject with the smallest value defined by (4) is chosen.

$$SubjectAvgK_x = \frac{\sum_{j=1}^{nk} I_j}{|S_{xk}|} \quad I_j \in G \tag{4}$$

where G is defined by:

$$G = \{I_p | p \in S_x\} \tag{5}$$

### 5.3 Adaptive K-nearest Neighbour

The K-nearest Neighbour algorithm is commonly used to solve pattern recognition problems. However, its performance suffers when subjects have differing numbers of training images. The Adaptive K-nearest Neighbour attempts to rectify this.

The top $k$ percent of images from the sorted list are chosen. The total number of images of each subject within the top $k$ percent of images is obtained. This total within $k$ for each subject is then divided by the total number of images of the subject in the database – thus forming a ratio of the subject which falls within the $k$ images. The subject with the highest ratio defined by (6) is chosen.

$$SubjectRatio_x = \frac{|S_{xk}|}{|S_x|} \tag{6}$$

### 5.4 $K\prime$ Subject Average

The top $k\prime$ percent of images of each subject are chosen. The average of the distances pertaining to the top $k\prime$ percent of images of a subject is calculated. The subject with the lowest average is selected. It must be re-emphasized that in this algorithm, the $k\prime$ percent is used for each subject, rather than the whole sorted list. The subject with the lowest average defined by (7) is chosen.

$$SubjectAvgK\prime_x = \frac{\sum_{j=1}^{n} I_j}{|S_x| k\prime} \quad I_j \in H \tag{7}$$

where H is defined by:

$$H = \{I_p | p \in S_{xk\prime}\} \tag{8}$$

### 5.5 Average

The average of all the distances for each subject is calculated. The subject which has the lowest average distance is then selected. Note that this algorithm is equivalent to $K\prime$ Subject Average with $k\prime = 100$. The subject with the smallest value defined by (9) is chosen.

$$SubjectAvg_x = \frac{\sum_{j=1}^{n} I_j}{|S_x|} \quad I_j \in G \tag{9}$$

### 5.6 Weighted Average

The average distance for each subject is calculated. However, the images belonging to a subject are given a weighting. The image with the largest distance is given a weighting of 1; the image with the second largest distance is given a weighting of 2, etc. Finally, if there are $|S_x|$ images of a particular subject, then the image with the smallest distance is given a weighting of $|S_x|$. The weighted sum can then be calculated using (10):

$$WeightedSum_x = \sum_{j=1}^{n} I_j w_j \quad I_j \in G \tag{10}$$

Table 1: ALGORITHM 1: WEIGHTED AVERAGE

1: sort(images)
2: **for** $i = 0$ to $n$ **do**
3:     Add the weight of image $i$ to the appropriate list in an array of lists $arr$, where each subject has its own list
4: **end for**
5: **for** $i = 0$ to $m$ **do**
6:     $w \Leftarrow arr[i].size()$
7:     **for** $j = 0$ to $arr[i].size()$ **do**
8:         $wSum \Leftarrow wSum + arr[i].get(j) * w$
9:         $w \Leftarrow w - 1$
10:     **end for**
11:     $total[i] \Leftarrow wSum/arr[i].size()$
12: **end for**
13: $lowestName \Leftarrow 0$
14: $wAvg \Leftarrow total[0]$
15: **for** $i = 1$ to $m$ **do**
16:     **if** $total[i] < wAvg$ **then**
17:         $lowestName \Leftarrow i$
18:         $wAvg \Leftarrow total[i]$
19:     **end if**
20: **end for**
21: return $lowestName$

When calculating the average, instead of dividing by the total number of images belonging to the subject, it is divided by the sum of the weights pertaining to the subject. The total weight can be calculated using (11):

$$TotWeight_x = \frac{|S_x|(|S_x| + 1)}{2} \tag{11}$$

Finally, the weighted average for a particular subject can be calculated using (12):

$$WeightedAverage_x = \frac{WeightedSum_x}{TotWeight_x} \tag{12}$$

The subject with the lowest weighted average is then selected.

See **Algorithm 1** for detailed pseudocode of this algorithm. Other weighting algorithms will follow similar pseudocode, but have a different weighting mechanism.

## 5.7 Reverse Weighted Average

This algorithm is the same as the Weighted Average algorithm except that the larger weights are applied to the images with larger distances. This algorithm attempts to find out if the less closely matched images are in fact better at distinguishing subjects.

## 5.8 Exponential Weighted Average

An average of the distances for each subject is calculated. However, each image belonging to the subject is given a weighting. The image of a subject which has the smallest distance is given an arbitrary weighting of 10.0. Subsequent images of the same subject are given weights

exponentially less by dividing the previous weight by the $|S_x|^{th}$ root of 10.0. So, if image $j$ has a weight of $w_j$, then the weight of image $j + 1$ can be calculated with (13):

$$w_{j+1} = \frac{w_j}{\sqrt[|S_x|]{10.0}} \tag{13}$$

To find the exponential weighted average, the weighted sum must be divided by the sum of the weights (total weight). The weighted sum and total weight are computed using (10) and (14) respectively.

$$ExpTotWeight_x = \sum_{j=1}^{|S_x|} 10^{\frac{j}{|S_x|}} \tag{14}$$

Finally, the exponential weighted average for a particular subject is calculated using (15):

$$ExpWeightedAverage_x = \frac{WeightedSum_x}{ExpTotWeight_x} \tag{15}$$

The subject with the lowest exponential weighted average is then selected.

# 6 Results and Discussion

In order to test the validity of results, three publicly available test databases were obtained, namely Caltech Faces, the Georgia Face Database and the ORL Database of Faces. The Feret database ( [10], [11]) is perhaps the most commonly used face database to benchmark the eigenfaces technique. However, the Feret database does not contain multiple images of each subject and hence is not useful for testing the novel classification algorithms proposed here.

## 6.1 Testing Procedure

A standard test procedure was used on each database. This involved the following:

1. Running the Viola and Jones [7] algorithm on each image in the database to extract faces.

2. Manually discarding all subjects from the database which do not have a minimum of 10 separate face detections from the Viola and Jones algorithm. This results in a reduction of the total number of images.

3. Setting aside a number of random images of each subject for testing. In this research, 5 per subject were used.

4. Performing training on the remaining images.

5. Performing the test procedure using the test images and the trained database.

6. Running 100 repetitions of steps 3-5 and taking the average as the final result.

7. Repeating steps 3-6 for each different classification algorithm.

Table 2: Caltech Faces Recognition Rates

| Classification Algorithm | Rate (%) |
| --- | --- |
| Top Match (Baseline, (*Literature*)) | 87.71 |
| Top-k Average (k=5) | 73.52 |
| Adaptive K-nearest Neighbour (k=5) | 77.39 |
| $K\prime$ Subject Average (k=40) | 90.14 |
| $K\prime$ Subject Average (k=60) | 92.04 |
| $K\prime$ Subject Average (k=80) | 91.05 |
| Average | 92.63 |
| Weighted Average | 94.54 |
| Reverse Weighted Average | 72.97 |
| Exponential Weighted Average | 93.75 |

Table 3: Georgia Face Database Recognition Rates

| Classification Algorithm | Rate (%) |
| --- | --- |
| Top Match (Baseline, (*Literature*)) | 58.26 |
| Top-k Average (k=5) | 51.46 |
| Adaptive K-nearest Neighbour (k=5) | 62.13 |
| $K\prime$ Subject Average (k=40) | 65.68 |
| $K\prime$ Subject Average (k=60) | 69.13 |
| $K\prime$ Subject Average (k=80) | 70.32 |
| Average | 71.67 |
| Weighted Average | 69.87 |
| Reverse Weighted Average | 64.67 |
| Exponential Weighted Average | 69.01 |

## 6.2 Caltech Faces

The Caltech face database, used by Kevenaar et al. [12], was obtained for testing. It contains 450 images of 27 subjects. The database is considered to be relatively easy since the faces are always upright, are uniform in presentation and never suffer from occlusion. Since the database does not provide a consistent number of images per subject, it was deemed necessary to ignore step 2 from the generic testing procedure. Thus, after performing face detection, the database was reduced to 435 images of 25 subjects with between 4 and 26 images per subject.

Table 2 shows that the Weighted Average algorithm improves on the baseline results by close to 7% (from 87.71% to 94.54%). This worked out to an extra 1441 correct recognitions over the 22400 image test. The results also show that the images with a smaller distance to the test image contribute more towards identifying the subject – since both Weighted Average and Exponential Weighted Average perform better than Average. The opposite is not true, with the Reverse Weighted Average (giving higher weightings to less closely matched images) does not perform well. Finally, it was envisaged that Top-k Average and Adapted K-nearest Neighbour would be used with small $k$ values, but they did not improve on the baseline. Using higher $k$ values would only result in the algorithms degenerating towards the Average classification algorithm.

## 6.3 Georgia Face Database

To determine whether the novel classification algorithms could raise recognition rates in sub-optimal conditions, a more difficult database was required. Thus, the Georgia Face Database,

Table 4: ORL Database of Faces Recognition Rates

| Classification Algorithm | Rate (%) |
|---|---|
| Top Match (Baseline, (*Literature*)) | 83.82 |
| Top-k Average (k=5) | 77.46 |
| Adaptive K-nearest Neighbour (k=5) | 82.44 |
| *K′* Subject Average (k=40) | 87.08 |
| *K′* Subject Average (k=60) | 88.62 |
| *K′* Subject Average (k=80) | 88.79 |
| Average | 88.24 |
| Weighted Average | 89.27 |
| Reverse Weighted Average | 81.27 |
| Exponential Weighted Average | 89.04 |

used by Chen et al. [13], was obtained. The database consists of 50 subjects and a total of 750 images, but this was reduced to 30 subjects and 355 images after steps 1 and 2 (pre-processing) in the testing procedure. The database is considered difficult because many of the faces are tilted, have different facial expressions and were taken under different lighting conditions. Further to that, the pictures were taken in separate sessions – thus, some subjects exhibited physical changes (e.g. grew a moustache).

Although the overall results from testing are worse than the Caltech Faces, Table 3 shows that the novel classification algorithms are still effective. In fact the best algorithm (Average) raises the recognition rate from 58.26% to 71.67% – an improvement of over 13%. It is interesting to note that the Average algorithm outperforms both the Weighted Average and Exponential Weighted Average. This is probably because the distance between the better images and the test image is relatively large (since the database is extremely difficult) and thus the distribution of distances for a particular subject is more even. With an even distribution of distance, weighting becomes superfluous.

### 6.4   ORL Database of Faces

The final test for the novel classification algorithms was to see how well they scaled. More specifically, would they still show improvements over the baseline if the number of subjects was increased? To test this, a third database was required. The ORL Database of Faces, created by Samaria and Harter [14], was obtained. The database consists of 40 subjects with 10 images per subject and all of these images remained intact after steps 1 and 2 of the testing procedure.

Table 4 shows that using *K′* Subject Average, Average, Weighted Average or Exponential Weighted Average as a classification algorithm will give better results than the baseline algorithm. In fact, Weighted Average and Exponential Weighted Average both show improvements of over 5% – even with the large number of subjects being used.

### 6.5   Algorithm Complexity

Tables 5, 6 and 7 shows the timing increase per classification which occurs when using a novel classification algorithm versus using the baseline algorithm (top match). The increase in classification time is minimal for all of the algorithms running on any of the databases and thus confirms that the algorithms are feasible for use in real-time applications such as streaming video at 25 fps. In fact, the roughly 2ms worst case increase would only become a factor if classifying thousands of faces (e.g. at a sports stadium). These results were generated using an Intel Core

Table 5: Caltech Faces Timing Increase In ms

| Classification Algorithm | Time |
|---|---|
| Top-k Average (k=5) | 0.58 |
| Adaptive K-nearest Neighbour (k=5) | 0.98 |
| $K\prime$ Subject Average (k=40) | 1.39 |
| $K\prime$ Subject Average (k=60) | 1.98 |
| $K\prime$ Subject Average (k=80) | 1.56 |
| Average | 1.99 |
| Weighted Average | 1.32 |
| Reverse Weighted Average | 1.85 |
| Exponential Weighted Average | 1.33 |

Table 6: Georgia Face Database Timing Increase In ms

| Classification Algorithm | Time |
|---|---|
| Top-k Average (k=5) | 1.07 |
| Adaptive K-nearest Neighbour (k=5) | 0.74 |
| $K\prime$ Subject Average (k=40) | 0.98 |
| $K\prime$ Subject Average (k=60) | 0.69 |
| $K\prime$ Subject Average (k=80) | 1.32 |
| Average | 1.48 |
| Weighted Average | 1.52 |
| Reverse Weighted Average | 1.23 |
| Exponential Weighted Average | 1.26 |

Table 7: ORL Database of Faces Timing Increase In ms

| Classification Algorithm | Time |
|---|---|
| Top-k Average (k=5) | 0.27 |
| Adaptive K-nearest Neighbour (k=5) | 0.79 |
| $K\prime$ Subject Average (k=40) | 0.86 |
| $K\prime$ Subject Average (k=60) | 0.84 |
| $K\prime$ Subject Average (k=80) | 0.95 |
| Average | 0.87 |
| Weighted Average | 0.88 |
| Reverse Weighted Average | 0.94 |
| Exponential Weighted Average | 0.86 |

2 Duo E8400 (3.0GHz) with 2GiB of RAM running Ubuntu Linux 10.10 64-bit.

# 7   Conclusions and Future Works

Methods for increasing face recognition rates have been investigated with the primary focal area being the classification algorithm. A number of the new classification algorithms show improvements of the literature results termed as the baseline results. It can be concluded that the best performing classification algorithm is Weighted Average with improvements over the baseline of 6.83%, 11.61% and 5.45% in the three test databases. Importantly, the algorithms are computationally efficient making them feasible for use in real-time applications.

So far, the novel classification algorithms have only been applied to the eigenfaces technique. Future research will involve applying the classification algorithms to other face recognition techniques to see if similar improvements are obtained.

# Bibliography

[1] A.W. Senior, R.M. Bolle (2002); *Face Recognition and its Applications: Biometric Solutions for Authentication in an E-World*, Kluwer Academic Publishers, 2002.

[2] Lin, Shang-hung (2000), An Introduction to Face Recognition Technology, *Informing Science The International Journal of an Emerging Transdiscipline*, 3(1): 1-7.

[3] M.A. Turk, A.P. Pentland (1991); IEEE Computer Society Conference on Computer Vision and Pattern Recognition, *Proceedings of Computer Vision and Pattern Recognition*, 586-591.

[4] H. Moon, P.J. Phillips (2001); Computational and performance aspects of PCA-based face-recognition algorithms, *Perception*, 30(3): 303-321.

[5] C. Liu, H. Wechsler (1999), Comparative assessment of Independent Component Analysis, *International Conference on Audio and Video Based Biometric Person Authentication, AVBPA'99, Washington D.C. USA*, 22-24.

[6] A.M. Bronstein et al (2003); 3D Face Recognition Without Facial Surface Reconstruction, *Technion – Computer Science Department*.

[7] Viola et al (2004); Robust Real-Time Face Detection, *Int. J. Comput. Vision*, 57(2): 137-154.

[8] G. Bradski (2000); The OpenCV Library, *Dr. Dobb's Journal of Software Tools*.

[9] H.A. Rowley et al (1995); Human Face Detection in Visual Scenes, *Advances in Neural Information Processing Systems 8*, 875-881.

[10] P.J. Phillips et al (1998); The FERET database and evaluation procedure for face recognition algorithms, *Image and Vision Computing Journal*, 16(5), 295-306.

[11] P.J. Phillips et al (2000); The FERET Evaluation Methodology for Face Recognition Algorithms, *IEEE Trans. Pattern Analysis and Machine Intelligence*, 22: 1090-1104.

[12] T.A.M. Kevenaar et al (2005), Face Recognition with Renewable and Privacy Preserving Binary Templates, *Proceedings of the Fourth IEEE Workshop on Automatic Identification Advanced Technologies*, 21-26.

[13] C. Ling et al (2005), Face recognition based on multi-class mapping of Fisher scores, *Pattern Recognition*, 38(6): 799-811.

[14] F.S. Samaria and A.C. Harter (1995); Parameterisation of a Stochastic Model for Human Face Identification, W*orkshop on Applications of Computer Vision*.

[15] L. Zhang et al (2011), Sparse Representation or Collaborative Representation: Which helps face recognition?, *Proceedings of the 2011 IEEE International Conference In Computer Vision (ICCV)*, 471-478.

[16] R. Khaji et al (2013), Collaborative Representation for Face Recognition based on Bilateral Filtering, *IJCSI International Journal of Computer Science*, 397-401.

[17] H. Zheng, J. Xie, Z. Jin (2012); Heteroscedastic Sparse Representation Based Classification for Face Recognition, *Neural Processing Letters*, 233-244.

[18] J. Wright et al (2009); Robust Face Recognition via Sparse Representation, *IEEE Transactions on Pattern Analysis and Machine Intelligence (PAMI)*, 233-244.

[19] W. Andrew et al (2012); Toward a practical face recognition system: Robust alignment and illumination by sparse representation, *IEEE Transactions on Pattern Analysis and Machine Intelligence (PAMI)*, 372-386.

[20] Z. Pengfei et al (2012), Multi-scale Patch based Collaborative Representation for Face Recognition with Margin Distribution Optimization, *Computer Vision-ECCV 2012*, Springer Berlin Heidelberg, 822-835.

[21] B. Mikhail, P. Niyogi (2003); Laplacian Eigenmaps for Dimensionality Reduction and Data Representation, *Neural Computation*, 1373-1396.

# A New Adaptive Fuzzy PID Control Method and Its Application in FCBTM

J.G. Lai, H. Zhou, W.S. Hu

**Jingang Lai\*, Hong Zhou, Wenshan Hu**
Department of Automation, Wuhan University
Wuhan, 430072, Hubei China
\*Corresponding author: henanlaijingang@163.com

> **Abstract:** The process of tension control for material testing using the Flexible
> Circuit Board testing machine (FCBTM) is featured with multi-variable, nonlinearity,
> time delays and time variation. In order to ensure the tension precision, the stability of
> servo motor' speed and the reliability of test results, this paper establishes an accurate
> system model for the FCBTM, in which a novel three-dimensional adaptive fuzzy
> PID controller is designed. Specially, the simulation results show that the proposed
> adaptive fuzzy control method is not only robust to the external disturbance but also
> with more excellent dynamic and steady-state characteristics than traditional ones.
> **Keywords:** Flexible Circuit Board testing machine (FCBTM); tension control; adaptive self-tubing, fuzzy PID control.

## 1  Introduction

With the development of science and technology, electronic products become increasingly
miniaturized, lightweight and thinner. Recent years have witnessed the increasing attention
on the Flexible Circuit Board (FCB) and its applications in the manufacturing and printing
of electronic components. Owning to the features of high wiring density, three-dimensional
wiring, light weight and thin, the FCB has been more and more directly used to the electronic
component of manufacture and printing in recent years, meanwhile the market demand is also
growing rapidly. However, the common FCBTM is quite obsolete, which results in the unstable
performance and low automation. This conflict between the huge market demand and the status
quo makes the design of new testing equipment for FCB material properties become very urgent.
Therefore, it is quite significance to research and design the new material FCBTM.

The servo motor and its controller circuit of FCBTM are composed of many mechanical and
electrical components which are highly nonlinear. They are used to load the measured object,
where the parameters of measured object exist uncertainty, nonlinear factors and others, thus,
by which the system is susceptible to be influent. During the test, in particular, the change of
hardness of FCB samples can cause changes of the load scale factor on the deformation of force
and displacement. With the dramatic increase of the required test fineness, it makes the precise
critical in the control process of FCBTM.

Traditional FCBTM usually uses the conventional PID algorithm. However, the control rate
of FCBTM varies greatly for the different material properties, which directly affects the rate
of change of the load. Fuzzy control theory is an effective solution, but simply because of the
lack of the integrator team, the steady state error and the disturbance rejection are difficult
to be eliminated. Especially in the case of classification variables are not enough, it often
produces small oscillations around the equilibrium point. The PID control method introduces
fuzzy controller and uses fuzzy reasoning, which will automatically implemented the optimum
adjustment for PID parameters $K_P$, $K_I$ and $K_D$ [1]- [3]. Because FCBTM is a nonlinear and
time-varying system, simple fuzzy control or PID control is difficult to achieve the desired effect.
The use of fuzzy PID composite control, combining the PID control and fuzzy control, which

can not only play the fuzzy control advantage of robustness, good dynamic response, fast rise time and overshoot small, but also have features of both quality and steady precision dynamic tracking characteristics. It can make system to obtain good static and dynamic characteristics.

In the testing machine system, fuzzy adaptive PID parameter controller is a PID controller on the conventional basis of the application of fuzzy set theory to establish binary continuous function between parameters $K_P$, $K_I$ and $K_D$, and absolute deviation value $|E|$ and absolute paranoia changes value $|EC|$. It should be pointed out that classical fuzzy PID controller requires a three-dimensional rule base which makes the design process more difficult [4]- [5]. To overcome this drawback and focus on reducing the dimension of fuzzy system, this paper presents a two-stage fuzzy PID controller with fuzzy switch and uses it to control the tension in a FCBTM. This controller uses two-dimensional inference engine (rule base) to perform reasonably the task of a three-dimensional controller.

$$\begin{cases} K_p = f_1\left(|E|, |EC|\right) \\ K_I = f_2\left(|E|, |EC|\right) \\ K_D = f_3\left(|E|, |EC|\right) \end{cases} \tag{1}$$

According to the different of $|E|$ and $|EC|$, it is able to online self-tubing parameters $K_P$, $K_I$ and $K_D$, which is the key to achieve fuzzy adaptive PID controller design [6]- [7].

In this paper, the goal is to improve the accuracy of load control of FCBTM. The new three-dimensional adaptive fuzzy PID controller could be used to universal testing machine.

## 2    The Establishment of FCBTM Model

In the course of testing FCB materials, first, the test sample is sandwiched between the movable beam and the base of testing machine, then by controlling the DC servo motor speed to drive the moving beam up and down via moving the transmission mechanism. Finally, the trial loading process is completed. The control parts of the whole system including: the DC motor control part, the mechanical transmission part, human machine interface(HMI), sensor signal feedback section and so on as shown in Figure 1. Interested readers can find further information about the detailed design and implementation of the hardware and software of FCBTM in [12].
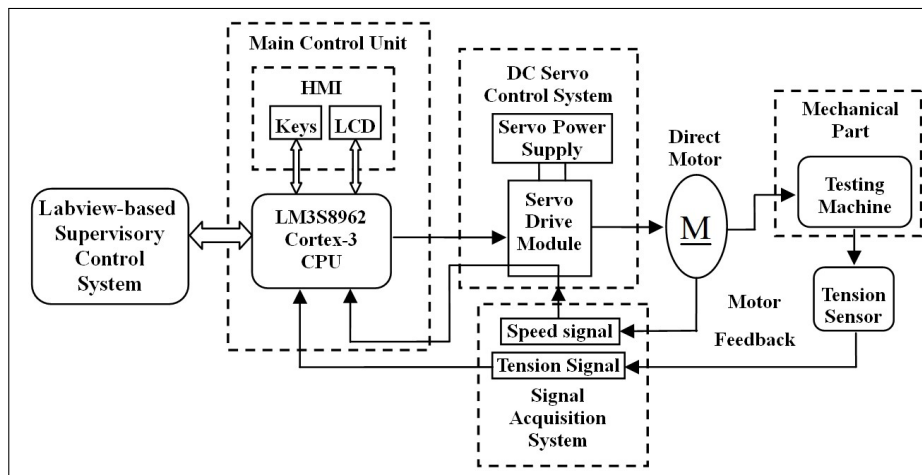


Figure 1: Structure diagram of control system of FCBTM

## 2.1 The DC Servo Motor Part

The equivalent circuit of DC servo motor is as follows: The field voltage of $U_a$ which is the system input signal; while $\theta$ is a motor shaft angle [8], [11], which is a system output.

$$J_a \frac{d^2\theta}{dt^2} + B\frac{d\theta}{dt} = M = Ki_a \tag{2}$$

The voltage balance equation of armature circuit of DC servo motor:

$$U_a = R_a i_a + L_a \frac{di_a}{dt} + e_a \tag{3}$$

Laplace transforms for (2) and (3), then collate them and get the system transfer function of DC motor :

$$F(s) = \frac{\theta(s)}{U_a(s)} = \frac{K}{s(L_a s + R_a)(J_s + B)} = \frac{K_m}{s(\tau_a s + 1)(\tau_e s + 1)} \tag{4}$$

where $K_m$ is the motor gain $K_m = \frac{K}{R_a B}$; $\tau_a = \frac{L_a}{R_a}$ is the electrical time constant of the motor; $\tau_e = \frac{J}{B}$ is the mechanical time constant of the motor; $J$ is the total moment of inertia converted to the motor shaft; $B$ is the viscous friction coefficient.

## 2.2 The Mechanical Transmission Part

In this part, $\theta$ is the motor rotation angle and it is the input signal. The axial displacement of the movable beam of test machine $Y$ is the output signal, the transfer function between the rotational angle input and movable beam is as follows [10]:

$$G_j(s) = \frac{Y(s)}{\theta(s)} \approx \frac{(\frac{Z_1}{Z_{2out}} \cdot \frac{Z_{2in}}{Z_4} \cdot \frac{L}{2\pi})K}{Js^2 + Bs + K} = \frac{Z_1}{Z_{2out}} \cdot \frac{Z_{2in}}{Z_4} \cdot \frac{L}{2\pi} \cdot \frac{w_n^2}{s^2 + 2\xi w_n s + w_n^2} \tag{5}$$

$Z_1$, $Z_{2out}$, $Z_{2in}$ and $Z_4$ are the motor outputs shaft gear, the external gear wheel transition, the internal tooth gear teeth and the axle, respectively; $L$ is ball screw pitch; $w_n = \sqrt{K/J}$ is the non-damped natural frequency; $\xi = B(2\sqrt{JK})$ is damping ratio of the mechanical system.

## 2.3 The Sensor Signal Transmitting Part

The sensor feedback transfer part of tension and displacement can be approximated as a proportional component, respectively, $K_c$ and $K_e$. The value of $K_c$ and $K_e$ is 1 according to the actual situation.

# 3 Dimensional Adaptive Fuzzy PID Controller Design

Fuzzy adaptive PID controller is mainly based on the system generated during the operation of error $E$, error rate $EC$ and acceleration of error rate $ER$ to online self-tubing PID parameters, which allows the system to ensure low overshoot and can achieve fast convergence. During the loading control process of FCBTM, conventional fuzzy adaptive PID controller only uses the error $E$ and error variation $EC$ as input to meet the self-tubing PID parameters requirements at different moments, which is also known as two-dimensional fuzzy controller [9]. The geometry detonation problem of multi-variable fuzzy control rule is solved, and a greater controllable scope is obtained. However, when the outputs of the control system of FCBTM enter the stage of steady-state approximation, the stability of this kind fuzzy PID control will decline, and the

controller will not be possible to generate error measure to eliminate this instability. At this point, if the acceleration $ER$ (the second derivative of the error) of the error changes $EC$ is added as fuzzy PID control input, it will make the system have a good steady precision. This is called three-dimensional fuzzy PID controller. However, the increase of dimension will definitely increase the difficulty of the control algorithm, and affect the control response speed.

Given the above analysis, in order to effectively use three-dimensional fuzzy PID controller to solve the contradiction of the traditional two-dimensional fuzzy PID controller requiring quick response and stability, when the controller of sample load was designed, if the error is large $|EC| \geq e_0$, then the conventional two-dimensional fuzzy PID control (hereinafter, the Fuzzy1) is selected as the controller, but when the error is small $|EC| < e_0$, the acceleration of change of error is introduced as a new input value, based on the positive negative to reselect a new fuzzy control rules to adjust the PID parameters online, the specific three-dimensional fuzzy PID control principle is shown in Figure 2.
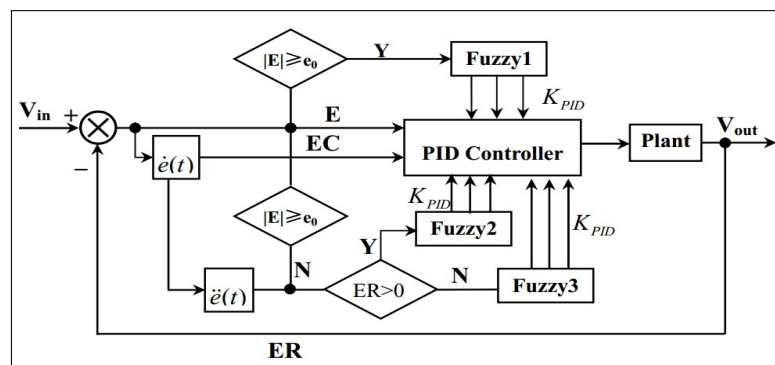


Figure 2: Structure of the proposed three-dimensional adaptive fuzzy controller

Based on experience to inform the error range of actual system and determine an error limit $e_0$, when the error meets $|EC| \geq e_0$, we choose the fuzzy rules Fuzzy1 of traditional two-dimensional fuzzy PID control; however, when the error meets $|EC| < e_0$, in accordance with $ER$ positive and negative reselect the fuzzy rules of three-dimensional fuzzy PID control. When $ER$ is bigger than 0, we select fuzzy rules Fuzzy2. Otherwise perform fuzzy rules Fuzzy3, in order to achieve the PID parameters $K_P$, $K_I$ and $K_D$ on-line modification and self-tubing. So when implement control action on the testing machine loading process, we have chosen to use two-dimensional fuzzy control table to achieve the three-dimensional fuzzy control function, essentially which can be seen as the dimensionality reduction of three-dimensional fuzzy control via reducing the number of dimensions to increase the response speed, at last form a three-dimensional fuzzy PID control on testing machine.

In the course of designing the three-dimensional fuzzy PID controller on testing machine, the most critical is to give fuzzy control rules adopted in different operating stages of the system. Next corresponding fuzzy control rules will be designed, depending on the system error variance at different times.

## 3.1    Select Input and Output Variables and Fuzzy Input Parameters

Due to the loading control of FCBTM including various tasks (such as tension and velocity control, etc.), it detects the value of error $E(k)$, error rate $EC(k)$ and the acceleration of error rate $ER(k)$ and adjusts $K_P$, $K_I$ and $K_D$ according to the fuzzy rules in each sample period. Then the DC servo drive unit is employed to tune the speed of motor, when fuzzy controller received the voltage signal from the fuzzy PID controller.

Therefore, fuzzy logic systems can make the error $E$, the error change $EC$ and change of acceleration $ER$ of each control period as input variables, and put the parameter adjustment values $K_P$, $K_I$ and $K_D$ as the output variables, at last form a three inputs and three outputs system. The calculation formula of each control cycle is as follow :

$$
\begin{cases}
K_P = K_{P0} + \Delta K_P, \\
K_I = K_{I0} + \Delta K_I, \\
K_D = K_{D0} + \Delta K_D,
\end{cases}
\tag{6}
$$

ĄĄ where $K_{P0}$, $K_{P0}$ and $K_{P0}$ is the initial setting of PID parameters which are able to be given in advance based on practical experience. Due to the high requirements on control quality, when fuzzy each input, we will quantify the system error $E$ and the error change $EC$ to 13 levels, with $-6, -5, -4, -3, -2, -1, 0, 1, 2, 3, 4, 5, 6$ representation.

Since the control system is to control two kinds physical of tension and speed, even if only to control tension rate, its rate range can also be within a wide range from 0 MPa/s to 5 MPa/s. Therefore, a simple fuzzy unification is not appropriate only based on the absolute value of $E$ and $EC$. However, if we respectively use different fuzzy methods according to the different control methods, then it is quite tedious and can not be exhaustive. So the relative values of $E$ and $EC$ are used to quantify and can be expressed as follows :

$$
\begin{cases}
e_r(k) = \frac{e(k)}{r(k)} \\
ec_r(k) = \frac{ec(k)}{e(k-1)}
\end{cases}
\tag{7}
$$

where $r(k)$ is the desired control value of the system, further designs the fuzzy quantitative equations are as follows:

$$
E(K) =
\begin{cases}
-6 & \lceil e_r(k) \times 100 \rceil < -5 \\
\lceil e_r(k) \times 100 \rceil & -5 \leq \lceil e_r(k) \times 100 \rceil \leq -0.5 \\
0 & -0.5 \leq \lceil e_r(k) \times 100 \rceil \leq 0.5 \\
\lceil e_r(k) \times 100 \rceil + 1 & 0.5 \leq \lceil e_r(k) \times 100 \rceil \leq 5 \\
6 & \lceil e_r(k) \times 100 \rceil > 5
\end{cases}
\tag{8}
$$

$$
EC(K) =
\begin{cases}
-6 & \lceil ec_r(k) \times 100 \rceil < -5 \\
\lceil e_r(k) \times 100 \rceil & -5 \leq \lceil ec_r(k) \times 100 \rceil \leq -0.5 \\
0 & -0.5 \leq \lceil ec_r(k) \times 100 \rceil \leq 0.5 \\
\lceil e_r(k) \times 100 \rceil + 1 & 0.5 \leq \lceil ec_r(k) \times 100 \rceil \leq 5 \\
6 & \lceil ec_r(k) \times 100 \rceil > 5
\end{cases}
\tag{9}
$$

Based on the style, the variables of $E$ and $EC$ are put into a certain one in the 13 quantization levels in each control period. The basic output domain of $\Delta K_P$, $\Delta K_I$ and $\Delta K_D$ of fuzzy PID controller can be properly selected based on experience. The basic domain of $\Delta K_P$, $\Delta K_I$ and $\Delta K_D$ were taken as [-0.3, 0.3], as [-0.06, 0.06] and as [-3, 3], respectively. The quantization levels of their fuzzy variables are the same as $E$ and $EC$.

## 3.2   Determination on The Set and Membership of The Fuzzy Controller

The selection of membership function has a certain impact on the whole fuzzy system control process. According to the foregoing analysis on the FCBTM load control principles and

procedures, in order to facilitate the calculation, this article uses the same kind of membership functions for the input variables $E$, $EC$ and output variables $\Delta K_P$, $\Delta K_I$ and $\Delta K_D$. The fuzzy subset of input and output variables is: NB, NM, NS, ZO, PS, PM, PB, respectively: Negative Big, Negative Middle, Negative Small, Zero, Positive Small, Positive middle, Positive Big. Figure.3 shows membership function of and in Fuzzy1. Its basic domain is [-3, 3], and its fuzzy domain is [-6, 6], where NB and PB are defined using Gaussian function as normal, the other fuzzy subsets are defined using trigonometric functions.
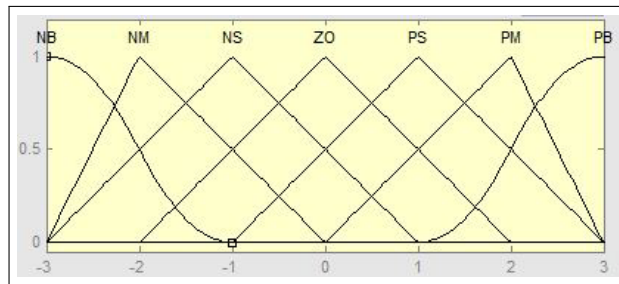


Figure 3: E and EC membership function in Fuzzy1

When the system enters the control later stages and the error is small $|E| < e_0$, then different fuzzy functions should be selected according to the positive and negative of the acceleration of error, in order to achieve high precision control for the testing machine. Fuzzy2 and Fuzzy3 are, respectively, the fuzzy controller when $ER > 0$ and $ER \leq 0$. The specific membership function is as shown in Figure.3, NB and PB are defined as normal Gaussian function, and the other fuzzy subsets are defined as using trigonometric functions. At this time, the basic domain of $E$ and $EC$ is still [-0.6, 0.6] and the fuzzy domain is still [-6, 6], and theirs membership function is as shown in Figure 4.
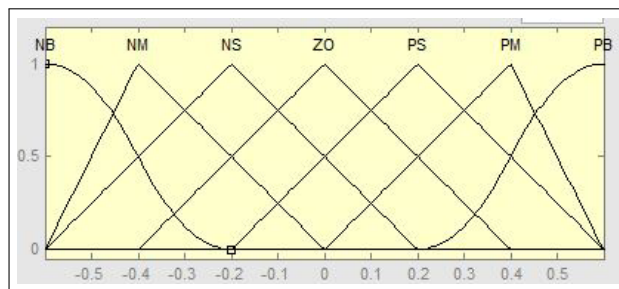


Figure 4: E and EC membership function in Fuzzy2 and Fuzzy3

The output variables ($\Delta K_P$, $\Delta K_I$ and $\Delta K_D$) of fuzzy controller have the same fuzzy subsets and membership functions. In Fuzzy1-3 the membership function of $\Delta K_P$ is as shown in Figure.5 and its basic domain is [-0.3, 0.3], the basic domain of $\Delta K_I$ is [-0.06, 0.06]. However, in Fuzzy1-2 the basic domain of $\Delta K_D$ is [-3, 3], compared to the Fuzzy3 is [-0.6, 0.6].

In this effort, when $EC$ changes, the tuning principles of PID parameters $K_P$, $K_I$ and $K_D$ are as follows:

Table 1 is the three-dimensional fuzzy PID control rules on the testing machine in the whole process. Fuzzy1 is employed when $E$ is larger, while Fuzzy2-3 is chose when $E$ is smaller. At this time, when $ER$ is lager than 0, we choose Fuzzy2; when $ER$ is not lager than 0, we use Fuzzy3. Thus the output of the system is tuned in the opposite direction.
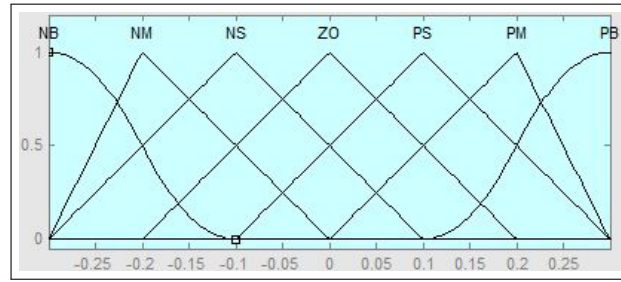
Figure 5: Domain and membership function of $\Delta K_P$

Table 1: Fuzzy1-3 control rule

| $\Delta K_P$ $\Delta K_I$ $\Delta K_D$ EC / E | NB | | | NM | | | NS | | | ZO | | | PS | | | PM | | | PB | | |
|---|---|---|---|---|---|---|---|---|---|---|---|---|---|---|---|---|---|---|---|---|---|
| NB | PB | PB | PB | PB | PM | PB | PM | PS | PM | PM | ZO | PS | PS | ZO | PS | ZO | NS | ZO | ZO | NS | NS |
|  | NB | NB | NB | NB | NM | NB | NM | NS | NM | NM | ZO | NS | NS | ZO | NS | ZO | PS | ZO | ZO | PS | ZO |
|  | PS | ZO | NS | NS | NS | NS | NB | NS | NB | NB | NM | NM | NB | NS | NS | NM | NS | NS | PS | ZO | ZO |
| NM | PB | PM | PB | PB | PB | PB | PM | PS | PM | PS | ZO | PS | PS | NS | ZO | ZO | NS | NS | NS | NM | NS |
|  | NB | NM | NB | NB | NM | NB | NS | NS | NM | NS | ZO | NS | NS | PS | ZO | ZO | PS | PS | ZO | PM | PS |
|  | PS | ZO | NS | NS | NS | NS | NM | NS | NB | NM | NS | NM | NM | NS | NM | NS | NS | NS | ZO | ZO | ZO |
| NS | PM | PM | PM | PM | PM | PM | PM | PS | PM | PS | ZO | PS | ZO | NS | ZO | NS | NM | NS | NS | NM | NS |
|  | NB | NM | NB | NM | NM | NM | NS | NS | NS | NS | ZO | NS | ZO | PS | ZO | PS | PM | PS | PS | PM | PS |
|  | ZO | ZO | ZO | NS | NS | NS | NM | NS | NM | NM | NS | NM | NS | NS | NM | NS | ZO | NS | ZO | ZO | ZO |
| ZO | PM | PM | PM | PM | PS | PM | PS | ZO | PS | ZO | ZO | ZO | NS | NS | ZO | NM | NM | NM | NM | NM | NM |
|  | NM | NM | NB | NM | NS | NM | NS | ZO | NS | ZO | PS | ZO | PS | PS | ZO | PM | PM | PS | PM | PM | PM |
|  | ZO | ZO | ZO | NS | ZO | NS | NS | NS | NM | NS | NS | NM | ZO | ZO | NS | NS | ZO | NS | ZO | ZO | ZO |
| PS | PS | PS | PM | PS | PS | PM | ZO | ZO | PS | NS | NS | ZO | NS | NS | NS | NM | NM | NM | NM | NM | NM |
|  | NM | NM | NM | NS | NS | NM | ZO | ZO | NS | PS | PS | ZO | PS | PS | PS | PM | PM | PM | PB | PB | PM |
|  | ZO | ZO | ZO | ZO | ZO | NS | ZO | ZO | NS | ZO | ZO | NM | ZO | ZO | NS | ZO | ZO | NS | ZO | ZO | ZO |
| PM | PS | PS | PM | ZO | ZO | PS | NS | ZO | PS | NM | NM | ZO | NM | NM | NS | NM | NM | NM | NB | NB | NM |
|  | ZO | NS | NM | ZO | NS | NM | PS | ZO | NS | PS | PS | ZO | PM | PM | PS | PB | PB | PM | PB | PB | PM |
|  | PB | PB | ZO | PS | PS | NS | PS | ZO | NS | PS | ZO | NS | PS | PS | NS | PS | PS | NS | PB | PB | ZO |
| PB | ZO | PS | PS | ZO | ZO | PS | NM | NS | ZO | NM | NM | NS | NM | NM | NS | NB | NM | NM | NB | NB | NM |
|  | ZO | ZO | NM | ZO | ZO | NS | PS | PS | ZO | PM | PS | ZO | PM | PM | PS | PB | PB | PM | PB | PB | PB |
|  | PB | PB | ZO | PM | PS | ZO | PM | PS | ZO | PM | PS | NS | PS | PS | NS | PS | PS | ZO | PB | PB | ZO |
| Fuzzy | fz1 | fz2 | fz3 | fz1 | fz2 | fz3 | fz1 | fz2 | fz3 | fz1 | fz2 | fz3 | fz1 | fz2 | fz3 | fz1 | fz2 | fz3 | fz1 | fz2 | fz3 |

## 3.3   The Fuzzy Reasoning and Precise Operation

In the course of real-time control of the FCBTM, the specific works are as follows:

1) Firstly we calculate a moment error value $E(k)$ on tension or speed, which is relative to the last moment. Then adopt the difference method to calculate the value of $EC(k)$;

2) Then we fuzzy quantification for $E$ and $EC$ according to formula (4)-(7), and find their memberships in the quantization interval;

3) Thirdly the corresponding inference calculations are launched according to the fuzzy control rules in table1, and find the membership corresponding language value on $\Delta K_P$, $\Delta K_I$ and $\Delta K_D$;

4) The gravity method is used to solve fuzzy, then makes $\Delta K_P$, $\Delta K_I$ and $\Delta K_D$ parameter mapping to the respective basic domain range, eventually obtained $\Delta K_P$, $\Delta K_I$ and $\Delta K_D$ the precise adjustment value;

5) The defuzzification uses the weighted average method. System after defuzzification gets

a good parameter tuning PID controller, who is then use to achieve the control of the loading process of FCBTM.

# 4    The Simulation on FCBTM

In this paper, we use SimuLink module in MATLAB software for numerical simulation. The parameters on DC servo motor are, respectively, $L_a = 0.02H$, $R_a = 1.36Omega$, $J = 1.05 \times 10^{-4}$, $B = 4.5 \times 10^{-4}$, the $K = 0.025$, $T_a = 0.015$, $T_e = 0.23$. Mechanical transmission part of the relevant parameters are as follow: $Z_1 = 30$, $Z_{2out} = 90$, $Z_{2in} = 30$, $Z_4 = 90$, $L = 5mm/rad$, then $\xi = 0.5$, $w_n = 100$. Taking the FCBTM introduced in section 3 as example to study the steady state and transient characteristics of the proposed control strategies incorporating the conventional PID, two-dimensional fuzzy PID and three-dimensional fuzzy PID controller.

## 4.1    Comparative Performance Analysis

In order to compare the differences between different control methods, firstly, the conventional PID control simulation model on the testing machine control system was built. The initial value of PID was gotten by the method of online debugging trial and the initial values were: 1, 0.5 and 0.03.

Secondly, the fuzzy the rules of fuzzy control in Table1 are compiled into incorporated into the fuzzy inference system editor, simultaneously, determine the input and output variables domain membership function. Then we can create one fuzzy controller in SimuLink. The quantization factors of output variables $\Delta K_P$, $\Delta K_I$ and $\Delta K_D$ were 0.5, 0.05 and 0.05. After that the conventional two-dimensional adaptive fuzzy PID control simulation model is built.

Finally build a three-dimensional FCBTM fuzzy PID controller simulation model as shown in Figure.6. The quantization factors of output variables $\Delta K_P$, $\Delta K_I$ and $\Delta K_D$ were: 0.5, 0.05 and 0.05.
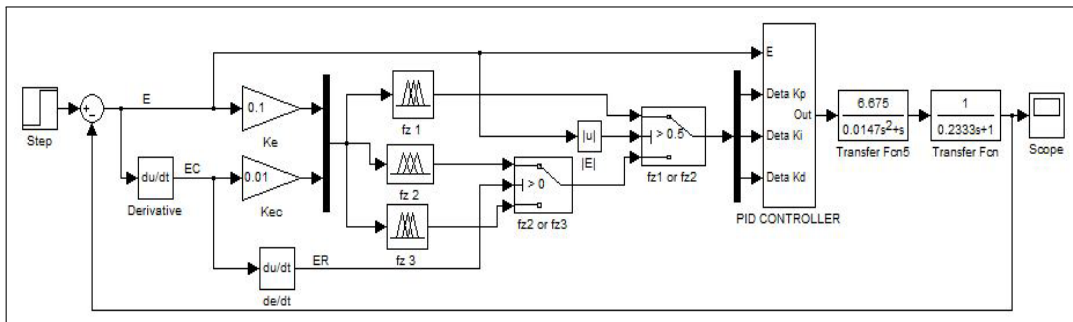


Figure 6: Dimensional Fuzzy PID controller simulation model

The loading process of FCBTM with constant strain rate can be equivalent to give a step input signal to the FCBTM system. Therefore, the three above-mentioned system simulation models all input a step signal, the corresponding curves are shown in Figure 7. The simulation time of this system is 15s, and the sample frequency is 0.01s. It can be seen that the tension responses of FCBTM under three controllers are approached and stabilized under the unit step input signal. As can be seen from the figure 7, the fuzzy PID controller using three-dimensional FCBTM control system has a small overshoot, and rise time, steady state can be achieved quickly.
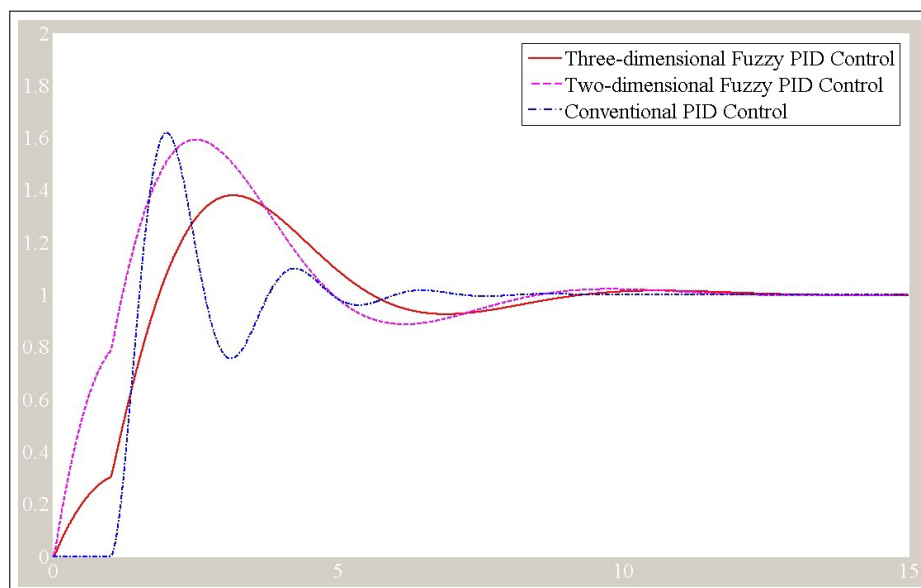
Figure 7: Comparison of tension response under three controllers

## 4.2   Robustness Analysis

Input and outer disturbance, system structure and parameter variation are the main measures to see about system robustness performance. Due to the interference of control systems are vulnerable to electromagnetic noise, in this section, outer periodic a step perturbation signal is used to analyze the robustness of the three controllers. We add a step perturbation to the FCBTM at 7s, which was used to analysis the anti-interference ability and stability of the three algorithms. The simulation results are shown in Fig.8. It can be seen that under the three controllers system can attain stability finally although the transient responses are influenced by the step perturbation signal more or less. The influence by disturbance under PID controller is much more than that of two-dimensional and three-dimensional fuzzy PID controllers. The variation of response under three-dimensional fuzzy PID controller may be ignored at certain error range. Further research shows that the robustness of the three-dimensional fuzzy PID control system is also excellent when the periodic pulse disturbance signal occurs at the input port.

## 5   Conclusion

This article adopts the fuzzy adaptive PID control method, (namely the two-dimensional fuzzy PID control system added a third variable that is the rate of change of the error), to reduce the response time of the FCBTM system while reducing overshoot and ultimately improve the steady-state performance. And three-dimensional fuzzy adaptive PID controller implementation process on FCBTM has been described in details. The salient feature of the proposed controller is that it does not require an accurate model of the controlled plant, and the design process is lower than that of the other PID controllers. The practical control effect and simulation based on the Matlab show that the proposed controller not only is robust, but also it gives excellent dynamic and steady-state characteristics compared with traditional controllers.
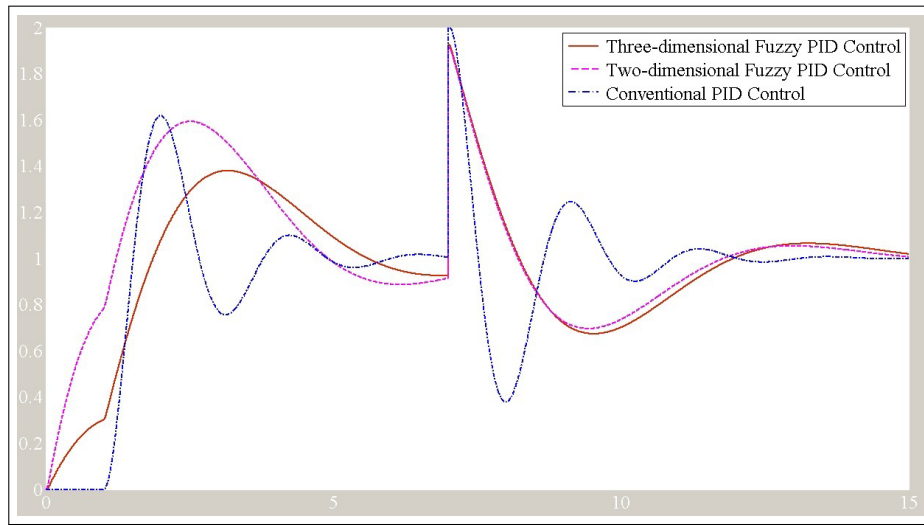
Figure 8: Comparison of tension response with disturbance

## 6    Acknowledgement

## Bibliography

[1] Duan X.G., Deng H., and Li H.X.(2013); A Saturation-Based Tuning Method for Fuzzy PID Controller, *IEEE Trans on Industrial Informatics*, 11: 5177-5185.

[2] Chalui H. and Sicard P. (2012); Adaptive fuzzy logic control of permanent magnet synchronous machines with nonlinear friction, *IEEE Trans on Industrial Informatics*, 59(2):1123-113.

[3] Benitez-Perez, H., Ortega-Arjona, J., Rojas-Vargas, J. A., and Duran-Chavesti, A. (2016); Design of a Fuzzy Networked Control Systems. Priority Exchange Scheduling Algorithm. *International Journal of Computers Communications & Control*, 11(2): 179-193.

[4] Du, Z., Lin, T. C., and Zhao, T. (2015); Fuzzy Robust Tracking Control for Uncertain Nonlinear Time-Delay System, *International Journal of Computers Communications & Control*, 10(6): 52-64.

[5] Hu B., Mann G., and Raymond Gosine G, (2001); A Systematic Study of Fuzzy PID Controllers Function Based Evaluation Approach, *IEEE Trans on Fuzzy Systems*, 9: 699-711.

[6] Hu B., Mann G., and Raymond Gosine G(1996); Theoretic and Gentic Designs of A Three-rules Fuzzy PI Controller, *IEEE Trans on Fuzzy Systems*, 16:489-496.

[7] Clarke D.W.(1996); Adaptive Control of a Materials-testing Maechine, *IEEE Trans on Fuzzy Systems*, 13:1-4.

[8] Han Z.G., Shen Y. (2010), An Improved Design Method of Three-dimensional Fuzzy Control, *Control Engineering of China*, 13(1):1-4.

[9] Liu X. J., Cai T.Y., etal.(1998); Structure analysis of three-dimensional fuzzy controller, *Control Engineering of China*, 24(2):230-235.

[10] Chen B., etal.(2006); *Electric drive control system*, Machinery Industry Press, Beijing, 2006.

[11] Lai, J.G., Zhou, H., Lu, X.Q., and Liu, Z.W (2016); Distributed power control for DERs based on networked multiagent systems with communication delays, *Neurocomputing*, 179:135-143.

[12] Lai J.G., Lu X.Q.(2012); The Application of Embedded System and LabVIEW in Flexible Copper Clad Laminates Detecting System, *International Journal of Information and Computer Science* , 1: 4-10.

# Influence of the QoS Measures for VoIP Traffic in a Congested Network

R.L. Luca, P. Ciotirnae, F. Popescu

**Robert Luca, Petrica Ciotirnae*, Florin Popescu**
Military Technical Academy
Romania, 050141 Bucuresti, Bdul George COSBUC, 39-49
robert.lucian.luca@gmail.com, ciotirnae@mta.ro, fdpopy@yahoo.com
*Corresponding author: ciotirnae@mta.ro

**Abstract:** The paper revolves around the subject regarding quality of service (QoS) in a telecommunication network. The chosen scenario is based on the transmission of data and voice packets using a WAN connection, which has a limited bandwidth and emphasize the need of implementing QoS mechanisms in order to fulfill the quality requirements of the traffic, especially for VoIP. This topology will outline the impact and importance of the QoS implementation, illustrated by the desired quality resulted through VoIP traffic simultaneously with maintaining the data conectivity using a lower bandwidth for applications which require a smaller amount of QoS properties, such as FTP.
**Keywords:** Quality of Service (QoS), VoIP, Weighted Fair Queuing (WFQ), Low Latency Queuing (LLQ), Class-Based Weighted Fair Queue (CBWFQ).

## 1 Introduction

This paper emphasize a method to implement mechanisms that provide Quality of Service (QoS) to VoIP services. The QoS problem is a subject that will be studied continuously, according to other papers which studied this matter [1], [2]. There are a few challenges that concern the VoIP implementation: finding solutions to transmit a real-time service using a data network, which offers no guarantees regarding the delivery of the service, by using the best effort mode. This type of technology is successful only if the features that inffluence the quality of service in data networks are being decreased: latency, jitter and packet loss (see [3]- [8]). Moreover, QoS represents one of the 4 characteristics which a network has to provide in order to fulfill the clients expectations, beside scalability, security and fault tolerance [9].

## 2 General description of the used mechanisms

In order to implement the QoS mechanisms, it is neccessary to use specific mechanisms depending on the type of network and service used. Some of them are described in the paragraphs below. The **Weighted Fair Queuing** (WFQ) [10] mechanism creates dinamically queues based on traffic flows. A packet can be asigned to a certain type of flow depending on the value obtained through applying a hash function on the source IP address and destination address, source port and destination port or ToS value.

This type of flow will have his own queue. The maximum number of queues that can be recorded on the interface is 4096, which is much higher than other similar mechanisms (ex: **Priority Queue** which allows the network administrator to configure four separate buffers with different priorities: high, normal, medium and low. Packets in buffer with higher priority are always processed before packets in lower priority buffer; **Custom Queue** - allows users to define up to 16 queues. Each queue is processed at a time and can be transmitted according to the

parameter "weight" (set by user) a certain number of packets or bytes). In **WFQ**, a flow exists as long as there are packets in that stream waiting to be transmitted. In other words, when the queue allocated to that stream is empty, it is removed . For this reason the number of queues in the system is changing rapidly .

The mechanism which allocates bandwidth among different streams is based on a factor (cost, weight), which depends on the **Precedence** field for the given buffer. When there is a free space in the hardware buffer, the WFQ mechanism takes a packet from the software buffers and places it in the hardware buffer. It will be chosen the packet with the minimum "Sequence Number" (SN) among all queues. SN value is assigned to a packet before it is placed in the queue of the associated stream and also before taking a decision on its eventual disposal (the WFQ mechanism uses a modified "tail-drop" algorithm which takes into account the SN value before discarding packets).

The formula used to calculate the SN of a packet:

$$SN = SN_{ant} + (w \times dim) \tag{1}$$

where: $SN_{ant}$ represents the $SN$ of the previous packet, $w$ represents the cost (weight)and has the formula:

$$w = \frac{32348}{I_{pp} + 1} \tag{2}$$

($I_{pp}$ represents the value of the IP Precedence Field) and $dim$ represents the packet dimension. From the expression (1) we can have some conclusions:

- The calculation of the SN takes account of packet size, being smaller for smaller packets;

- Packets arriving in queues that already have a large number of packets will get a higher SN whereas the calculation of the SN takes account of the previous packet SN ;

- It can be seen that the SN varies inversely with the value of the Precedence field. The higher the priority of a flow, the lower the cost value "w" and hence the SN.

In **Fig. 1** it can be seen how the packets are scheduled for transmission in two different queues that have the same cost $w$.

If the $A$ flow from **Fig. 1** would have a bigger cost than the cost of stream $B$ it would be possible that SN A1 be greater than SN B1 and the packet "B1" may be transmitted before the transmission of packet "A1", situation which is graphically depicted in **Fig. 2**.

WFQ algorithm automatically creates eight queues with smaller weights (high priority) for management traffic generated by the router (messages from routing algorithms, control traffic of OSI layer 2, etc.). WFQ works well for networks where delay sensitive traffic requires less bandwidth than the average of other flows. The method has the advantage that it does not require manual configuration of classes and can thus be used as the default method when traffic characteristics are unpredictable and classification is difficult [12].

Disadvantages of this method: no guarantees for the delivery of a specific type of traffic and the fact that this algorithm doesn't have a high priority queue that would provide minimum values for delay and jitter for VoIP traffic.

Another mechanism that can be used for providing QoS measures is **Class-Based Weighted Fair Queue (CBWFQ)** [10], [11]. This congestion management mechanism permits the classification of packets into classes with costs (weights) according with the bandwidth specified by the administrator for each class. CBWFQ band division is performed inversely to the cost assigned
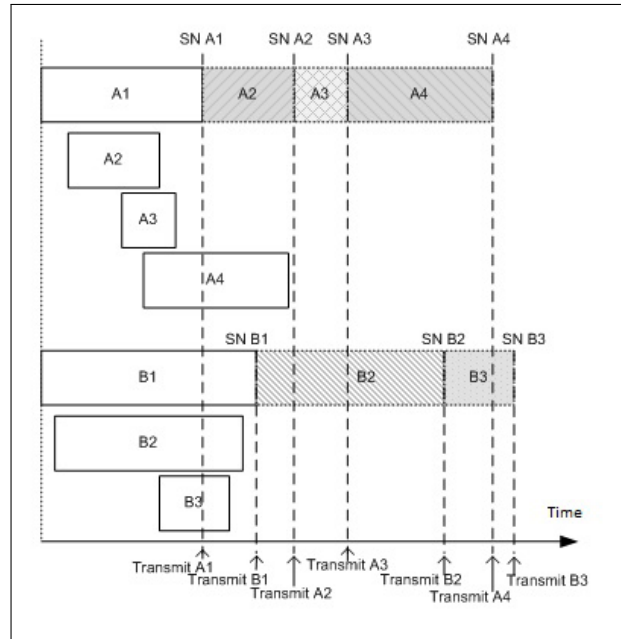
Figure 1: Programming packet transmission according to the SN (same cost $w$) [14]
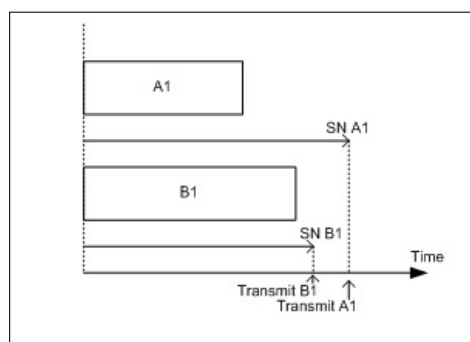


Figure 2: Programming packet transmission (different cost, $w(A) > w(B)$)

to the flow. The method in which bandwidth is shared between the streams is described by the following equation :

$$share(k) = \frac{w(1) + w(2) + ... + w(k) + ... + w(N)}{w(k)} \tag{3}$$

Equation *(3)* outlines the fact that the flows which have a smaller "w" cost get more bandwidth. Unclassified traffic (which does not fall within any user-defined class) is sent to a special class (default) using WFQ mechanism and the weights defined by it according to the equation *(2)*.

The cost of user-defined classes can be determined from the following formulas based on how the bandwidth command is applied to a certain class (as the number of bits or as a percentage of the total bandwidth) according to the following equations:

$$w(k) = ct\frac{B_{w_{tot}}}{B_w(k)} \tag{4}$$

,where $ct$ depends on the number of queues in the system (inversely to the number), $B_{w_{tot}}$ represents the available bandwidth on an interface and $B_w(k)$ is the bandwidth configured for a specific class as the number of bits.

$$w(k) = \frac{ct \times 100}{B_{w_{percentage}}(k)} \tag{5}$$

$B_{w_{percentage}}(k)$ represents the bandwidth configured as a percentage from the total bandwidth.

Each manually configured class represents a separate queue managed by a FIFO algorithm that receives a percentage of the total bandwidth depending on how the packets are chosen for transmission to the hardware buffer. After configuration, the CBWFQ algorithm works similar to WFQ, which means that it is based on the SN value defined by the same formula as in WFQ, equation *(2)*. It can be demonstrated that any user-defined class dominates the dynamically determined flows (WFQ) almost all the time (except when certain classes are configured with a very low percentage 1.5%, which is unlikely) [13].

Same as WFQ, a predefined set of queues is allocated for the CBWFQ mechanism called "Link Queues" that the system uses for transmission of network management traffic. These buffers are set at a fixed cost $w = 1024$, a cost which is much better compared to the cost of any dynamic flow and about the same level as the traffic classified by the user. Due to the fact that this type of traffic is intermittent, the bandwidth distribution is not affected. Moreover, there is a rule that user-defined traffic classes should not reserve more than 75% of the available bandwidth on an interface, such that these special buffers do not remain without bandwidth [15].

**Low Latency Queuing** mechanism (LLQ) or "**CBWFQ with Priority Queue**" [11] complements CBWFQ mechanism and allows you to specify a traffic class with high priority and therefore minimal latency. The delay sensitive traffic can be transmitted before other types of traffic by using a special buffer with the highest priority (cost w = 0). In **Fig. 3** it can be seen the essential difference between LLQ and CBWFQ mechanism, namely the existence of the priority buffer. This is a buffer with the minimum cost (0) which means total priority. In other words, the traffic that will be selected to use this buffer will always be sent before other types of traffic. For this class it applies a "policing" mechanism (when the configured rate is exceeded, packets are automatically discarded) to avoid the situation in which traffic with priority monopolizes all available bandwidth on an interface and starves other traffic classes that have been configured for guaranteed bandwidth. Due to the fact that in the case of VoIP, traffic packets are sent at

regular intervals, the transmission rate is relatively constant and for that reason VoIP is the best choice for the priority buffer. Due to the advantages of minimum values for delay and jitter,LLQ is one of the most recommended method of "queuing" in literature and represents the version tested in the practical application presented below.

On the low-capacity links, LLQ can be used with other QoS mechanisms such as header compression and fragmentation and interleaving (to avoid the situation in which voice packets must wait for the transmission of large data packets, which would lead to significant delays and jitter).
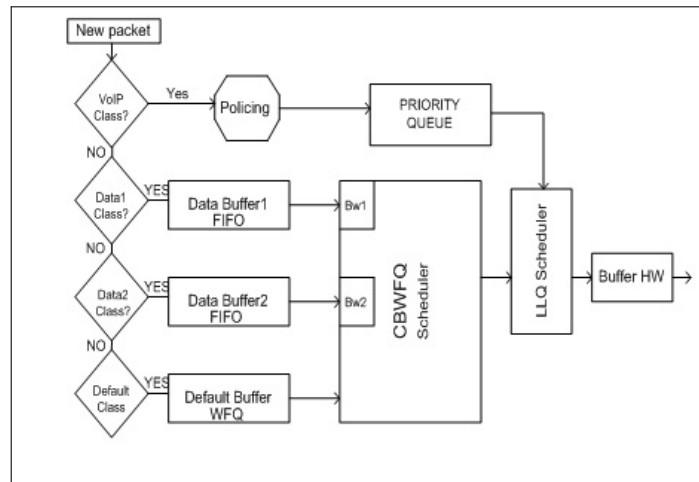


Figure 3: LLQ mechanism operation [16]

# 3 Experimental results

For laboratory testing the following scheme was used for the interconnection of the equipments (**Fig. 4**):
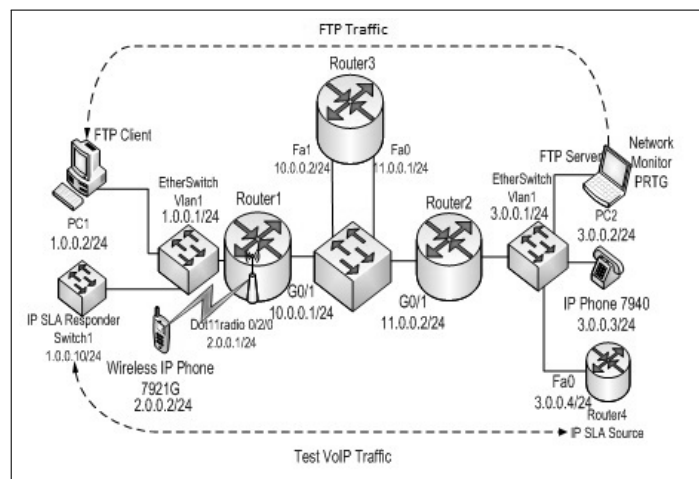


Figure 4: Logical scheme of the equipments interconnection

The aim of the laboratory tests is to highlight and compare the statistical values obtained for voice traffic in VoIP format in two distinct situations. The first case refers to a congested

network in which it does not take into account the priority of traffic classes and the second situation where specific QoS measures are applied.

Functional laboratoty platform description:

- VoIP service is provided by the CME server (Call Manager Express) on router 1 for the wireless network 2.0.0.0/24 and CME server on router 2 for the network 3.0.0.0/24. Between the two servers there is a trunk for data link;

- computer at IP 1.0.0.2 will play the role of a FTP client that will receive multiple streams of data from the laptop with the address 3.0.0.2 that will be the FTP server. Between router 1 and router 2 it will be generated so much traffic as possible so that congestion occurs.

- in addition, on the link between router 1 and router 2 the rate is limited at 500 kbps. This limitation has been achieved using an additional router (router 3) configured in such a way that it receives all the traffic transmitted between router1 and router 2.

- traffic received by the router 3, regardless of its source or nature is selected by access lists and configured on router 3 as a single class of traffic. For this class it applies a shaping policy at 500 kbps (limiting the transfer rate at a given value while maintaining the packets in a buffer when the limit is exceeded).

To analyze the quality of voice traffic was used an mechanism available on Cisco equipments called "Cisco IP SLA." This application may generate packets similar with VoIP packets with predetermined characteristics depending on the type of the codec used. Router 4 is used as the source and the probe and Switch 1 as the device addressed. Generated packets go through the network to the switch 1 and then return to the probe device to calculate the value for delay, jitter and number of packets lost.

Shortly after the initiation of data traffic congestion occurs in the network and the quality of voice traffic will be affected by high latency, variations in delay and packet loss. A range of objective assessments can be achieved by using a VoIP traffic generator (router 4) whose statistics are taken, analyzed and displayed in charts by a program called PRTG Network Monitor. This application identifies network devices by IP and assignes them "sensors" which return various statistics such as CPU load, system temperature, check the ping response time etc. Such a sensor that receives and interprets VoIP statistics is called Cisco IP SLA VoIP and can be associated with a router / switch Cisco that operate as transmitter of IP SLA test packets (probe). So, before this program can collect statistics from a VoIP device it must be configured to generate test traffic.

IP SLA VoIP UDP jitter mechanism can generate packets similar to VoIP packets with characteristics that are preset depending on the type of codec used, e.g. G.711, G.729. After the values for delay , jitter and packet loss have been collected an approximate value for the R factor is calculated which is an objective measure of voice quality (E-model), which in turn is converted into an equivalent value called MOS (MOS-CQE that Conversational Quality Estimated).

Therefore, IP SLA generates VoIP traffic statistics: delay, jitter, packet loss, MOS, and these statistics are retrieved and displayed in intuitive charts by the dedicated sensor in PRTG. Thus, the degradation of voice quality that comes with the installation of congestion can be confirmed by objective means (up to 1.2 seconds delay, packet loss up to 50% and jitter up to 20 ms.), shown in **Fig. 5** and **Fig. 6**:

Router 1 and router 2 are connected by a link that is limited in terms of available bandwidth. When the traffic rate tends to exceed that available bandwidth, every packet will be dropped regardless of the class to which it belongs. To avoid this, it is applied a policy to all the traffic
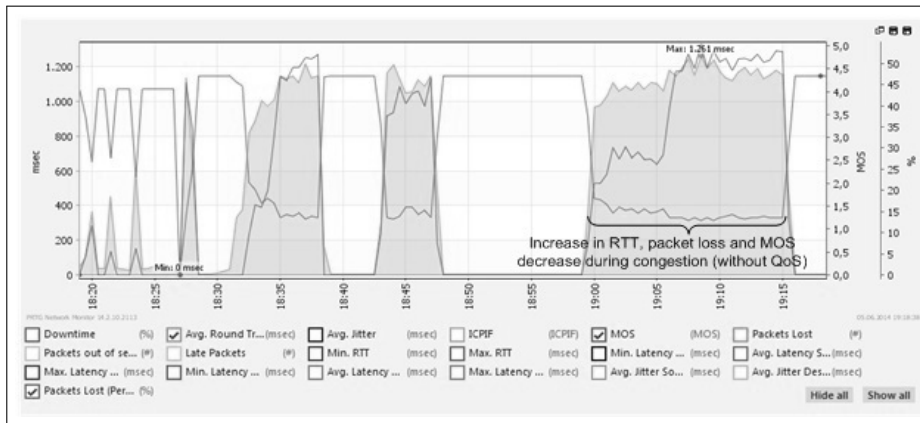
Figure 5: **MOS**, **RTT** (average values) and **packet loss** statistics for a congested network without QoS measures (for VoIP SLA traffic)

leaving the interface (higher level policy), so the transfer rate is less than the maximum available bandwidth. In this way, it will move the congestion from the router 3 on the output interfaces of the border routers (router1 and router2) where the quality requirements of traffic can be managed (in a lower-level policy). In this application it has been studied Low Latency Queuing algorithm performance.
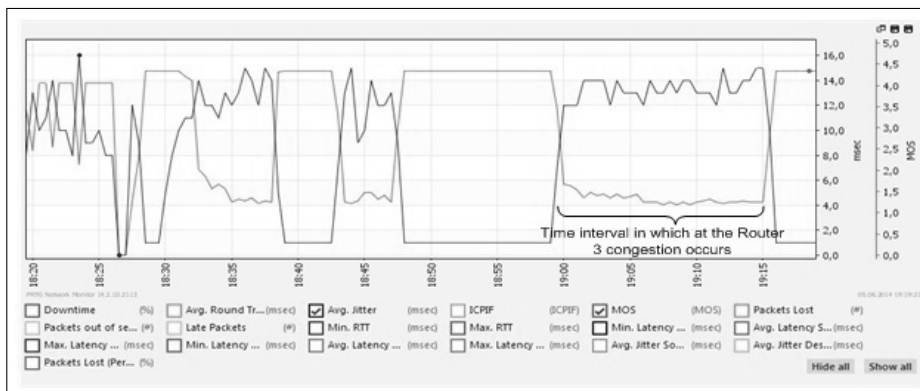


Figure 6: Highlighting the increse of **jitter** values during congestion

So there will be an aggregate traffic consisting mainly of VoIP traffic, FTP traffic and management traffic (ARP, DHCP) that will have a maximum output rate of 480 kbps (limitation imposed by the higher-level policy). From this rate a part will be allocated for VoIP traffic(with priority, 190 kbps), another part will be guaranteed for FTP traffic (150 kbps) and the remainder will be allocated to other types of traffic. This last category will share the remaining bandwidth with a WFQ policy type. LLQ algorithm must be carefully implemented because a poor setting may have unintended consequences (packet loss) on delay sensitive traffic (VoIP class in this case) due to the "policing" rule applying to it. If LLQ is implemented correctly, the traffic that is found in the priority buffer will never exceed the configured rate.

When hierarchical QoS policy is applied to the output interface of the two border routers it will be seen an immediate increase in MOS values and also the call quality (subjective) is much better in the absence of packet losses and delays as it can be seen in **Fig. 7**.

In **Fig. 7** it may be noted that packet losses have decreased from high levels of $40 - 50\%$ to 0 and the delays have also decreased to values of a few ms.
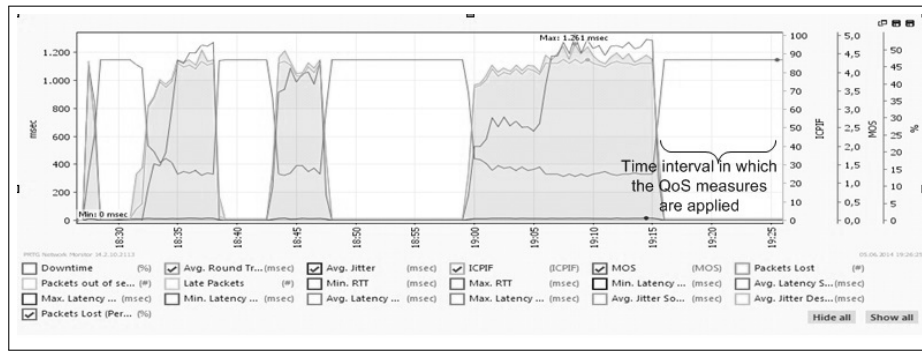
Figure 7: **MOS**, **ICPIF**, **jitter**, **RTT** statistics (average) and **packet loss** for VoIP SLA traffic with QoS measures applied

In **Fig. 8** it can be seen a comparison between the results obtained for delay and jitter when the mechanism used is CBWFQ and LLQ mechanism respectively.

Although apparently the differences between the two are small and don't affect speech quality in the lab scenario, in a real situation where there can be multiple nodes and multiple paths between source and destination the values for delay and jitter in the case of CBWFQ can grow significantly and can sum up and degrade the quality of voice traffic. Hence the importance of using a high priority buffer for voice traffic.
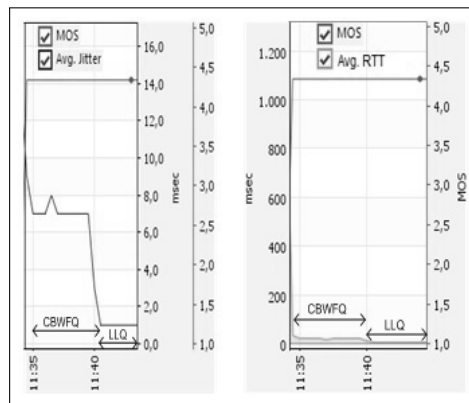


Figure 8: Highlighting the differences for **jitter** and **RTT** between CBWFQ and LLQ

## 4    Conclusions

Using appropriate QoS mechanisms it can be achieved the desired quality for VoIP traffic while maintaining the operation at lower rates for other types of traffic. Thus, by applying the appropriate QoS measures we have achieved a considerable improvement of MOS index from values of about 1.5 to ideal levels (about 4) which indicates a very good quality for VoIP traffic. The increase in MOS is due to improvements in the values of delays (from hundreds, thousands of milliseconds to a few milliseconds); lost packets (at levels of about $40-50\%$ to 0%) and jitter (from 15msec to 1 msec).

LLQ is a highly effective mechanism to meet QoS requirements because it allows control of service quality based on traffic classes that can be defined with precision.

Also, analyzing the mechanism behind CBWFQ (LLQ) it can be concluded that none of the classes is not restricted to the configuration set up if there is enough bandwidth available.

We also demonstrated the necessity of using a high priority buffer for VoIP traffic through a comparative analysis of the results obtained in the two cases LLQ and CBWFQ which showed that values for delay and jitter can be minimized by using Low Latency Queuing.

# Bibliography

[1] P. Sharma (2014); Challenges of Quality of Services in Mobile Ad Hoc Networks, *International Journal of Advance Research in Computer Science and Management Studies*, 2(3): 342-347.

[2] R.D. Albu, I. Dzitac, F. Popentiu-Vladicescu, I.M. Naghiu (2010); Input Projection Algorithms Influence in Prediction and Optimization of QoS Accuracy, *International Journal of Computers Communications & Control*, 9(2): 132-139.

[3] V. Fineberg (2002); A practical architecture for implementing end-to-end QoS in an IP network, *IEEE Communications Magazine*, 40(1): 122-130.

[4] W. C. Hardy (2003); *VoIP Service Quality: Measuring and Evaluating Packet-Switched Voice*, McGraw-Hill, 2003.

[5] T. Wallingford (2005); *Switching to VoIP*, O'Reilly, 2005.

[6] O. Hersent, J.P. Petit, D. Gurle (2005); *Beyond VoIP Protocols: Understanding Voice Technology and Networking Techniques for IP Telephony*, John Wiley and Sons, 2005.

[7] J. Davidson, J. Peters (2000); *Voice over IP Fundamentals*, Cisco Press, 2000.

[8] Cisco Systems, Inc.(2001); *Cisco IP Telephony QoS Design Guide*, www.cisco.com.

[9] M. A. Dye, R. McDonald, A.W. Rufi (2008); *Network Fundamentals CCNA Exploration Companion Guide*, 2008 Cisco Press.

[10] Cisco Systems, Inc (2014); *QoS: Congestion Management Configuration Guide, Cisco IOS XE Release 3S*, www.cisco.com.

[11] T. Szigeti, R. Barton, C. Hattingh, K. Briley Jr. (2014); *End-to-End QoS Network Design: Quality of Service for Rich-Media and Cloud Networks*, Second Edition, Cisco Press, 2014.

[12] http://mynetworkingwiki.com/index.php/Weighted_Fair_Queuing

[13] http://myway2ccie.blogspot.ro/2009/04/qos-weighted-fair-queuing-and-class.html

[14] http://www.perihel.at/2/rno/03-QoS-Queuing-Methods.pdf

[15] http://blog.ine.com/2008/08/17/insights-on-cbwfq/?s=wfq

[16] http://josephmlod.files.wordpress.com/2010/12/llq-pq.jpg

# Efficient Opinion Summarization on Comments with Online-LDA

J. Ma, S. Luo, J. Yao, S. Cheng, X. Chen

**Jun Ma, Senlin Luo**
School of Information and Electronics
Beijing Institute of Technology
Beijing, China
{junma,luosenlin}@bit.edu.cn

**Jianguo Yao*, Shuxin Cheng**
School of Software
Shanghai Jiao Tong University
800 Dongchuan Road
Minhang, Shanghai 200240, China
{jianguo.yao,reallytrue1262}@sjtu.edu.cn
*Corresponding author: jianguo.yao@sjtu.edu.cn

**Xi Chen**
School of Computer Science
McGill Universiy
Montreal QC Canada
xi.chen7@mail.mcgill.ca

**Abstract:** Customer reviews and comments on web pages are important information in our daily life. For example, we prefer to choose a hotel with positive comments from previous customers. As the huge amounts of such information demonstrate the characteristics of big data, it places heavy burdens on the assimilation of the customer-contributed opinions. To overcoming this problem, we study an efficient opinion summarization approach for a set of massive user reviews and comments associated with an online resource, to summarize the opinions into two categories, i.e., positive and negative. In this paper, we proposed a framework including: (1) overcoming the big data problem of online comments using the efficient online-LDA approach; (2) selecting meaningful topics from the imbalanced data; (3) summarizing the opinion of comments with high precision and recall. This framework is different from much of the previous work in that the topics are pre-defined and selected the topics for better opinion summarization. To evaluate the proposed framework, we perform the experiments on a dataset of hotel reviews for the variety of topics contained. The results show that our framework can gain a significant performance improvement on opinion summarization.
**Keywords:**Opinion summarization, Latent Dirichlet Allocation (LDA), online - LDA, imbalanced data, big data.

## 1 Introduction

The rapid development of the Web 2.0 application makes tremendous and diverse information flood the web. We have to admit that the information shows a wide variety of the meanings which may hardly grasp without summarization. Even worse, the data contained this information shows the characteristics of big data and brings the challenge to the efficiency of the data processing. With more and more user-contributed reviews and comments on the Web, the corresponding websites can become more popular resources that reflect the attitudes and interests of the users in a way that depart from the advertisement and the content of the underlying information resource itself.

Many techniques have been developed to extract concise information from these contents, such as sentiment classification, text summarization and topic modeling [3] [4] [7]. Nevertheless, the comments on the web are updated unceasingly, it is hard to perform online opinion summarizing with these current techniques. Even though these comments are meant to be useful, the vast opinions summarized are still not easily digested and exploited by the users.

When we want to make a comparison of electronic products such as cell phones and laptops, common attributes of the products under consideration include ease of use, battery life, sound quality, Add on s etc. Actually, on most of eCommerce websites, these attributes are pre-defined topics/features and mainly describe hardware performance. Let we say laptops, because of the system's original configuration, the user's experiences can be completely different even with the same hardware. And the after-sales services are also a major concern of the user which only can be reflected in the comments. Thus the pre-defined topics do not demonstrate much diversity on different products. The user's comments are valuable information resource that needs to be summarized.

On *tripadvisor*[1], in order to make an easy comparison of hotels, the scalar rating mechanism is built on the websites for users. But the scalar ratings, e.g. scores between 1 and 5, are not very helpful for hotel managers or tourists because the numeric value does not provide the subjectivities or opinions that come from customer experiences. Also, these scalar ratings are not comparable: for example, when a 3-star hotel receives a high score from 10 tourists while a 4-star hotel receives a medium score from 1 tourist, that does not imply that the former one is better than the latter. In this situation, how to obtain valuable information from users' comments is more important. Furthermore, personal experiences about each hotel cannot totally the same. Consider two typical hotel comments shown in figure 1. These two comments discuss several different topics of the hotel, such as price, room, food etc. The same topics are also in the comments, such as room, breakfast. Apparently, the topics in hotel comments show more diverse topics than electronics products comments. It is impossible to list all the topics tourists may share. Extracting meaningful topics from the comments is not an easy task.

Hotel comments show a very interesting phenomenon of imbalance. The hotels with more comments imply that this hotel is popular and the tourists posting the comments are more likely to share their good experience with others. So the positive comments are far more than the negative comments. The situation of the less popular hotel is quite different, in that less comments will be posted if the tourists had a bad experience. The imbalanced data is the big problem for summarization in form of binary classification.

In our framework, we use scheme of online topic extraction in coping with big data problem. Online inference is employed to handily analyzes the huge number of comments in stream form. There is a superior advantage that makes online LDA process massive collection without heavy computational cost and memory necessity.

Due to the imbalance of the hotel comments, the meaningful topic selection is another challenging problem to opinion summarization. In our framework, topic selection is carried on with multi-facets of consideration. In comparing with three *ROC* based topic selection methods, FAST [19] is the best one in handling the extracted topics with the problem of the imbalance, and relative low computation is needed. Furthermore, better opinion summarization is obtained with any redundancy topics filtered out and accuracy in classification. In our evaluation, we observe that our framework avoids several problems faced by supervised classification approach.

The aim of the present work is to study the manner in which hotel comments can be summarized into positive and negative opinions with meaningful selected topics, so that the obtained summary can be used in real life. Our main contributions are summarized as follows:

---

[1]www.tripadvisor.com

Figure 1: Different Topics on Hotel Comments

- We present a framework of comments summarization and the online variational methods are used to handle huge amounts of comments from the web in coping with the big data.

- We address the problem of data imbalance of hotel comments. Different from existing works on pre-defined topics, topic selection is performed with the consideration of the more positive comments and less negative comments.

- The ratable topics can be a form of summary and the opinion summarization is performed with these topics for easy digest and exploitation. The experiments are conducted on comments crawled from *tripadvisor*. Several metrics are used for the evaluation, and experimental results show that our proposed framework can summarize the comments in a good manner.

The rest of the paper is organized as follows. Section II surveys existing studies on comments summarization in topic models. In Section III, we propose a framework of the opinion summarization and discuss the topics/features involved in this task and the challenges it implies, in comparison to other LDA based text summarization. In Section IV, we propose a different approach to analyze data imbalance. The evaluation results using several metrics are reported in Section V. In Section VI, we offer insights on the challenges of opinion summarization and point out clear directions in which further improvements can be made.

## 2   Related Work

We first review the research works related to topic modeling. We then give a brief overview of opinion summarization using other techniques, and we discuss the difference between our framework and sentiment classification lastly.

**Topic modeling.** Topic Sentiment Model (TSM) [17] is based on the pLSI model [7] which is used to extract the topics. While they set the topics into three sub-topics: neutral, positive and negative topics, the generation progress of documents is considered as first choosing the sub-topics, then choosing the topics in these sub-topics. Y. Lu et al. [13] used a two-step strategy to integrate the opinions with a pulse. The first step is to divide the opinion documents into expert opinions and ordinary opinions. They called it semi-supervised pLSA because the topics are found from expert opinions on the second step, then use as the defined aspect to cluster ordinary opinions.

Latent Dirichlet Allocation (LDA) [3] is another representative topic model which provides a basis for textual-level summarization in an unsupervised way. Supervised latent Dirichlet allocation (sLDA) model [4] accommodates a response variable to make the LDA model work under a supervised condition with the facility of the classification. Multi-grain LDA (MG-LDA) model [10] manipulates the LDA model to induce multi-grain topics. The main idea of the model is to find a ratable aspect within texts on a given topic and use this rating information to identify more coherent aspects. Labeled LDA [5] model is a supervised model with the ability of the k-classification. Joint sentiment/topic (JST) model [11] is a four-layer probabilistic model with the extension of three hierarchical layers LDA which can perform sentiment classification under fully unsupervised way. Z. Ma et al. [21] proposed two topic models, MSTM and EXTM to extract the topics from the documents and its comments respectively, then select representative comments from comment clusters.

Opinion summarization with the LDA related model is multi-faceted and very involved. These approaches can have scalability issues.

**Comments summarization.** Comments summarization involves two major steps, topic identification and classification. Generally existing research is to classify the comments according to their polarity, which is positive or negative [1] [2] [?]. This kind of summarization on comments can give a very general notion of what the users feel about the product. The accuracy of the classification heavily depends on the identified topics and the distance measure. LDA models are one way of topic identification. NLP-based techniques are the other ways to identify topics in the text [13] [14] [15] [16] employed pointwise mutual information and cosine distance as distance measures to perform the binary classification and found that the latter one leads to better accuracy.

Our proposed framework is different from the LDA with the employment of online inference in handling big data. And we also address the imbalance problem of hotel comments. Our work aims at improving the accuracy and scalability of opinion summarization model and inferring meaningful topics for better summarization of the comments.

## 3   A Better Way to Extract the Topics

In this section, we demonstrate the framework of our model. A brief analysis is given to hotel comments. Then we compare different approaches of topic extraction and highlight the advantage of online inference LDA model for comments topic extraction.

### 3.1   The Framework

Imagine booking a hotel on the web. We may not review every comment on each hotel and furthermore we could not find the sentiment changes within a long term. So how can we manage and digest the large information other tourists provided? LDA model is well-known algorithm for discovering the main themes of large and unstructured documents. Our framework is combining the LDA model and a *ROC*-based topic selection.

Opinion summarization includes three steps. The first step is topic extraction, the online inference for the LDA model is used for improving its scalability. The potential topics of the comments may not be evaluated properly because the topic number $k$ of LDA is pre-defined by the user. This means that not all the topics extracted are meaningful for opinion summarization, or good for the classification of positive and negative. So we perform the topics selection (extracted topics are the features for classification) in a second step. The third step is opinion summarization or binary classification. As we can see in figure 2, the collected comments show
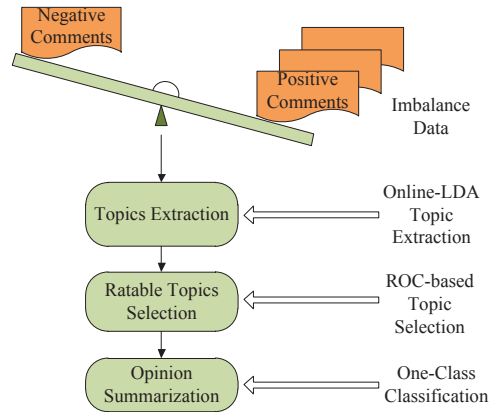


Figure 2: Framework of our model

the characteristic of imbalance (We detail the reason in the next section) which pose a server problem on classification. The *ROC*-based topic selection is used in our framework for better classification. The relevant algorithm is described in section 3.

## 3.2　Topic Extraction on Comments

There are several probabilistic models to extract the topics - unigram model, multi-gram model, policy model and LDA model. The fundamental idea of these models is that the comments analyzed are considered to have one or some pre-defined topics. The difference is that each one is based on different statistical assumptions.

Probabilistic latent semantic indexing (pLSI) model introduces two probability layers to reduce the constrains on the number of topics and mixture weights of each topic. The probability of a comment is:

$$p(d, w_n) = p(d) \sum_z p(w_n|z)p(z|d). \tag{1}$$

But these topics mixtures are only for those training comments and cannot be used for previously unseen comments. Furthermore, pLSI is a model prone to overfitting in training. So this model is not a well-defined generative model either.

Latent Dirichlet Allocation (LDA) is an extension of the pLSI which introduce a Dirichlet prior on topics. Here we denote as $\theta$. The generative process includes two steps: one is to choose $\theta$ for the Dirichlet prior on topics, then choose a word from $p(w_n|\theta, \beta)$.

This process is a continuous mixture distribution:

$$p(c_i|\alpha, \beta) = \int p(\theta|\alpha) \left( \prod_{n=1}^{N} p(w_n|\theta, \beta) \right) d\theta, \tag{2}$$

$p(\theta|\alpha)$ are the mixture weights on topics.

In this work, LDA is used to extract topics from hotels comments collection. A unified topic model is trained on the integrated content by combining the multiple text fields within each comment together. Given a comments collection $C = c_1, c_2, , c_N$ where $N$ denotes the comments number, each comment $c_i$ is assigned a distribution over K topics learned from the comments collection where $K$ denotes the pre-defined topic number.

Hotels comments are updated frequently on their pages. A model using a supervised learning algorithm cannot well generalize profiles of new comments. LDA model can be used for new comments and can characterize the comments under the unsupervised form in term of the estimated posterior distribution. Usually this posterior cannot be computed directly [3], and is mostly approximated using Markov Chain Monte Carlo (MCMC) methods or variational inference. The realization of the particular MCMC method, the Gibbs sampling algorithm [18], is widely used to LDA based comments collection modeling.

The applicability of Gibbs sampling depends on the ease with which the sampling process creates separate variables for each piece of observed data and fix the variables in question to their observed values, rather than sampling from those variables. Gibbs sampling generates a Markov chain of variables, each of which is correlated with nearby variables. Each step of the Gibbs sampling procedure involves replacing one of the variables with a value drawn from the distribution of that variable conditioned on the values of the remaining variables. Thus the algorithm converges much slowly when handling high-dimensional data.

As we know, the variational method is a deterministic alternative to sampling-based algorithms. The only assumption made for variational method is the factorization between hidden variables and visible variables. Thus, the inference problem is transformed into an optimization problem as the equation shows:

$$\mathcal{L}(\omega, \phi, \gamma, \lambda) \triangleq \mathbb{E}_q[\log p(\omega, z, \theta, \beta|\alpha, \eta] - \mathbb{E}_q[\log q(z, \theta, \beta)] \tag{3}$$

$\phi$, $\gamma$, are the parameters of $z$ and $\theta$, $\lambda$ is the parameter of the topics $\beta$. The variational inference may converge faster than Gibbs sampling. However, it still requires a full pass through the entire collection each iteration. It can therefore be time and memory consuming in the application to large and stream coming comments collection.

Hoffman et al. [8] proposed a much faster online algorithm for the variational inference of LDA. This time a fully factorized variables is used, then the lower bound is defined as

$$\mathcal{L} \triangleq \Sigma_d \ell(n_d, \phi_d, \gamma_d, \lambda), \tag{4}$$

The online variational inference comes from the best setting of the topics $\lambda$. After estimating the $\gamma(n_d, \lambda)$ and $\phi(n_d, \lambda)$ on seen comments, then set $\lambda$ to maximize

$$\mathcal{L}(n, \lambda) \triangleq \Sigma_d \ell(n_d, \gamma(n_d, \lambda), \phi(n_d, \lambda), \phi_d), \tag{5}$$

The convergence of the online inference had been analyzed and proved much faster than other variational methods.

The hotel comments on *tripadvisor* keep increasing dramatically as we have seen. The scalability is an unavoidable challenge for processing the data set in real time. Online variational inference for LDA can be much more useful in dealing with a high volume of data and it can handily analyze massive collections of comments. Moreover, online LDA need not locally store or collect the comments- each can arrive in a stream and be discarded after one look. Refer to [8] for a detail analysis of online variational inference for LDA.

# 4  Opinion Summarization from Topic Selection

In this section we briefly illustrate the data imbalance problem and two topics selection methods, then we describe the algorithm, used in our framework for opinion summarization from imbalanced data topic selection.

Further to the topic extraction described in the previous section, we explore the impact of the topics on the summarization performance. Intuitively, opinion summarization can be different from the summarization of factual data, as comments regarded as informative from the factual point of view may contain little or no sentiment. So, eventually, they are useless from the sentimental point of view. The main question we address at this point is: how can we determine the informative extracted topics for opinion summarization.

The comments collection we clawed from *tripadvisor* demonstrates the imbalance problem of more positive and less negative. The data imbalance presents a unique challenge to classify the comments from the extracted topics. Precision and recall are widely used measurements for classification performance. The precision for a class is the number of true positives divided by the total number of elements labeled as belonging to the positive class. Recall is the number of true positives divided by the total number of elements that actually belong to the positive class. Consider the two topics sets on text classification, the first topic set may yield higher precision, but lower recall, than the second topics set. By varying the decision threshold, the second topic set may produce higher precision and lower recall than the first topic set. Thus, one single threshold cannot tell us which extracted topic set is better. The topic selection needs serious consideration.

Commonly, there are two methods to select topics: the first is rank topics in descending order with the related criteria, such as $ROC$, then choose the top, say, $l$ topics. The second is more complicated with computation of cross-correlation coefficient between topics. Scatter matrices are belong to the first method.

$$J_3 = \text{trace}\{S_w^{-1} S_b\} \tag{6}$$

where $S_w = \sum_{i=1}^{c} P_i S_i$, $P_i$ is the a priori probability of class $w$, $S_i$ is the mean vector of class $w$, $S_w$ is the within-class scatter matrix, and $S_b$ is the between-class scatter matrix.

The cross-correlation coefficient is the second method to topic selection. Let $i_1$ be the best topic selected using the first method.

$$i_2 = \max_j \{a_1 R_j - a_2 |\rho_{i_1,j}|\}, \quad j \neq i_1 \tag{7}$$

This equation considers the cross-correlation $(\rho_{i_1,j})$ between the best topic and topic $j \neq i_1$. The rest of the topics are ranked according to

$$i_k = \max_j \{a_1 R_j - \frac{a_2}{k-1} \sum_{r=1}^{k-1} |\rho_{i_r,j}|\}, \tag{8}$$

$$j \neq i_r, \quad r = 1, 2, \ldots, k-1$$

These two methods are designed for well-balanced data and if the data dimension is high, the effectiveness of the topic selection is a severe problem for classification. Most comments we crawled from *tripadvisor* are about the length of 150 words. In generalizing the comments with the LDA model, the pre-defined topic number $k$ is set to 20, 30 rather than 100 because of the relative short length of each comment. Even this moderate number may produce high dimension problems for the topic selection. The detailed analysis is presented in section V. Meanwhile, the computational cost is another bottleneck, even we employ the topic extraction with online-LDA,

the topic selection is a time-consuming task with these two methods because of the computing of matrix inverse. So in the proposed framework, we use FAST [19] to perform the topic selection for opinion summarization. The topic selection metric is based on an $ROC$ curve generated on optimal simple linear discriminants. Then those topics with the highest $AUC$ (Area Under Curve) are selected as the most relevant. This method is designed for the topics selection of imbalanced data classification.

A $ROC$ curve is a criterion for ranking the topics, FAST employs a new threshold determination method which fixes the number of points to fall in each bin to obtain the threshold for $ROC$. Bin means the width of data separation. We use more bins in high density data areas and fewer bins in sparse data area, each bin containing the same number of data. Thus more thresholds computed from each bin are placed into the density area for the calculation of the $ROC$. On the opposite, fewer thresholds placed into the sparse area. This effective procedure can be described as following pseudo-code in Algorithm 1:

---

**Algorithm 1** Pseudo-code of effective procedure.

---

K: number of bins
N: number of comments
T: number of topics
InBin=0 to N with a step size T/20
**for** $i = 1$ to $T$ **do**
    Sort $T_i$ ($T_i$ is the ith value of vector T)
    **for** $j = 1$ to $K$ **do**
        Bottom=round(InBin(j))+1
        Top=round(InBin(j+1))
        Threshold=mean($T_i$(Bottom to Top))
        Classify $T_i$
    **end for**
    Calculate the AUC (Area Under Curve)
**end for**

---

The detailed analysis of the algorithm is in [19]. The benefit applied is not merely about selected topics for classification, the computational cost of the algorithm is relatively low because no matrix inverse is calculated. Because the area under the $ROC$ curve is a strong predictor of performance, especially for imbalanced data classification problems, we can use this score as our topic selection: we choose those topics with the highest areas under the curve because they have the best predictive power for comment collection.

## 5   Experiments

The experiments is to evaluate the model that produces opinion summaries of comments, in the context of which we assess the best manner to use summarization opinion for the users to quickly digest. In this section, we will present and discuss the experimental results of topic selection and opinion summarization on the hotel comments dataset.

### 5.1   Dataset

We crawled 250,004 hotel comments from *tripadvisor* in one month period (from Nov, 2012 to Dec, 2012). The comments in the dataset are labeled according to 5 scales of 'star' expressing the polarity of the opinion of the reviewers (1, 2 corresponding to negative comments and 4,

5 corresponding to positive comments). Since we summarize the opinions into two classes of sentiment (positive and negative), the neural comments (scale 3) are excluded from the comments collection. Figure 4 shows the statistical information about the comments collection. Most comments are within a length of 150 words.
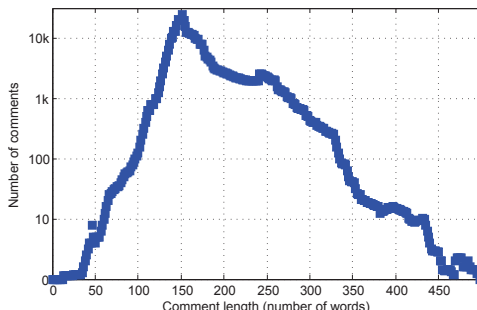


Figure 3: The statistical information of the comments collection

## 5.2   Topic Selection

The first experiment is performed to evaluate the generalization performance of the online-LDA model. As we pointed out in Section III that the LDA with online inference can handle massive datasets much faster than other methods such as variational inference, Gibbs sampling. We need to verify that there is no generalization performance degeneration using online inference for LDA. We compared online-LDA model with pLSI models and LDA model described in Section 3. In this experiment, we used all the comments crawled from *tripadivor* containing 250,004 comments. We held out 10% of the collection for test purposes and trained the models on the remaining 90%. We have found $\alpha = 50/T$ and $\beta = 0.01$ to work well with hotel comments collection for LDA model and online-LDA model.

The perplexity [3] is used as the measurement for the evaluation of the models. As it is the standard metric and it measures the model's ability of generalizing unseen data; lower perplexity indicates the higher likelihood and better model performance.

We trained these three models using EM with the stopping criteria, that the average change in expected log likelihood is less than 0.001%.

Figure 4 presents the perplexity for each model in terms of the comments analyzed. Three models were trained from the crawled comments without looking at the same comment twice. It can be seen that the online-LDA model have a lower perplexity than pLSI and LDA model after analyzsis of the same number of comments. This superior advantage comes from the fact that the online variational inference converged much faster than variational bayes used in LDA [8]. After analyzing the total comments collection, both LDA models reached the same level of perplexity about 1700. The generalization performance of online-LDA is as good as the LDA with an extra advantage of much faster fitting to the comments. The perplexity of pLSI is 1900. So the results show that online-LDA is more adapted to coming comments under online environment.

Besides fast topics extraction, our summarization framework employed a lower cost topics selection method in coping with the imbalanced nature of hotel comments. The experiment performed next is to evaluate the performance of topic selection. The balanced error rate (BER) is the main judging criterion for the topic selection [20].BER is the average of the error rates of positive comments and negative comments. If these two classes are balanced, the BER is equal to the error rate as the rate of inverse recall [6]. We evaluated the performance of selected topics
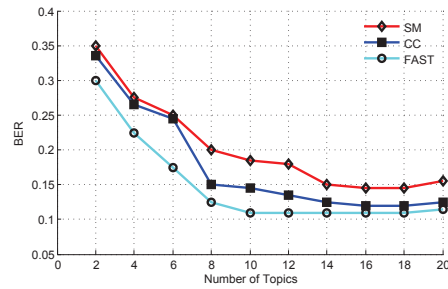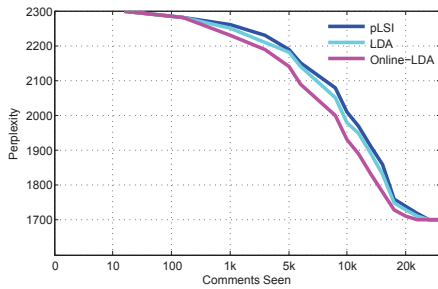
Figure 4: The perplexity results for pLSI, LDA and Online-LDA.

Figure 5: BER with $k = 20$ using $SVM$.

in our framework (FAST) with the comparison of the topics selected by scatter matrices (SM) and cross-correlation coefficient (CCC). The main concern in our framework is the performance of the topic selection metric, so we simply choose the popular SVM classifier to evaluate the performance without the detail analysis of the difference with other classifiers. Table 2 presents the description of the comments used in BER evaluation.

Table 1: Comments used in evaluation of BER

|  | Number of Topics | Ratio |
|---|---|---|
| Positive Comments | 180,023 | 95.5% |
| Negative Comments | 8,053 | 4.5% |

These comments collection demonstrates the strong imbalanced nature that the negative comments are less than 5% of the total comments. From the previous analysis of data set, we know that most of the comment length is less than 260. So we set $k = 20$, 30 respectively for the online-LDA model, then the extracted topics are used for BER evaluation with the methods described in our work.

Figure 5 and 6 show the result of the performance in terms of BER. We can see that the BER changes dramatically with the different numbers of the topics. We observe that BER decreases as the topics increase when the topics number is less than 9. And then the BER reaches to the relatively stable values of 0.15, 0.1 and 0.08 respectively to SM, CC and FAST. The explanation for this behavior is that the redundant topics have little impact on the performance of the classifier. This robustness might be useful to redundant topics for classification. But our goal is comment summarization rather than classification. Redundant topics can bury informative topics and make the user hard to exploit.

The topics selected using FAST significantly outperformed SM and CCC topics with lower BER when using the SVM classifier. Several experimental results reveal that the lowest BER comes from the 9 selected topics. I.Tiov et al. [10] show that 9 topics out of 45 LDA topics correspond to ratable aspects. This is a quite interesting discovery that the topics we selected are same as the ratable aspects defined by a manual analysis of the documents, as the more topics used in classification, the more freedom we can have to distinguish the polarity of the comments in a finer granularity. But the performance of the classification remains stable to a certain level. The optimal topics come from selected topics with the emerging of this level. This suggests that topic extracted using LDA is not a sufficiently representative topic of the importance of comments for summarization purposes. Thus, using $ROC$-based topic selection that has proven useful for opinion summarization can yield better results.
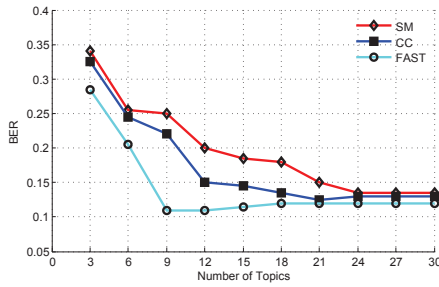
Figure 6: BER with $k = 30$ using $SVM$.
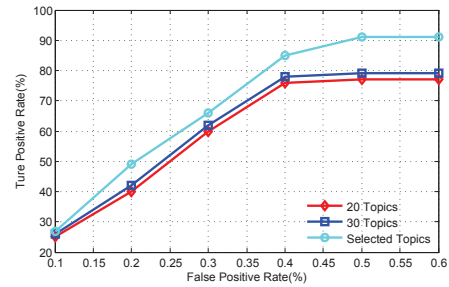
Figure 7: Performance of Summarization in term of $ROC$.

## 5.3  Opinion Summarization

As discussed before, a significant advantage of our framework over existing models in topic selection and classification is the lower computational cost in topic extraction and topic selection in imbalanced comments. We only consider the positive and negative comments given data set, with the neutral comments being ignored. There are two main reasons. Firstly, hotel comments opinion summarization in our case is effectively a binary classification problem, i.e. comments are being classified as either positive or negative, without the alternative of neutral. Secondly, the selected topics merely contribute to the positive and negative words, and consequently there will be much more influence on the summary results of positive and negative comments given data set. Furthermore, the classification with less negative comments shows the unique similarity of the outlier detection. As a result, we choose to evaluate the overall performance of the opinion summarization indirectly through outlier detection based on the selected topics. More specifically, we apply one-class SVM classifier on the comments with selected topics.

$$f(x) = \text{sign}((\omega \cdot \Phi(x)) - \rho). \tag{9}$$

The regularization parameters $\omega$ and $\rho$ solve the quadratic programming problem of the $\nu$-SVM. The classification using these methods is computationally simple and does not require significant memory.

The main problem we encountered is that the lexicon is needed first in our proposed summarization framework. In our case, however, comments are often composed of ungrammatical sentences and, additionally, a high number of unusual combinations of escape characters (corresponding to the vivid sentiment expressed), which make the comments much noisier and harder to process than the standard data sets traditionally used for summarization evaluation. Nevertheless, the online-LDA, being a generative model, proved to be quite robust to variations in the input data and, most importantly, to the change of the domain (Micro-blog etc.) [8]. There are $10,314$ words in our lexicon for the experiments.

Table 2: Performance of Opinion Summarization

| Topics | Positive Comments Detection Rates | Negative Comments Detection Rates |
|---|---|---|
| Selected Topics | 89% | 91% |
| 20 topics | 80% | 77% |
| 30 topics | 80% | 79% |

The results of the opinion summarization are shown in Table 2. The first thing to note in Table 2 is that the opinion summarization model is doing a much better job at classifying the
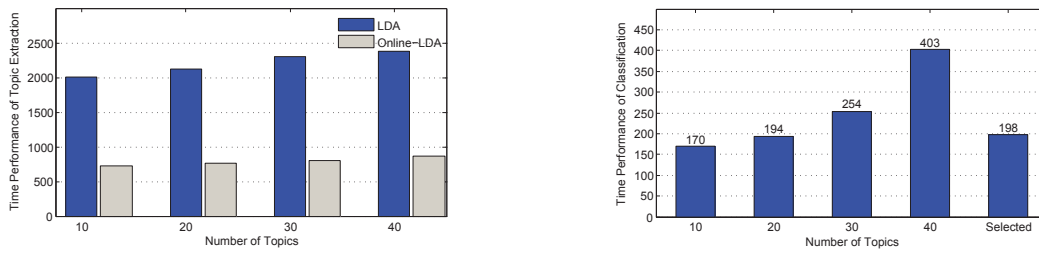
Figure 8: Time Performance of the Topic Extraction.



Figure 9: Time Performance of The Classification.

comments according to its polarity than the solo LDA model, the main problem with the latter being a relatively low precision. The main reason for this is an insufficient number of annotated negative examples when performing the topic selection.

The results show that the model is capable of reliably identifying negative comments (Figure 7). It can be observed that there is a considerable improvement in classification accuracy after performing the topics selection with FAST, with 5.3% improvement for our framework.

We evaluate the topic extraction time. We extract the 10, 20, 30 and 40 topics with LDA and online-LDA respectively. Results show that the online-LDA model outperforms the LDA model (Figure 8).

We evaluate the framework's time performance. We extract the 10, 20, 30 and 40 topics with online-LDA, and then perform the topic selection with two topics sets, 20 and 30 topics. We classify the comments in two ways: the first is to classify the comments with original topics, the second is to classify the comments with selected topics. The time performance of the second classification is averaged over two selected topics.

The topic selection used more time when classifying but the classification time does not increase dramatically due to the lower dimension of the data. Results show an extra 28 seconds in comparison with 10 topics (Figure 9) due to the time-consumption of the topic selection. We believe, however, that for the best performance of summarization a 28 second period is considered low enough in handling over $200,000$ comments so that our results indicate an acceptable time performance penalty.

# 6   Conclusion

In this paper, we have presented a new framework for the summarization of hotel comments. The most useful usage of opinion summarization is a web application. While most of the existing approaches to opinion summarization have not put into much consideration of the scalability of the models. Scalability is the most important task in our proposed framework. The online-LDA model is used for extracting the topics from the huge and increasing comments collection. The generalization performance remains the same but the computational cost is lower in comparison with LDA model. We address the imbalance problem of the comments. And the topics selection method, FAST is used for better classification performance. The selected topics are informative and easy for the user to digest the comments.

There are several directions we plan to investigate in the future. One is the best comments selection when the aim is to brief the comments collection. Another one is the ratable aspects regression analysis for certain kinds of reviews.

# Bibliography

[1] A. Divtt and K. Ahmad (2007); Sentiment polarity identification in financial news: A cohesion-based approach, *In ACL'07*, Prague, Czech Republic, June 2007, 1-8.

[2] B. Pang, L. Lee and S. Vaithyanathan (2002); Thumbs up?: sentiment classification using machine learning techniques, *EMNLP'02: Proc of the ACL'02 conference on Empirical Methods in Natural Language Processing, Morristown, NJ, USA*, 10: 79-86.

[3] D.M. Blei, A. Ng and M. Jordan (2003); Latent Dirichlet Allocation, *Journal of Machine Learning Research*, January 2003, 3:993-1022.

[4] D.M. Blei and J.D. McAuliffe (2007); Supervised topic models, *In NIPS'07*, Vancouver, B.C., Canada, 1-8.

[5] D. Ramage, D. Hall, R. Nallapati and C.D. Manning (2009); Labeled LDA: a supervised topic model for credit attribution in multi-labeled corpora, *In EMNLP'02: Proc. of the ACL'02 conference on Empirical Methods in Natural Language Processing*,Stroudsburg, PA, USA, 2009.

[6] D.M.W. Powers (2001); Evaluation: Precision, Recall and F-measure to ROC, Informedness, Markedness & Correlation, *Journal of Machine Learning Technologies*, 2(1):37-63.

[7] T. Hofmann (1999); Probabilistic latent semantic indexing, *In SIGIR'99: Proc. of the 22nd Annual Intl. ACMSIGIR Conf. on Research and Development in Information Retrieval*, New York, NY, USA.

[8] M.D. Hoffman, D.M. Blei and F. Bach (2010); On-line learning for Latent Dirichlet Allocation, *NIPS2010, Proceedings of the 22nd annual international ACM SIGIR conference on Research and development in information retrieval*, Lake Tahoe, Nevada, USA, 50-57.

[9] H. Wang, Y. Lu and CX. Zhai (2011); Latent Aspect Rating Analysis without Aspect Keyword Supervision, *KDD'11, Proc. of the 17th ACM SIGKDD intl. conf. on Knowledge discovery and data mining*, San Diego, California, USA, 618-626.

[10] I. Titov and R. McDonald (2008); A Joint Model of Text and Aspect Ratings for Sentiment Summarization, *Proc. of ACL'08*, Columbus, Ohio, USA, 308-316.

[11] C. Lin and Y. He (2009); Joint Sentiment/Topic Model for Sentiment Analysis, *CIKM'09, Proceedings of the 18th ACM conference on Information and knowledge management*, Hong Kong, China, 375-384.

[12] L.-W. Ku, Y.-T. Liang and H.-H. Chen (2006); Opinion extraction, summarization and tracking in news and blog corpora, *AAAI-CAAW'06, Proceedings ofAAAI-CAAW-06, the Spring Symposia on Computational Approaches to Analyzing Weblogs*, Stanford, California, USA, 1-8.

[13] Y. Lu, C. Zhai and N. Sundaresan (2009); Rated aspect summarization of short comments, *WWW'09, Proceedings of the 18th international conference on World wide web*, ACM, NY, USA, 131-140.

[14] P.D. Turney (2002); Thumbs up or thumbs down?: semantic orientation applied to unsupervised classification of reviews, *ACL'02, Proceedings of the 40th Annual Meeting on Association for Computational Linguistics*, Morristown, NJ, USA, 417-424.

[15] P.D. Turney and D.L. Littman (2003); Measuring praise and criticism: Inference of semantic orientation from assocation, *ACM Trans. Inf. Syst.*, 21(4):315-346.

[16] P. Stenetorp, S. Pyysalo, G. Topic, S. Ananiadou and J. Tsujii (2012); BRAT: a web-based tool for NLP-Assisted text annotation, *EACL '12 Proceedings of the Demonstrations at the 13th Conference of the European Chapter of the Association for Computational Linguistics*, Avignon, France, 102-107.

[17] Q. Mei, X. Ling, M. Wondra, H. Su and C. Zhai (2007); Topic sentiment mixture: modeling facets and opinions in weblogs, *WWW '07 Proceedings of the 16th international conference on World Wide Web*, Banff, Alberta, Canada, 171-180

[18] B. Walsh (2002); Markov chain Monte Carlo and Gibbs sampling, *Lecture notes for EEB 596z*, 2002.

[19] X. Chen and M. Wasikowski (2008); Fast: A roc-based feature selection metric for small samples and imbalanced data classification problems, *Proceedings of the ACM SIGKDD International Conference on Knowledge Discovery and Data Mining*, 124-132.

[20] YW. Chen and CJ. Lin (2015); Combining SVMS with various feature selection strategies, *Available: www.csie.ntu.edu.tw/ cjlin/papers/fearutes.pdf*.

[21] Z. Ma, A. Sun, Q. Yuan and G. Cong (2012); Topic-Driven reader comments summarization, *CIKM'12*, Maui, HI, USA, 265-274.

# Checking Multi-domain Policies in SDN

F.A. Maldonado-Lopez, E. Calle, Y. Donoso

**Ferney A. Maldonado-Lopez**
Systems and Computing Engineering Department
Universidad de los Andes, Bogotá, Colombia
fa.maldonado1897@uniandes.edu.co

**Eusebi Calle**
BCDS, Broadband Communication and Distributed Systems
Universitat de Girona, Spain
e.calle@udg.edu

**Yezid Donoso\***
Systems and Computing Engineering Department
Universidad de los Andes, Bogotá, Colombia
*Corresponding author: ydonoso@uniandes.edu.co

**Abstract:** Programmable Network like SDN allows administrators to program network infrastructure according to service demand and custom-defined policies. Network policies are interpreted by the centralized controller to define actions and rules to process the network traffic on devices that belong to a single domain. However, actual networks are *multi-domain* where several domains are interconnected. Then, because SDN controllers in a domain cannot define nor monitor policies in other domains, network administrators cannot ensure that their own policies, origin policies are being enforced by the domains not directly managed by them (i.e. foreign domains). We present AudiT, a multi-domain SDN policy verifier that identifies whether an origin policy is enforced by foreign domains. AudiT comprises (1) model for network topology, policies, and flows, (2) an Audit protocol to gather information about the actions performed by network devices to carry the flows of interest, and (3) a validation engine that takes that information and detects security policy violations, and (4) an extension to the OpenFlow protocol to enable external auditing. This paper presents our approach and illustrates its application using an example considering multiple SDN networks.
**Keywords:** Network Operating Systems, Software-Defined Networking, Network management, Policy Verification

## 1 Introduction

In Software-Defined Networking (SDN), network administrators use software languages to define how network traffic is processed and delivered. They use these languages to implement network policies, concrete rules about how a network must deal with specific types of traffic known as *flows*. For instance, these languages can be used to specify which users or network machines can connect to specific servers; which network devices must be used to deliver specific types of traffic, or which bandwidth can be assigned to specific flows.

SDN is based on the separation of control and data planes. On one hand, the control plane remains on a centralized server called *controller* that makes decisions about how the traffic is processed. The controller is responsible for managing connections, addressing, and routing protocols. Applications at the controller use specific-SDN protocols such as OpenFlow [14] to instruct elements in the data plane how to process and deliver the network traffic. The data plane consists of network devices, or datapaths, responsible for packet forwarding and switching.

In the SDN architecture, a single controller manages policies and behavior of a network domain. Only the domain controller has access to the rules used by each network device in its own domain. Thus, neither a network device nor a controller can access information about rules from other network domains. Although this is perfect to deal with policies in a single domain, a network administrator cannot observe how a external network, out of its domain, handles the traffic.

With the current SDN architecture, the administrator is not able to enforce nor monitor multi-domain policies. That is because forwarding rules must be implemented on multiple domains. For instance, today is very common that network traffic is delivered using a internal network such as LANs, and external networks such as WANs and Internet. If the network administrator wants to enforce or monitor a network policy, she can define applications in her own network domain but cannot do it in the external domains. Unfortunately, she cannot check if external domains enforce a network policy because she cannot determine how the traffic is delivered in those external networks.

This situation can be specially critical in network security policies. For example, essential traffic that is delivered through external networks can be duplicated or redirected to other network machines using a simple application in the external domain SDN controllers. Due to network administrators cannot get access to the rules in the external networks, they are disabled to detect these situations neither validate if a policy is achieved.

We propose a mechanism to audit network policies in multiple domains called AudIt. Our approach overcomes these SDN limitations and allows to network administrators to validate if the network policies are enforced by a external domain. AudiT comprises three modules: an extension to the OpenFlow protocol to enable external auditing, the AudIt interface for network devices that gathers information about the actions performed in external domains to carry the flows of interest, and a validation engine that runs into the internal network controller and detects policy violations.

Other mechanisms were suggested to check network policies. For example, Hinrichs [4] developed a declarative language called Flow-based Management Language (FML) to describe network policies and configuration in a high-level and declarative approach. This FML is a high-level declarative language, based on flows, that checks the first packet of every flow against the policy. Lately, Monsanto et. al. [16] introduce a declarative language called NetCore. It is a high-level declarative language that describes the desired behavior of the network but does not deepen the implementation of that behavior. With NetCore is possible to express packet forwarding policies for SDN. Afterwards, Soulé et. al. present Merlin [21]. Merlin is also a declarative language based on logical predicates and regular expressions with which a network administrator can write network policies.

In contrast to previous works, we propose to express network policies as predicates but use a SAT solver and a model finder to evaluate predicates, find inconsistencies and detect policy violations. AudIt uses Alloy [6] to describe the network topology, policies and network traffic. Mirzaei *et al.* proposed used Alloy to verify network properties in [15]. In this case they model internal states of a network and OpenFlow switches.

In summary, we introduce the foreign controller verification problem, we define multi-domain policies in programmable networks, a mechanism to gather information from external SDN domains, and a validation engine that uses gathered information to check if a network policy is enforced by the external domain.

Rest of this paper is organized as follow: Section 2 explains the problem of auditing own policies at external domains; then we present a model to illustrate network topology, paths, forwarding rules and policies in Section 3. Then, Section 4 introduces AudiT protocol and functionality, and presents an example. Finally, Section 5 concludes the paper and presents

future work.

## 2    Auditing policies in multi-domain networks

A *Network policy* is a set of conditions, constraints, and settings about how a specific type of traffic must be managed by a network. It also includes which users and hosts are authorized to create connections, and the circumstances under which they can or cannot connect. Network policies are the accurate and unambiguous way to specify the traffic behavior.

Initially, Stone *et al.* proposed a path-based policy language (PPL) that abstracts topological (physical) paths and flows to check network properties [22]. Now, with programmable networks as SDN, new network policy abstractions are under development, therefore the challenges in policy checking open a rich field of study. High-level declarative language were proposed to represent network policies with more expressiveness. Declarative languages such as FML [4, 5] express network policies in terms of flows. For general purposes, Hinrichs developed a declarative language called Flow-based Management Language (FML) to describe network policies and configuration in a high-level and declarative approach [4]. FML is based on flows, and checks the first packet of every flow against the policy. FML identifies a network flow by: *source* and *target* for users, hosts, and access points, in addition to protocols and requests

A flow is the specification of a traffic, sometimes is called a *session*, that contains common attributes such as source, destination, protocol, but also can specify more granular characteristics as duration, valid time, users, data format and so on. Then those policies are processed using DATALOG to find matching flows. Other languages were designed for SDN are Merlin and NetCore. Merlin [21] is a framework to write network policies for SDN. NetCore [16] is a language for describe forwarding rules and it is integrated with another framework called Frenetic, a project from Cornell and Princeton universities. These languages allow network administrators to define policies in a single-domain networks. They did not contemplate checking policy enforcement on a third-domain.

In contrast to previous approaches, AudIt offers not only the ability to write and check network policies, it is unified with the controller and extract forwarding data and check it. AudIt also uses the flow specification and checks if the set of flows is valid for a given topology. Moreover, AudIt reports inconsistencies in terms of flows not only as instructions at the hardware implementations.

For example, suppose that a network policy defines *only computers assigned to members of IT department can get access to database servers*. We can write this *policy* as:

$$allow(\texttt{src},\texttt{target}) \mid \texttt{src} \in IT \wedge \texttt{target} \in DataBase \qquad (1)$$

$$deny(\texttt{src},\texttt{target}) \mid \texttt{src} \notin IT \wedge \texttt{target} \in DataBase \qquad (2)$$

Expression (1) means that the network must allow flows from IT to database servers. Due to this policy must be closed, (2) denies any flow from other machines to the same servers. In SDN networks, policies are enforced by its domain controller which rules the behavior of every forwarding device –switch– in its domain. The big question is: Can the network administrator monitor that this policy is achieved?

### 2.1    Policies in Multi-domain networks

In multiple-domain networks, each domain is managed by its own controller. In our example scenario depicted in Figure 1.a, the domain A is ruled by its *controller* CA, and operates the IT department and its users. The external domain B, managed by the controller CB, operates

a) Multi-domain network scenario.
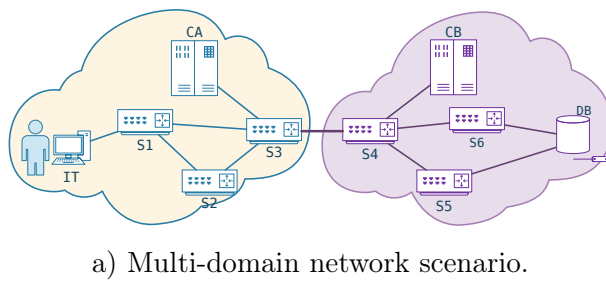
**S1 flowtable**

| Match | Action |
|---|---|
| Src = IT ∧ Dst = DB | ⟨ Fwd S3 ⟩ |

**S3 flowtable**

| Match | Action |
|---|---|
| Src = IT ∧ Dst = DB | ⟨ Fwd S4 ⟩ |

b) Flowtables for devices in domain A.

Figure 1: Domain A may send a policy to be implemented in domain B, but there is not guarantee B implements the policy correctly.

the database servers. Network administrator supervises her own controller CA, and may install forwarding rules on devices S1, S2, and S3 to deal traffic generated by the IT department. Network controller CA cannot access the rules in forwarding devices in the domain B neither compel controller CB to install required forwarding actions into the devices S4, S5, and S6.

A *multi-domain policy* must be enforced by own and external domains. The controller CA may share the policy with the controller CB, and awaits that CB implements the policy in its devices. However, there is not certainty that delivered traffic in the external domain B obeys any policy defined by A. Following the example, the administrator of domain A cannot enforce policies related to deliver traffic to the database servers, because the domain B is external.

## 2.2   Challenges in multi-domain networks

Each network controller is in charge of configuring switching devices on its domain. Figure 1.b shows the required configuration installed on devices in the path of domain A that process the flow until it reaches the next domain. *Network configuration* are rules that implements the policy. In this case, the configuration conducts the *flow traffic* from IT department to database servers. This traffic arrives to switch S1, then is forwarded to switch S3, and finally it is forwarded to domain B interface, switch S4. Clearly, A controller unknowns and cannot handle implemented configurations in external domains. However, administrator want to know if their policies are enforced in external domains. Because of database servers are located in external network, for instance it is hosted by another company, the above policy redirects flows from the IT department to external servers but deny the flows originated from sources other than IT department. However, usually companies rely on external networks such as WANs and Internet to deliver network *flows*.

Since the configuration of network device is protected information, it is only accessed by its own domain controller, and administrator wants to check if the external controller applies a policy on its domain, we have identified a main challenge: how to detect if a policy is enforced by a external domain? and how to audit the policy enforcement without reveal risky information?

## 2.3   Policies in Programmable Networks

In SDN environment there are some languages to describe network policies. For example, NetCore is a high-level declarative language that describes the desired behavior of the network but does not deepen the implementation of that behavior. With NetCore is possible to express packet forwarding policies for SDN networks [16]. Another work, Merlin [21] is also a declarative language but based on logical predicates and regular expressions which can be solved using linear programming to determine forwarding paths.

Verification of SDN configurations is focused on check network properties that follow a rule. For instance VeryFlow [10] creates a network-wide invariants and checks them against rules. FatTire [19] uses regular expressions and writes policies in this way to be able to validate. Other works attend to find *conflict rules*, rules that contradict earlier ones. In such a way FortNOX [18] checks new flow-rules against a flow-constraint set, and authenticates the source of rules by means of digital signatures. Another illustration is NetPlumber [9] that searches if a candidate rule introduces network misconfigurations or policy violations . It executes a procedure called Header Space Analysis (HSA) over dependency graphs to find conflicts. These approaches examine the forwarding tables from each network device and could check if they conform with the specified policy. However, none of these approaches support the validation of policies in external domains.

**From policies to flow-rule implementation**   Network applications – or functionality– run on a controller and define the general behavior or *policies* by installing specific configurations on each switching device. Regularly, those programs use OpenFlow (OF) [17] to communicate controllers and forwarding devices, and install, modify, or get *flow-rules* that specify how a device deals with specific traffic. A flow-rule is a pair `<match,action>` map on the device's *flowtable*. A flow-rule defines which `action` is performed once a packet header matches the `match` pattern.

OF defines a set of messages to control the internal information on each device, and rules used to process a flow. In summary, OF messages can add, modify, and query rules from device's flowtable. Actions also include: dropping a packet (`DROP`), forwarding a packet to a specific port (`FWD`), or report the set of installed rules (`STATUS`). The rule-set is *closed*, and the packet is reported to the controller if its header does not match any rule.

## 3    Topology and Policy Models

We describe a model that involves the physical topology and paths; and network operation definitions such as flows, policies, and conflicts. First, we use the following specification for networks. We will use the *relation of correspondence* later on when we write the model in Alloy.

**Definition 1** (Network Graph)**.** A network graph $\mathcal{G}$ is a duple $(N, L)$ such that $N$ is the set of nodes, and links $L := (N, N, C)$ is the *correspondence C* with domain and co-domain $N \to N$.

Considering the links relation $L$, we write the function $\mathsf{links}(n)$ to denote $\{m|(n,m) \in L\}$, the set of all the nodes $m$ connected to a node $n$. In addition, for convenience, we write $n \to m$ to express *from n to m* sometimes instead of $(n,m) \in L$. A well-formed network $\mathcal{G}$ must satisfy the following rules: 1) Network is connected, $\forall n \in N | \mathsf{links}(n) \neq \emptyset$, i.e. there are not isolated nodes; 2) no self-loops, $\nexists n \in N | n \to n$, i.e. there are not links from a node to itself; and, 3) for all link, there is an arrival node, $\nexists n \in N | \mathsf{links}(n) \cap n = \emptyset$.

It is important to note that nodes in our model does not represent a network device – router nor switch–, a node denotes a *device port*. Then under this abstraction, the link relation represents forwarding rules, not just physical links in the topology.

**Definition 2** (Path)**.** A path $p$ is a tuple $(s, t, N_p, L_p)$. A source node $s$, a target node $t$, a subset of nodes $N_p = \{n_1, n_2, \ldots, n_k\}$, and a subset of links that creates the sequence $L_p = \{(s, n_1), (n_1, n_2), \ldots, (n_{k-1}, n_k), (n_k, t)\}$.

A path, can be described as a list of nodes that maintains a sequence. Path nodes $N_p \subset N$, path links $L_p \subset L$. A well-formed path satisfies: 1) all implicated nodes in the links belong to node set, $\forall (n_a, n_b) \in L_p \implies \{n_a, n_b\} \in N_p$, 2) $\{s, t\} \in N$, source and target nodes are in the network, and 3) source node *opens* and target node *finishes* a path, $\nexists (n_1, n_2) \in L_p | n_2 = s \lor n_1 = t$.

At this point is appropriated to describe the *transitive closure*. We use this concept to tackle the reachability property when describe a path. A binary relation $R$ is *transitive* if contains tuples in the way $a \to b$ and $b \to c$, but also contains $a \to c$. This relation is noted as $R^+$ and contains $R$. Finally, a path has no loops, considering the relation $L$ and the function $\mathsf{links}^+(n)$ is the set of all nodes that can be reached from $n$. Then a path has no loops if $\nexists n \in N_p | n \in \mathsf{links}^+(n)$. Also for convenience, we denote a path as a node sequence as $\langle s, n_1, n_2, \ldots, t \rangle$. We include a wildcard symbol $(*)$ to denote any unspecified node or sequence of nodes. For example, the path $p = \langle A, *, C \rangle$ is the path that starts at node $A$ and ends at $C$.

## 3.1 Traffic flows

Flow is the fundamental abstraction for our model. For the reader it is similar to *communication session* supported by a set of paths and device configurations. Traffic flow defines the high-level network parameters needed to create a competent communication channel. A flow provide enough detail to describe a set of feasible sessions, and provides a form to group and manage these sessions.

**Definition 3** (Flow). A flow is a sequence of traffic constraints $f = (f_1, \ldots, f_n)$. Each term $f_i$ is a restriction over a traffic characteristic, strongly related to filters on packet fields.

Due to we illustrate flows as traffic constraints. Reader should note we indicate packet-field match as those constraints. The used definition allows us to construct flexible and composed communication flows. A term of flow involves transport-layer protocol, source / destination at third layer, or applications. Also, we use set operators over these packet fields to define the flow. For instance, $flow_a = \{\texttt{protocol = TCP}, \texttt{src\_ip = 192.168.5.10}, \texttt{dst\_ip = 192.168.7.10}\}$ details a traffic flow between those IP addresses and TCP as transport protocol. Note that this flow only defines the traffic in one way. It means, the other direction is not under this definition.

However, flow definition is only associated to communication characteristics and packet fields, but not the set of paths that supports the flow.

## 3.2 Policies, conflicts and semantics

In order to define the set of paths that implements a policy and then identify policy conflicts and violation we follow the guidelines of Harel and Rumpe [8] to specify a modeling language Ł describing the *syntactic domain* $\mathcal{L}_L$, the *semantic domain* $\mathcal{S}_L$ and the *semantic function* $\mathcal{M}_L : \mathcal{L}_L \to \mathcal{S}_L$, also traditionally written $[\![\cdot]\!]_L$.

The policy is a set of rules that achieves a management procedure. Forwarding rule is the action that a node executes to forward a packet into a computer network. Rules are described in terms of flows, by the previous definition.

**Definition 4** (Policy). A network policy is a tuple $\pi = (f, P, C, \alpha)$ s.t. $f$ is the target flow composed of packet-field values, $P$ is the set of paths that support the flow, $C$ is a set of conditions, over the flow $f$ or path $P$, and $\alpha$ is an action, regularly $\{permit, deny\}$.

Essentially, a policy resolves whether allow the flow $f$ over the set $P$ conclude on a specific action $\alpha$. It is decisive and produces a configuration network that allows or deny the traffic flow. For example, the network administrator wants to apply the policy: *Ana is a user with profile of IT member, who is in the subnetwork 192.168.5.\*/24 (S1), is allowed to access the database at subnetwork 192.168.7.\*/24 (S6) and port 1521, and her traffic must go through the router S3.*

Now the manager has to detail the policy. In order to do that she solves the following steps:

1. path `S1_S6 := <S1,*,S3,*,S6>`,

2. transport protocol: = TCP,

3. port number: = 1521;

4. the conditions  user = Ana, and Ana ∈ IT member;

5. finally the policy decision: *permit*

In this way, we can find $\omega$, the set of configurations and instructions that implements the paths and the policy $\pi$. Note that IP addresses, user groups, traffic class and protocols should be modeled as *sets*. On the other hand, ordered items such as *time* are modeled as *sequences* to be able to compare them using $\leq$ and $\geq$ operators.

$$\omega = impl(p : path|(\texttt{S1\_S6}) \wedge \texttt{protocol} = \texttt{TCP} \wedge \texttt{port} = \texttt{1521} \wedge \texttt{Ana} : user \in \texttt{IT member}) \quad (3)$$

This representation of a policy, utilizing logical conjunctions, allows us to express this policy as a conjunctive normal form *predicate* (CNF), and logically solve it. Moreover, we are able to check a formal solution using a model finder as Alloy [7], compare solutions, or find inconsistencies.

**Definition 5** (Policy Semantic). A semantic of a policy $[\![\pi, \mathcal{G}]\!]$ is the set of paths that implements the flow over a path on $\mathcal{G}$ and achieves the policy.

$[\![\Upsilon]\!] = \Omega$ is the semantic of all network policies and produces the set of all paths implemented on the network. The complete network configuration is denoted by $\Omega$. The semantic function $[\![\pi, \mathcal{G}]\!]$ of a policy contains the sets of paths, flow definitions, conditions and the network $\mathcal{G}$ that satisfies the policy $\pi$. Obviously, the policy $\pi$ is valid in a network $\mathcal{G}$, if $[\![\pi, \mathcal{G}]\!]$ is not empty.

**Definition 6** (Policy Conflict). A policy conflict occurs when a set of policies are not implemented by any path or there are inconsistencies that prevent the generation of a path.

Essentially, if the semantic of a policy is empty, means that there is not set of configuration of paths that satisfies the policy. Given two valid policies $\pi_1$ and $\pi_2$, they are not conflicting in the network $\mathcal{G}$ if $[\![\pi_1 \cup \pi_2, \mathcal{G}]\!]$ is not empty. That is, two policies are not conflicting if there is a set of paths, flows, and restrictions in the network $\mathcal{G}$ that satisfies both policies. In contrast, we say that two policies $\pi_1$ and $\pi_2$ are conflicting in $\mathcal{G}$ if $|[\![\pi_1 \cup \pi_2, \mathcal{G}]\!]| = 0$.

**Definition 7.** (Minimal diagnosis) Given a set of policies $\pi \subseteq \Upsilon$ such that $[\![\Upsilon \setminus \pi]\!] \neq \emptyset$, the minimal set $\pi$ is the minimal diagnosis.

We refer to this minimal set as the littlest configuration applicable without conflicts. Now, we need a tool, called a *verifier*, able to find (calculate) the semantic function $[\![\pi, \mathcal{G}]\!]$ and verify if that set is empty and the minimal diagnosis of that set. We use similar tools also for validating paths on network infrastructure [12], and recently we show how to use of minimal diagnosis to detect and prevent firewall-rule conflicts on software-defined networking [13].

## 4   Checking multi-domain policies with AudIt

AudIt is an auditing extension for OpenSwitch protocol and OpenFlow controller that allows domain controllers to validate security policies on a foreign domain. Our proposal creates a language definition and transformation to audit network policies. We use Alloy to obtain a set of tuples that satisfy the policies (exactly the semantic function). If Alloy does not find any element (the set is empty), the policy set is invalid or conflicting.
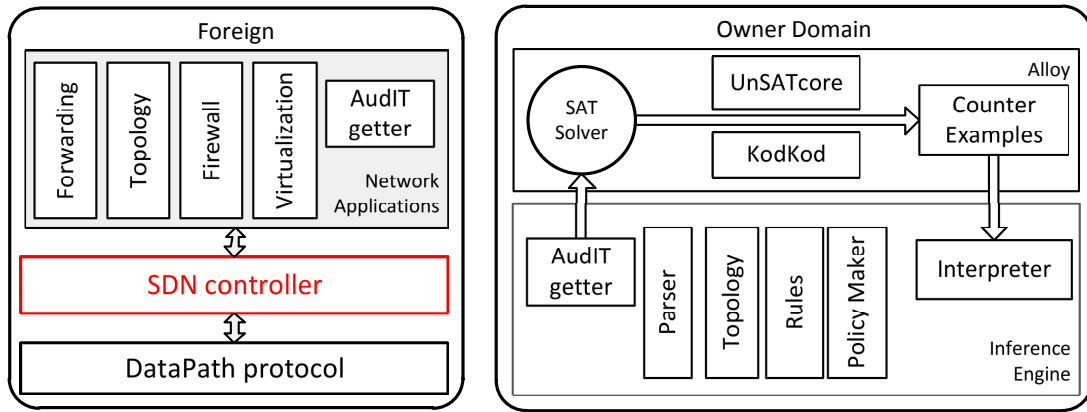
Figure 2: AudIt architecture

AudIt works as a validation protocol that allows a controller to gather auditing information from external domains and validate the origin policy. It performs two phases: gathering network information and validation process. First, the controller in the origin domain gets information we called *audit packets* that is routed through the network as regular traffic. Then, when auditor packet reaches devices in the external domain, these network devices report a subset of its own flowtable to the controller in the origin domain. Finally, the controller in the origin domain process the gathered flowtables to obtain all the processing rules related to the flows of interest, and executes the *validation engine* that checks if the external domain is accomplishing the security policy.

## 4.1   AudiT Extension

OpenFlow specifies a set of control messages between controller and forwarding devices. Control messages include: *modify-state* to add or delete flowtables in the device, *collect-statistics* to read counters and device statistics, *managing* groups of flowtables. Controller is also able to request device *status*, where the device reports the flowtable to the controller. AudIt uses regular controller primitives to request information from the flowtable on devices of external domain.

**Information gathering**   Once the controller enables AudIt on each network device, and the audit packet arrives, the device invokes `OFPMP_TABLE_FEATURES` and the header match to filter a subset of the rule table that matches the header. Thereby, it extracts a set of all the *related flowtable entries* (RFE).

$$\text{RFE} = \{e | e.\texttt{src} \odot p.\texttt{src} \cup e.\texttt{target} \odot p.\texttt{target}\} \tag{4}$$

For simplicity, our example only considers IP addresses and masks in the IT-database scenario. Our RFE are defined by (4). Where $p$ is the policy and $\odot$ is the match relation.

**AudIt message**   Figure 3 shows the structure of an AudIt message. It comprises the same flow header in order to be routed through the same path; moreover, it includes origin controller identifier, controller authentication data, other AudIt settings, and the list of fields and rules to be filtered by the device.

| Flow header | Origin Controller ID | AudiT settings | Controller Signature |
|---|---|---|---|
| List of fields | | List of policies | |

Figure 3: Structure of an AudIt packet. The list of policies are constraints over packet fields.

## 4.2 AudIt protocol

Figure 4 shows the proposed protocol that allows controllers to enable AudiT protocol, gather information from foreign devices, and check policies.

1. Involved domains subscribe an *audit agreement* that specifies the permission to create, send and process audit packets. Then, all implicated domains update their module that recognizes the audit request and overwrites `AUDIT_ENABLE` variable.

2. Origin domain A shares the traffic policy over IT's traffic with B. Security Policy described in section 1 - 2: *DataBase is only accessed from IT department.* External-domain controller CB enforces the security policy in its network, translates the policy into rules applicable to its infrastructure.

3. Origin controller creates an audit packet. Audit packet contains all packet fields of the flow traffic. This procedure request information about how the traffic is delivered. Thus, foreign network devices process the audit packet as they process regular data flow, or use a interface to return the Related Flowtable Entries (RFE).

4. Foreign devices reply the audit packet with the RFE. The list of entries from its flowtable.

5. At the origin, the controller of A executes the validation engine, determines if there is a subset of rules that violates the policy, and writes a conflict report.
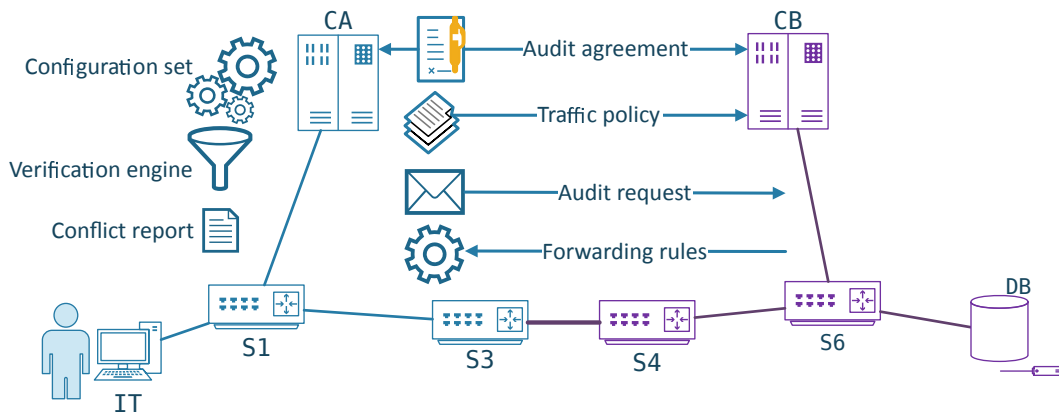


Figure 4: AudiT protocol execution. Devices from domain B report packet rules to CA, then A verifies traffic policy and generates an auditing report.

## 4.3 Multi-domain Policy Checking

At the end, origin controller owns all rules related with the traffic policy that comes from the external domain, and validates the set of related flowtable entries (RFE) against the policy to identify violations. Figure 5 shows the set RFE that AC gathers from domain B. It is a list of rules related with the traffic policy defined in expressions 1 and 2. Then, the validation engine

determines if this subset of rules violates the policy. This policy-rule validation engine could be similar to [9].

| S4 flowtable | | S6 flowtable | |
| --- | --- | --- | --- |
| Match | Action | Match | Action |
| Src = IT ∧ Dst = DB | ⟨ Fwd S6 ⟩ | Src = IT ∧ Dst = DB | ⟨ Fwd DB ⟩ |

Figure 5: Related flowtables entries from devices in domain B.

## 4.4 Inference Engine based on SAT

We develop an *inference engine* able to check implementation procedures against network policy. Topology is defined as a set of *nodes*. *Links* is a closure relation of arity two over the node set. Specifically for this project, we model device ports as nodes, and links by a closure relation over nodes. Figure 6 shows how the topology is represented in terms of device ports. A forwarding rule, the simplest instruction that redirects a packet from one port to another is represented as part of the path. Under this perspective, the configuration is part of the topology. Forwarding rules are shown in the figure as dotted lines. These soft-links are considered as regular topology once the model is built.

An optimization opportunity arises due to forwarding rules create *soft-links* that are interpreted as part of the topology. If the traffic policy is quite specific, the resultant topology is disconnected graph, even is reduced to some paths. This abstraction of nodes as device ports, and soft-links can reduce the complexity at evaluation time.
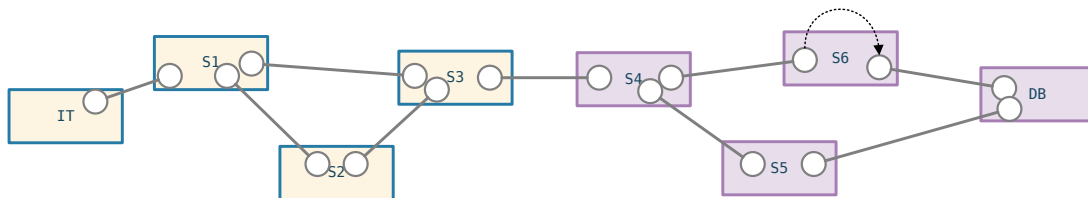


Figure 6: Representation of a network topology based on ports from the original deployment. Blocks are network devices and circles are ports. Forwarding rules are depicted as dotted lines that connect two ports.

Flow is depicted as the list of constraints over packet header, traffic movement sense, and topological considerations. For example, the flowtable described in Figure 1.b is the interpretation of constraints, source and destination addresses, over fields of a packet header. Reader should note that flowtable also denotes the *soft-link* between two ports generated by the forwarding rule. Nevertheless, this soft-links are part of the topology equally as wired links do. In other words, the model does not discerns one from another. Communication details such as protocols or port numbers are considered sets if these elements are part of the packet header. Due to our work uses set theory notion of order is not considered in this model, for that reason we cannot have policies with arithmetic conditionals. For example, the expression *if the number port is greater that 1024, then ...* is invalid in our approach.

Our inference machine is implemented on Alloy [6]. It is fed with external-domain information gathered by the audit procedure or through services that exposes forwarding information.

# 5    Conclusions and Future Work

We presented OpenFlow AudIt, a mechanism that checks if foreign domains are enforcing multi-domain network policies. AudIt helps to overcome policy-checking limitations of the SDN architecture. It comprises (1) an extension to the OpenFlow protocol to enable external auditing, (2) an Audit protocol to gather information about rules applied to specific network *flows*, and (3) a validation engine that uses flow information and determines if the external network is enforcing specific traffic policies. Additionally, Audit can identify policy violations. It informs the network configuration, rule of flow that infringes the policy and its identifier. In general terms, AudIt allows network administrators to gather information from external domains and determine if network policies are enforced in multiple domains.

## 5.1    Experiments and results

We implement and test our AudIt protocol using the Floodlight controller [1]. Test cases are divided into two groups: information gathering, and violation inferencing. We run the controller on a server and deploy a test-network using mininet [2], which operate as external domain and implement the example topology used by Sethi in [20]. From another terminal, which operates as owner domain, we run our AudIt interface and extract traffic information from the controller. AudIt implementation creates a topology representation, a policy inventory, and a configuration repository. Thereafter, the inference engine is executed. AudIt writes, policies, configurations and topology as Alloy instructions and executes the satisfiability solver.
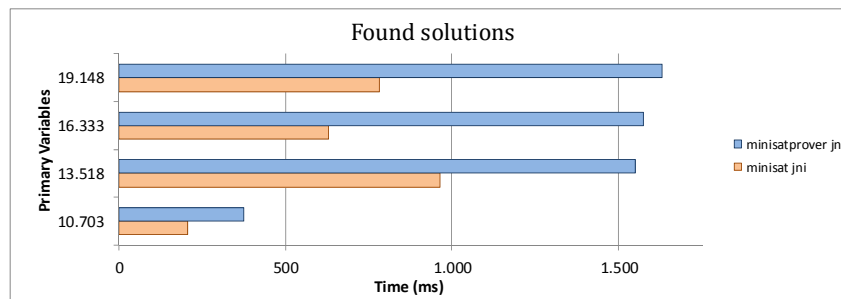


Figure 7: Solutions from Alloy implementation. The same implementation is evaluated using two solvers: minisat and minisatprover with minimal unsatisfiable core.

Figure 7 shows two evaluations over the same topology and set of policies. We implement the same FatTree topology also described in [20] to compare our approach. AudIt takes less than a second using the minisat solver, which only finds if an instance accomplishes the set of policies. On the other hand, if the network administrator wants to determine the set of policies violated by the external domain, she executes AudIt with the minisatprover option and could take up to $1.5s$. These measures are lower than the values reported on [20], for the same Fat Tree topology composed of 20 switches, 16 hosts, and 48 links. We test forwarding and reachability on a Intel i5 at 3.0 GHz, with 3.74 GB RAM. With the intension to show how state explosion and variable affect the performance we test AudIt for 930K, 1.5M, 2.2M and 2.8M of states, which are represented on primary variables shown in Figure 7.

However, AudIt does not have complete information about the network as opposed to Net-Plumber [9]. Moreover, Audit requires the deployment of our OpenFlow extensions into the

---

[1] http://www.projectfloodlight.org/floodlight/
[2] mininet.org

network devices in those external domains. Commercial products (i.e. switches from companies such as IBM or HP) do not support the deployment of new extensions without a firmware update. We expect that future experimental implementation shows the benefits of Audit and can be a foundation to introduce multi-domain policy validation into the standard.

Letting external domains gather information about network flow processing may represent a potential security risk for external controllers. In addition, controllers in external domains may include programs that hide information or mimic policy enforcement. Future work focuses on evaluating security risks on our experimental implementation in order to determine which additional mechanisms are required to ensure safe auditing of multi-domain policies.

## Acknowledgment

## Bibliography

[1] Al-Shaer, E.; Marrero, W.; El-Atawy, A.; Elbadawi, K. (2009); Network configuration in a box: towards end-to-end verification of network reachability and security, *17th IEEE International Conference on Network Protocols, ICNP 2009*, 123-132.

[2] Canini, M.; Venzano, D.; Perešíni, P.; Kostić, D.; Rexford, J. (2012); A NICE way to test OpenFlow applications, *Proceedings of the 9th USENIX conference on Networked Systems Design and Implementation*, USENIX Association, 10-10.

[3] Gude, N.; Koponen, T.; Pettit, J.; Pfaff, B.; Casado, M.; McKeown, N.; Shenker, S. (2008) NOX: towards an operating system for networks, *SIGCOMM Comput. Commun. Rev.*, ACM, 38: 105-110.

[4] Hinrichs, T. L.; Gude, N. S.; Casado, M.; Mitchell, J. C.; Shenker, S. (2009); *Expressing and Enforcing Flow-Based Network Security Policies*, University of Chicago, Technical report, 1-20.

[5] Hinrichs, T. L.; Gude, N. S., Casado, M.; Mitchell, J. C.; Shenker, S. (2009); Practical Declarative Network Management, *1st ACM Workshop on Research on Enterprise Networking, 2009*, 1-10.

[6] Jackson, D. (2002); *Alloy: A Lightweight Object Modelling Notation*, ACM Trans. Softw. Eng. Methodol.; April 2002.

[7] Jackson, D. (2006); *Software Abstractions: Logic, Language, and Analysis*, The MIT Press, 2006.

[8] Harel, D. and Rumpe, B. (2004); Meaningful Modeling: What's the Semantics of "Semantics"?, *Computer*, IEEE Computer Society Press, 37: 64-72.

[9] Kazemanian, P.; Chang, M.; Zheng, H.; Varghese, G.; McKeown, N. (2013); Real time Network Policy Checking Using Header Space Analysis, *Proceeding on Network System Design and Implementation (NSDI)*, USENIX, 99-112.

[10] Khurshid, A.; Zou, X.; Zhou, W.; Caesar, M.; Godfrey, P. B. (2013); VeriFlow: Verifying Network-Wide Invariants in Real Time, *10th USENIX Symposium on Networked Systems Design and Implementation (NSDI), Proceeding HotSDN '12 Proceedings of the first workshop on Hot topics in software defined networks*, 49-54 .

[11] Mai, H.; Khurshid, A.; Agarwal, R.; Caesar, M.; Godfrey, P. B.; King, S. T.(2011); Debugging the data plane with Anteater, *SIGCOMM Comput. Commun. Rev.*, ACM, 41: 290-301.

[12] Maldonado-Lopez, F.; Chavarriaga, J. and Donoso,Y. (2014); Detecting Network Policy Conflicts Using Alloy, *Abstract State Machines, Alloy, B, TLA, VDM, and Z*, Springer Berlin Heidelberg, 8477: 314-317.

[13] Maldonado-Lopez, F. A.; Calle, E. and Donoso, Y.; (2015);Detection and prevention of firewall-rule conflicts on software-defined networking, *Reliable Networks Design and Modeling (RNDM), 2015 7th International Workshop on*, 259-265.

[14] McKeown, N.; Anderson, T.; Balakrishnan, H.; Parulkar, G.; Peterson, L.; Rexford, J.; Shenker, S.; Turner, J. (2008); OpenFlow: enabling innovation in campus networks, *SIGCOMM Comput. Commun. Rev.*, ACM, 38: 69-74.

[15] Mirzaei, S., Bahargam, S. and Skowyra, R. (2013); *Using Alloy to Formally Model and Reason About an OpenFlow Network Switch*, Technical Report, http://hdl.handle.net/2144/11416.

[16] Monsanto, C.; Foster, N.; Harrison, R.; Walker, D. (2012); A Compiler and Run-time System for Network Programming Languages, *SIGPLAN*, ACM, 47: 217-230

[17] Open Networking Foundation *OpenFlow Switch Specification*, v.1.3.1, ONF Open Networking Foundation, 2012

[18] Porras, P.; Shin, S.; Yegneswaran, V.; Fong, M.; Tyson, M.; Gu, G. (2012) A security enforcement kernel for OpenFlow networks *Proceedings of the first workshop on Hot topics in software defined networks*, ACM, 121-126.

[19] Reitblatt, M.; Canini, M.; Guha, A.; Foster, N.(2013); FatTire: declarative fault tolerance for software-defined networks, *Proceedings of the second ACM SIGCOMM workshop on Hot topics in software defined networking*, ACM, 109-114.

[20] Sethi, D.; Narayana, S. and Malik, S. (2013); Abstractions for model checking SDN controllers, *Formal Methods in Computer-Aided Design (FMCAD), 2013*, 145-148.

[21] Soulé, R.; Basu, S.; Kleinberg, R.; Sirer, E. G.; Foster, N. (2013); Managing the Network with Merlin, *12th workshop on Hot Topics in Networks, HotNets'13, Nov. 2013*, 1-8.

[22] Stone, G.; Lundy, B. and Xie, G. (2001); Network Policy Languages: A survey and a new approach, *IEEE Network*, 15: 10-21.

# A Fuzzy Logic Software Tool and a New Scale for the Assessment of Creativity

I. Susnea, G. Vasiliu

**Ioan Susnea\*, Grigore Vasiliu**
Dunarea de Jos University of Galati
Romania, 800008 Galati, Domneasca, 47
ioan.susnea@ugal.ro; grigore.vasiliu@ugal.ro
\*Corresponding author: ioan.susnea@ugal.ro

**Abstract:** It is difficult to measure something we cannot clearly define. No wonder that, for the over 100 definitions of the creativity proposed in the literature, there are almost as many scales and assessment tools. Most of these instruments have been designed for research purposes, and are difficult to apply and score, especially in the educational environment. Not to mention that they are expensive.

The research described in this paper is aimed to develop a free, fast, and easy to use software tool for the assessment of creativity in the educational context. To this purpose, we have designed a new scale with 20 items, based on a novel approach focusing on detecting the factors known to block the creativity, like stereotypical thinking, and social conformity. The user input is collected through a web based interface, and the actual interpretation of the results is automated by means of a fuzzy logic algorithm. The proposed solution is interesting because it can be easily integrated in almost any e-learning platform, or used as a stand-alone tool for tracing the evolution of the students involved in courses for the development of creative thinking skills, and also for possible other applications.

**Keywords:** assessment of creativity, e-learning, fuzzy logic

## 1 Introduction

The world of the 21'st century is very different from what it used to be just a couple of decades ago. New professions emerge overnight (think of *Android developer*, *market research data mining specialist*, or *cloud services engineer*), while others quickly fade out (postal services, newspaper delivery, travel agents, word processors, and many others).

To help students succeed in this world, the educational system should create new skills and should be able to assess these new skills ( [5]). One of the fundamental skills required in our rapidly changing society is creative thinking ( [27], [11], [31]).

This is the reason why the modern School has been intensely criticized ( [23], [22]) for it is unable to foster the creativity of the students, or - even worse - for killing their innate creativity.

By reviewing the vast literature dedicated to creativity, it appears that the real reason why we don't have serious initiatives to foster creativity in School is that we still don't fully understand this construct ( [20]). There are currently over 100 definitions of the creativity ( [33], [1]), many explanatory theories ( [29], [12], [26]), an ocean of literature *about* creativity, but very few initiatives explicitly aimed to develop educational content for the education *for* creativity ( [28]).

The lack of consensus of the researchers concerning the many facets of the creativity is also manifest in the field of formal education: though most teachers declare that they value and encourage the creativity of the students, most of them can barely recognize it and are totally unprepared to stimulate it ( [7]).

An additional obstacle is the lack of easy to use assessment tools to trace the evolution of the students involved in creativity courses, and to demonstrate the efficiency of the specific educational content.

The existing assessment tools are hard, if not impossible, to apply in the educational environment, either because they are too complex and difficult to score, like the famous TTCT ( [32]), or simply because they are not free (e.g. rCAB - Runco Creativity Assessment Battery, www.creativitytestingservices.com) . Considering the fact that, the first creativity lesson in any course is that "there are no right and wrong answers", it results that the Moodle-style evaluation tests, wherein the students must select one or more "correct"answers from a predefined list are totally useless.

For these reasons, the main objective of the research described here is to develop a new creativity assessment tool that is free, easy to use, and score, and compatible with most existing e-learning platforms.

Unlike the vast majority of the existing psychometric approaches, which treat the tendency towards social conformity as a bias, in our study we assumed that the social conformity is a clue indicating a type of "stereotypical thinking"that blocks creative thinking itself, not the process of measuring it. In other words, in our approach, the social conformity is treated as a signal, not as noise.

The automatic scoring is performed by means of a fuzzy logic algorithm starting from two subscales, each having 10 items, focused on different "dimensions"of the creativity: one subscale assessing the ideational behavior, the other aimed to measure the stereotypical thinking and social conformity.

Beyond the present introduction, this work is structured as follows:

Section 2 is a brief review of the related work aimed to clearly define the context of this study.

Section 3 contains the description of the proposed solution, and Section 4 is reserved for discussion and conclusions.

## 2   Related Work

Given the polymorphic nature of the creativity, it's no wonder that the assessment instruments are equally diverse as the definitions of creativity. For this reason, it is convenient to present the assessment tools from the perspective of the 4 P's (*Person, Product, Process*, and *Press/Place*) commonly used to illustrate the definitions of the creativity.

Other, more comprehensive reviews of the state of the art in the field of creativity assessment are available in ( [24], [13], [4]).

There are many tests that focus on traits or behaviors specific to *creative persons*, which is understandable considering that most researchers of the creativity are psychologists. Among this type of tests, it is worth to mention: The Kirton Adaptor-Innovator Inventory ( [16]), SCAB - The Scale for Creative Attributes and Behaviors ( [14]) and RIBS - Runco Ideational Behavior Scale ( [25]).

In another approach, the tests focus on creative behaviors from the past. Examples of products based on this idea are SPCA - The State of Past Creative Achievements ( [6]) and The Creative Achievement Questionnaire ( [8]).

The tests that evaluate the creativity by analyzing the *creative products* are, in most cases, based on the measure of the divergent thinking by means of open ended prompts. These are by far the most frequently used, which determined Kaufman ( [13]) to ironically note:

"One of the great ironies of the study of creativity is that so much energy and effort have been focused on a single class of assessments: measures of divergent thinking. In other words, there's not much divergence in the history of creativity assessment. "

It is not unlikely that this preference for the divergent thinking tests is connected with the popularity of TTCT (The Torrance Test of Creative Thinking, [32]). However, beyond the

incontestable success, the divergent thinking measures have their critics ( [21], [15]), who note that applying and scoring these tests are cumbersome and their predictive value is questionable.

In the same class of product oriented tests it is worth to mention CAT - The Consensual Assessment Techniques ( [2]), which is based on a methodology of evaluating the creative products by independent experts.

The creativity assessment tools based on the analysis of the *processes* leading to creative outcomes are far less common. One example is CPAC - Cognitive Processes Associated with Creativity ( [19]).

In what concerns the assessment of the influence of the *environment* on creativity, this is a difficult and less studied problem. One notable example in this direction is the KEYS test ( [3]).

There are also complex tests containing specific subscales for multiple P's of the creativity. For example, CSQ-R - Creativity Styles Questionnaire - Revised. ( [17]) contains 78 items organized in the following subscales: Belief in Unconscious Processes (person), Superstition (person), Final Product Orientation (product), Use of Techniques (process), Use of Other People (process), and Use of Senses (process), and Environmental Control (press).

In what concerns the way to collect the user's responses, the most popular solution is the Likert scale, but there are also tests that use the simplified dialogue based on binary responses Yes/No, or True/False.

From the perspective of the software implementation, the problem of creating the GUI (Graphic User Interface) to collect the user's responses is quite simple. However, things become considerably more complex when it comes to automate the interpretation of multiple subscales addressing distinct "dimensions"of the creativity. See next section for details on how we solved the problem of computing a global creativity quotient CQ.

We will conclude this brief presentation of the state of the art in the field of the creativity assessment by citing again the opinion of Kaufman: "Creativity assessment is a work in progress - we know far less about creativity and its measurement than we would like to know - but that is not to say that we know nothing at all. "( [13]).


## 3   Description Of The Proposed Solution

Probably the most common fallacy about creativity is to confound it with the divergent thinking. In fact, divergent thinking is just one of the many facets of the construct called creativity (see figure 1).

When dealing with such complex concepts, the evaluations based on a single dimension of the creativity - be it divergent thinking or any other - have, inevitably, a limited reliability, and in the same time, addressing multiple dimensions leads to large and cumbersome scales (e.g. CSQ-R, described in [17] with 78 items). One possible approach to facilitate the understanding of complex intellectual constructs is to consider their opposite, or their associated "negative space"(see figure 2 for a graphical metaphor that illustrates this idea)

So, what is the opposite of creative thinking? One possible answer is "thinking inside a box", a style of thinking heavily biased by stereotypes, prejudices, illicit generalizations, superficiality and conformism. Starting from this idea we have developed a scale that attempts to indirectly assess the individual creativity by considering the factors that indicate stereotypical thinking. The proposed scale, called IACEST (Indirect Assessment of Creativity through the Estimation of Stereotypical Thinking) contains two subscales as shown in Tables 1 and 2. See [19] and [10] for details on how the items of similar scales are formulated.

Note: In order to prevent the attempts to learn by heart the "right"answers, a third set of items containing 5 additional filler statements has been included in the online implementation
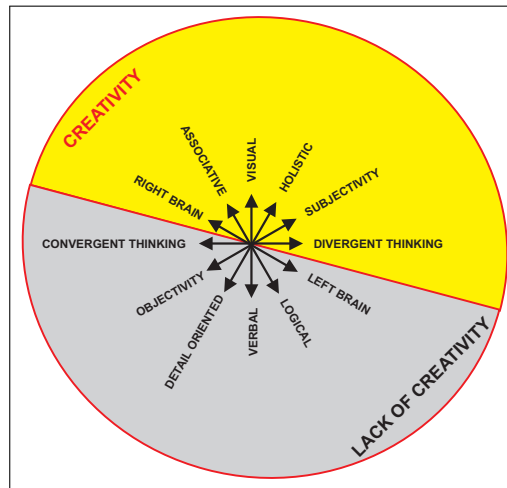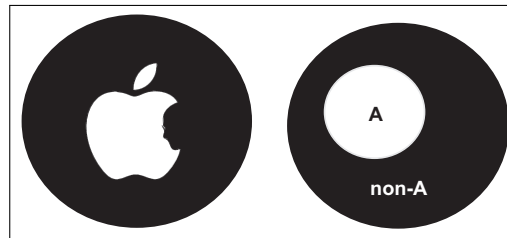
Figure 1: The multiple facets of creativity



Figure 2: The Apple logo redesigned by Jonathan Mak a metaphor based on the negative space

Table 1: Subscale 1. Creative personality and thinking style items.

| Item | Statements |
|------|-----------|
| 1 | An image is worth a thousand words. |
| 2 | People say I am a bit lazy and scatterbrained. |
| 3 | I have a great sense of humor, and I always see the funny side of life. |
| 4 | Sometimes I get obsessed with a problem, and I keep trying until I find a solution. |
| 5 | A bit of adrenaline is always welcome. Life is boring without it. |
| 6 | I am very curious. |
| 7 | People think that I am good at finding solutions to common problems. |
| 8 | I enjoy trying to find new solutions to problems. |
| 9 | I have lots of ideas in every domain. |
| 10 | One plus one does not always equal two |

of the scale. (The answers to these items are simply ignored in the evaluation.) For the same reason, the items are presented in random order each time the test starts.

The graphic user interface implementing the five point Likert scale for collecting the user's responses is presented in figure 3.

Each answer is scored with a numeric value between 0 (totally disagree) and 4 (definitely agree). For each subscale we compute a total score:

$$< ss_1 = \sum_{i=1}^{10} A_i >; < ss_2 = \sum_{i=11}^{20} A_i > \tag{1}$$

Table 2: Subscale 2. Items for detecting stereotypical thinking and other blocking factors for creativity.

| Item | Statements |
|------|------------|
| 1 | I always play by the rules. |
| 2 | My parents were very strict with me. |
| 3 | If anything can go wrong, it will. |
| 4 | I am very disciplined and diligent. |
| 5 | Sometimes I use oracles when I need to make difficult decisions. |
| 6 | I know exactly what I will do next summer. |
| 7 | I always trust reputable scientists. |
| 8 | I like to solve the problems one by one. |
| 9 | I like to quote the opinions of wiser people. |
| 10 | I feel very embarrassed if I fail. |
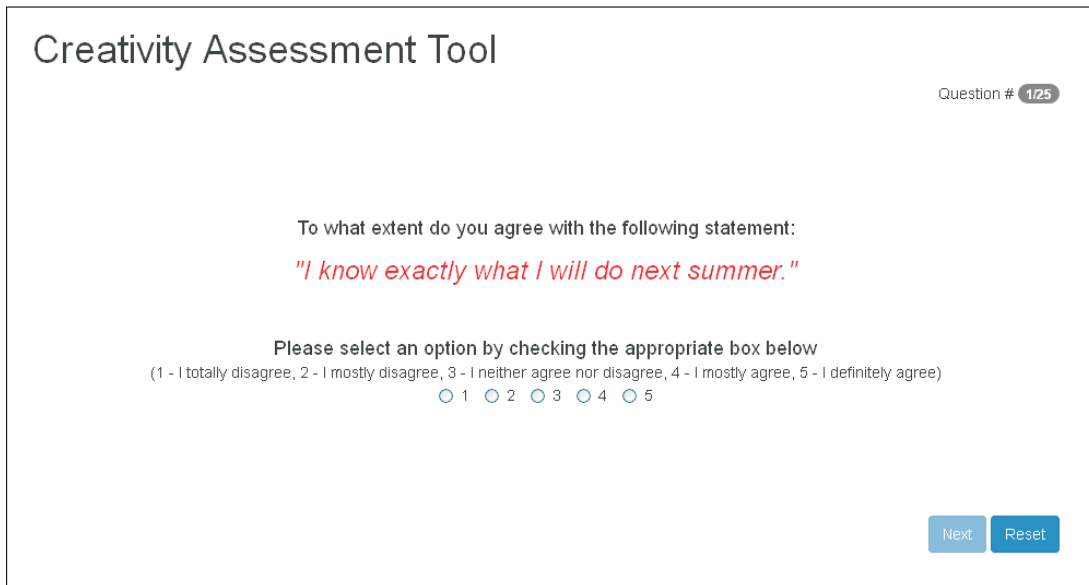


Figure 3: A snaposhot of the GUI of the application

Obviously $ss_1, ss_2 \in [0, 40]$. While a high score for the first subscale indicates a high creativity, the second subscale is aimed to detect social conformity tendencies, and stereotypical thinking. A high score for the second subscale is likely to indicate the existence of important blocking factors for the subject's creativity.

Since the two subscales address distinct factors of the creativity, it is not possible to compute the final creativity quotient - CQ by simply adding or substracting the scores of the subscales.

Assuming that the domain od variation for CQ is the interval [0,100], one possible way to compute this quotient is:

$$CQ = 50 * (1 + \tanh(k * (ss1 - ss2))) \qquad (2)$$

where k is a scaling factor, empirically set to the value $k = 0.07$.

Though this heuristic method of computing CQ spreads the user responses reasonably well over the interval [0,100] when using exactly two subscales that reflect opposite influences, we preferred to use a fuzzy inference algorithm to compute CQ. This solution is proven effective in

many other difficult problems (see for example [9]), provides superior flexibility, and the resulting code is largely reusable in other applications.

For this experimental version, and considering the limitations of the PHP language required by the dedicated web based application, we chose the simplest implementation with three fuzzy domains for $ss1$ and $ss2$ and linear membership functions, as shown in figure 4.
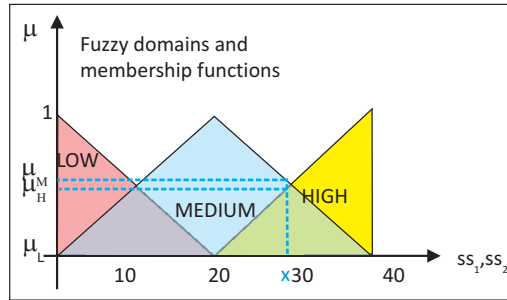


Figure 4: Fuzzy domains and membership functions for ss1, ss2

With these assumptions, the knowledge base for the actual interpretation of the scores ss1 and ss2 for computing CQ is described by the set of rules presented in Table 3:

Table 3: The fuzzy rule base

| ss1 | ss2 | CQ |
|--------|--------|--------|
| LOW | LOW | LOW |
| LOW | MEDIUM | LOW |
| LOW | HIGH | LOW |
| MEDIUM | LOW | MEDIUM |
| MEDIUM | MEDIUM | MEDIUM |
| MEDIUM | HIGH | LOW |
| HIGH | LOW | HIGH |
| HIGH | MEDIUM | HIGH |
| HIGH | HIGH | MEDIUM |

Each line of Table 3 should be read as an IF/THEN statement of the following type:

IF (ss1 is LOW) AND (ss2 is LOW) THEN CQ is LOW

The truth values $\mu_L, \mu_M, \mu_H$ of the statements (ss1 is LOW), (ss1 is MEDIUM), (ss1 is HIGH), (ss2 is LOW), (ss2 is MEDIUM), (ss2 is HIGH), for the particular values of ss1, ss2 derived from the user's responses are determined using the equations of the membership functions. And the truth value of the entire statement for the rule i is:

$$Z_i = min(\mu_1, \mu_2) \tag{3}$$

Assuming that the output domain is $CQ \in [0, 100]$, we can choose constant values for the output fuzzy domains ("singletons", Si) e.g. $S_{LOW} = 10, S_{MEDIUM} = 50, S_{HIGH} = 100$. With these notations, the final "crisp" value of CQ is the center of gravity of the entire knowledge base:

$$CQ = \frac{\sum_{i=1}^{9} Zi * Si}{\sum_{i=1}^{9} Zi} \tag{4}$$

For details on the tehory behind the above implementation, see [30].

Figure 5 is a snapshot of the screen presenting the results of the test and the computed value of CQ.

The actual implementation contains additional software modules for user authentication, and report generation. The results of the tests are stored in a database.

A beta version of the web application can be tested at http://dev.ugal.ro/creativity/



Figure 5: A snaposhot of the final screen presenting the result of the test

## 4    Discussion and conclusions

The validation of the proposed scale is in progress. A simple pretest for internal consistency has been conducted with N=30 undergraduate students of the Faculty of Automation, Computers, Electrical and Electronics Engineering resulting in statistically acceptable values of the Cronbach quotient $\alpha = 0.73$ for subscale 1, and $\alpha = 0.78$ for subscale 2.

Though this research has been conducted in the context of an educational project partly funded by EACEA - The Education, Audiovisual and Culture Executive Agency of the European Commission - (namely TECRINO- Teaching creativity in engineering, 538710-LLP-1-2013-1-CY-LEONARDO-LMP), for unknown reasons, the EACEA representatives stubbornly denied all the requests for permission to disseminate the results of this work through scientific publications, and to allocate funds, within the same budget, to deepen this study. Due to lack of funding, our work in this direction is much slower than we hoped.

Therefore, for this moment, we must align to the expectations formulated by Miller in ( [18]): "It should also be noted that validation of any instrument is an ongoing procedure.... Once a measure has been adequately developed, it is the responsibility of all researchers in the field to further the generation of evidence for its validity."

Obviously, further validation studies using a larger sample are definitely required.

The preliminary results are promising: the proposed tool is free, simple, easy to use, easy to integrate in almost any e-learning platform, and serves the purpose of assessing the evolution of the students enrolled in creativity training courses. And the idea of using a fuzzy algorithm for automated scoring of psychometric scales may have other interesting applications.

**Acknowledgment**

# Bibliography

[1] Aleinikov, A., Kackmeister, S., and Koenig, R. (Eds.). (2000); *Creating creativity: 101definitions*, Midland, MI: Alden B. Dow Creativity Center, Northwoods University.

[2] Amabile, T.M. (1982); Social psychology of creativity: A consensual assessment technique, *Journal of Personality and Social Psychology*, 43: 997-1013.

[3] Amabile, T. M., Conti, R., Coon, H., Lazenby, J., and Herron, M. (1996); Assessing the work environment for creativity, *Academy of management journal*, 39(5): 1154-1184.

[4] Batey, M. (2012); The measurement of creativity: From definitional consensus to the introduction of a new heuristic framework, *Creativity Research Journal*, 24(1): 55-65.

[5] Binkley, M., Erstad, O., Herman, J., Raizen, S., Ripley, M., Miller-Ricci, M., and Rumble, M. (2012); Defining twenty-first century skills, *Assessment and teaching of 21st century skills*, Springer Netherlands, 17-66.

[6] Bull, K.S. & Davis, G.A. (1980); Evaluating creative potential using the statement of past creative activities, *Journal of Creative Behavior*, 14: 249-257.

[7] Cachia, R., Ferrari, A., Kearney, C., Punie, Y., Van den Berghe, W.,and Wastiau, P. (2009); Creativity in schools in Europe: A survey of teachers in Europe, *European Commission-Joint Research Center-Institute for Prospective Technological Studies, Seville.*

[8] Carson, S., Peterson, J.B.,& Higgins, D.M. (2005); Reliability, Validity, and Factor Structure of the Creative Achievement Questionnaire, *Creativity Research Journal*, 17(1): 37-50.

[9] Dzitac, I., Vesselenyi, T., Tarca, R. C. (2011); Identification of ERD using fuzzy inference systems for brain-computer interface, *International Journal of Computers Communications & Control*, 6(3): 403-417.

[10] Fields, Z., & Bisschoff, C. A. (2014); Developing and Assessing a Tool to Measure the Creativity of University Students, *J Soc Sci*, 38(1): 23-31.

[11] Florida, R. (2006); The Flight of the Creative Class: The New Global Competition for Talent. *Liberal Education*, 92(3): 22-29.

[12] Kasof, J. (1995); Explaining creativity: The attributional perspective, *Creativity Research Journal*, 8:311-366.

[13] Kaufman, J. C., Plucker, J. A., & Baer, J. (2008); *Essentials of creativity assessment*, John Wiley & Sons, 53.

[14] Kelly, K.E. (2004); A brief measure of creativity among college students. *College Student Journal*, 38: 594-596.

[15] Kim, K. H. (2006); Can we trust creativity tests? A review of the Torrance Tests of Creative Thinking (TTCT), *Creativity research journal*, 18(1): 3-14.

[16] Kirton, M. (1976); Adaptors and innovators: A description and measure. *Journal of Applied Psychology*, 61: 622-629

[17] Kumar, V. K., Kemmler, D., & Holman, E. R. (1997); The Creativity Styles Questionnaire–Revised. *Creativity Research Journal*, 10(1): 51-58.

[18] Miller, A. L. (2009), *Cognitive processes associated with creativity: Scale development and validation* (Doctoral dissertation, Ball State University).

[19] Miller, A. L. (2014); A self-report measure of cognitive processes associated with creativity, *Creativity Research Journal*, 26(2): 203-218.

[20] Parkhurst, H. B. (1999); Confusion, lack of consensus, and the definition of creativity as a construct, *The Journal of Creative Behavior*, 33(1): 1-21.

[21] Plucker, J.A., Runco, M.A. (1998); The death of creativity measurement has been greatly exaggerated: Current issues, recent advances, and future directions in creativity assessment, *Roeper Review*, 21: 36-40.

[22] Resnick, M. (2007); Sowing the Seeds for a More Creative Society, *International Society for Technology in Education*, 35(4): 18-22

[23] Robinson, K. (2011); *Out of our minds: Learning to be creative.* Capstone

[24] Runco, M.A. (1999); Appendix II: Tests of creativity. In M.A. Runco and S.R. Pritzker Eds.), *Encyclopedia of creativity*, San Diego, CA: Academic Press, 755-760).

[25] Runco, M. A., Plucker, J. A., & Lim, W. (2001); Development and psychometric integrity of a measure of ideational behavior. *Creativity Research Journal*, 13(3-4): 393-400.

[26] Sawyer, R. K. (2011); *Explaining creativity: The science of human innovation*, Oxford University Press.

[27] Susnea, I., Pecheanu, E., Tudorie, C. and Cocu, A. (2014); The education for creativity - the only student's tool for coping with the uncertainties of the future, *MAC ETEL 2014 - International Conference on Education, Teaching and e-Learning*, Prague , Oct. 2014.

[28] Susnea, I. Pecheanu, E. Tudorie, C. (2014); Initiatives towards and Education for Creativity, The 6th International Conference Edu World 2014 *Education Facing Contemporary World Issues*, 7th - 9th November 2014. Also published in Procedia - *Social and Behavioral Sciences, 2015* 180: 1520 - 1526.

[29] Sternberg, R. J. (1988); A three-facet model of creativity. In R. J. Sternberg (Ed.), *The nature of creativity*, Cambridge: Cambridge University Press, 125-147.

[30] Tanaka, K. (1997); *An introduction to fuzzy logic for practical applications*, Springer Verlag.

[31] Thorsteinsson, G., Page, T., & Niculescu, A. (2010); Adoption of ICT in supporting ideation skills in conventional classroom settings, *Journal of Studies in Informatics and Control*, 19(3): 309-318.

[32] Torrance, E. P. (1974); *Torrance Tests of Creative Thinking: Norms and technical manual.* Bensenville, IL: Scholastic Testing Press

[33] Treffinger, D. J. (1996); *Creativity, creative thinking, and critical thinking: In search of definitions.* Sarasota, FL: Center for Creative Learning.

# Author index